Online treatment adaptation strategies for the 1.5T MR-linac: first implementation and evaluation for lymph node oligometastases

Dennis Winkel

Online treatment adaptation strategies for the 1.5T MR-linac: first implementation and evaluation for lymph node oligometastases
PhD Thesis, Utrecht University, The Netherlands, D. Winkel, 2019

The research described in this thesis was performed at the Department of Radiotherapy of the University Medical Center Utrecht

Manuscript

Cover image:	Dennis Winkel
Cover layout:	Ilse Modder
Lay-out:	Dennis Winkel
Typeset:	LaTeX
Printed by:	Gildeprint
ISBN:	978-946323-831-1

Publication of this thesis was financially supported by the UMC Utrecht Department of Radiotherapy and Elekta. Part of this work was supported by the Dutch Cancer Society (KWF 2015-0848)

Online treatment adaptation strategies for the 1.5T MR-linac: first implementation and evaluation for lymph node oligometastases

Strategieën voor online planaanpassingen voor de 1.5T MR-linac: eerste implementatie en evaluatie voor lymfeklier oligometastasen

(met een samenvatting in het Nederlands)

Proefschrift

ter verkrijging van de graad van doctor aan de Universiteit Utrecht
op gezag van de rector magnificus, prof. dr. H.R.B.M. Kummeling,
ingevolge het besluit van het college voor promoties
in het openbaar te verdedigen
op donderdag 17 oktober 2019 des middags te 2.30 uur

door

Dennis Winkel
geboren op 18 februari 1989
te Tiel

Promotor:	Prof. dr. B.W. Raaymakers
Copromotoren:	Dr. G.H. Bol
	Dr. ir. P.S. Kroon

Contents

Chapter 1

General introduction

Radiotherapy, or radiation therapy, is an important pillar of cancer therapy in which ionizing radiation is applied to the patient [1, 2]. The aim is to use the ionizing radiation to damage the DNA of cancerous tissue leading to cellular death [3]. Radiotherapy can be given with intent to cure (curative). Additionally, radiotherapy can also be applied with a palliative intent, where cure is not possible, to achieve long-term local control with postponement of toxic systemic treatments or for symptomatic relief. Radiotherapy can also be applied as an adjuvant treatment in which radiotherapy is applied combined with another type of treatment such as surgery, chemotherapy, hormonal therapy and other systemic therapies.

In external beam radiotherapy (EBRT) a pre-defined dose distribution is given to the tumor and surrounding tissue with a linear accelerator through a high energy megavoltage (MV) photon beam [4]. Higher doses to the tumor often result in higher tumor control probabilities (TCP) [5]. To avoid unnecessary high dose levels in healthy tissue while achieving high dose levels in the target, dose is delivered through multiple beam angles using a cross-fire technique. As such, the beams traverse the body and dose is deposited along the beam trajectory which cause cell damage of healthy tissue outside of the tumor [3]. EBRT is therefore often delivered through fractionated treatment schemes to allow normal tissue to recover [6, 7].

Prior to dose delivery, the treatment is prepared by acquiring pre-treatment imaging of the patient. Typically these are computed tomography (CT) and magnetic resonance (MR) scans and sometimes positron emission tomography (PET) scans. On these scans the physician can identify relevant anatomical structures, such as the target and surrounding organs. From the CT scan additional physical properties such as the electron density (ED) of tissues can be derived which are used for accurate dose calculations. A physician delineates the gross tumor volume

(GTV), which is the visible part of the tumor, as well as surrounding organs at risk (OARs). In case the tumor has microscopic tumor spread, a clinical target volume (CTV) is defined as an expansion of the GTV. In addition to the GTV or CTV, a planning target volume (PTV) margin is added to account for geometric inaccuracies and uncertainties such as machine uncertainties, delineation inaccuracies, patient setup errors, as well as potential target motion throughout dose delivery. The exact margin is often determined on population statistics [8].

The PTV is thus required to ensure that even given all geometric uncertainties, the target is receiving the prescribed dose. The PTV often overlaps with surrounding OARs which, as a result, may also receive high amounts of radiation [9]. This makes it ever desirable to reduce the margin, which is often done through image-guidance or the use of fixation devices, such as masks for inter- and intra-fraction motion or abdominal corsets for intra-fraction motion [10, 11].

Based on the pre-treatment imaging and the delineations a radiotherapy treatment plan is generated using a treatment planning system (TPS). A plan is created to deliver the prescribed dose in Gray (Gy) to the treatment volume, without violating tolerance levels of surrounding OARs. A dose engine is used to calculate the delivered dose to the patient, taking into account the electron densities and properties of the linear accelerator such as the beam energy, angle, shape and intensity profiles [12]. For conformal radiotherapy a treatment plan is created using forward planning in which the operator creates a treatment plan by modifying the angles and shapes of each beam [13]. Modifying the shape can be done using a multi-leaf collimator (MLC), which is mounted on the linear accelerator. This process is highly dependent on the skill and experience of the human operator. Treatment planning for intensity modulated radiotherapy (IMRT) [3, 14], which allows for non-uniform beam profiles, is often performed in an inverse manner [15]. The operator defines a set of planning objectives for the target, as well as dose constraints for the surrounding tissues. The TPS then iteratively changes shape and intensity of the beam to create a treatment plan that satisfies all of these planning aims. The resulting treatment plan is converted to a set of machine actions which allow the linear accelerator to deliver the radiotherapy treatment as intended. The need to deliver high doses to the tumor and to spare surrounding tissue as much as possible to reduce the probability for toxicity and other adverse effects, makes certain trade-offs unavoidable.

In the last decade automated treatment planning solutions were introduced [16–21]. This increases the efficiency and reduces inter- and intra-planner variability [22]. Automated treatment planning also allows for efficient generation of a library of plans [23]. For the latter, multiple plans are generated based on

expected variations in the patient anatomy and the best suitable plan can be selected based on online image guidance [24, 25]. In addition to direct clinical use, automated radiotherapy treatment planning algorithms have also been applied to supportive tools such as plan quality assessment and verification. It can also be used to predict what type of dose distribution can be achieved for a certain patient [26–28].

Image-guided radiotherapy

In the past decades image-guided radiotherapy (IGRT) has vastly developed and it is currently indispensible in modern radiation therapy [3, 29]. In IGRT, image-guidance is used to improve the precision and accuracy of treatment delivery. Linear accelerators are equipped with special imaging technology that enables the operator to visualize the tumor before, or even during treatment delivery, while the patient is positioned on the treatment table. With image guidance, the acquired images can be compared to reference images and adjustments to the patient position can be made in order to more precisely target the tumor and avoid OARs. IGRT increases accuracy, which as a result may facilitate a PTV reduction and decreases dose to the OARs, while maintaining or improving TCP.

Most modern radiotherapy systems are equipped with cone-beam computed tomography (CBCT) systems. Volumetric scans are reconstructed making use of kV-imaging systems mounted on the rotating gantry. This makes it possible to acquire 3D images with CT-like contrast while the patient is on the table [30]. These scans can be used to adapt the patient position accordingly, but yield poor quality compared to a diagnostic CT and is not suitable for on-line delineating or accurate tissue identification, in particular not for soft-tissues.

To accurately identify the target and correct the position of the patient using CBCT, it may be desirable to make use of surrogates such as fiducial markers [31, 32]. These surgically implanted markers are landmarks to facilitate correct localization of the tumor. The use contributes to precise and accurate dose delivery and can greatly reduce the PTV margin, but is however invasive and cause additional burden for the patient. Another surrogate method is to make use of bony anatomy or other anatomic landmarks in the vicinity of the target. When the target is however not connected to these landmarks, movement may be independent and this method contains more uncertainties, which leads to larger PTV margins [33].

MRI is gaining a more important role in modern day radiotherapy. In recent years, MRI-guided radiotherapy systems became commercially available and are nowadays used in clinical practice for image guidance purposes [34–36]. MRI yields a superior soft-tissue contrast compared to CBCT, which means that both the tumorous tissue and surrounding OARs can more clearly be visualized [37,38]. Further benefits are that MRI acquisition does not require ionizing radiation and that imaging of the patient anatomy can be acquired with different contrast and dynamics and in any desired orientation. Also, the trade-off can be made freely between spatial and temporal resolution.

MR-guided online adaptive radiotherapy

The research described in chapter 3 – 7 of this thesis is conducted for the 1.5T MR-linac machine. The 1.5T MR-linac is a radiotherapy system which has been designed and developed at the radiotherapy department of the University Medical Center Utrecht (Utrecht, The Netherlands) in collaboration with Philips (Best, The Netherlands) and Elekta AB (Stockholm, Sweden). The 1.5T MR-linac, is commercialized by Elekta as the Unity. It consists of a MRI system with a field strength of 1.5T surrounded by a ring-shaped gantry on which a 7 MV linear accelerator has been placed. Active shielding coils in the magnet avoid interference between the main magnetic field and the linear accelerator, while a beam window, allows for an irradiation field of 22cm in cranial caudal and 57cm in lateral direction at the isocenter of the system. The 7 MV flattening filter free (FFF) photon beam is shaped by a MLC with 80 leaf pairs. The first patients were treated on this system in May 2017 [36].

The 1.5T MR-linac system can provide diagnostic quality imaging of the patient anatomy before, during and after dose delivery. The superior soft tissue quality that the 1.5T MR-linac provides good visualization of the patient anatomy and allows for online delineation of the target and surrounding OARs. Being able to accurately identify the target and surrounding tissues, does not only allow for more precise patient position, but opens up opportunities for plan adaptation [39] and motion characterization. MR imaging prior to dose delivery can yield high spatial resolution anatomical images. The pre-treatment delineations can be propagated to the daily MRI using deformable image registration and/or can be adjusted when necessary. The updated anatomical information can then be used as input for adaptive treatment planning, in which the treatment plan can be shifted towards the current patient position or be partially or completely re-optimized as is also described in chapter 3.

Stereotactic body radiation therapy of lymph node oligometastases

Local treatment of lymph node oligometastases is commonly performed using stereotactic body radiation therapy (SBRT) [3]. SBRT is a minimally invasive therapy in which experience has primarily been gained for inoperable patients with liver and lung oligometastases [40, 41]. In SBRT a relatively high irradiation dose is delivered in a limited number of fractions to the target in a highly conformal manner with steep dose gradients to achieve good sparing of the OARs [42,43]. Recently SBRT is also commonly applied as standard clinical care for the treatment of lymph node [44–46], adrenal gland [47, 48] or bone oligometastases [49]. Treatment of individual metastatic lesions is being used to treat patients with limited metastatic disease as a means to improve progression-free- or overall survival and delay systemic therapies without compromising the quality of life.

In the majority of the patients treated for lymph node oligometastases, the affected lymph nodes originate from prostate cancer and have a low alpha/beta ratio [50]. Because of this a high biological effective dose (BED) can be achieved of >100 Gy which is associated with improved local control [51]. In general, SBRT of lymph node oligometastases also gives relatively low toxicity. Because of these properties, systemic treatment for this patient group can be delayed with approximately 8-13 months [52, 53] and therewith maintaining the patients quality of life by avoiding androgen deprivation therapy (ADT) related side-effects [54].

SBRT of lymph node oligometastases has been mainly applied using CBCT image guidance or CyberKnife systems with fractionation schedules ranging from 55–10Gy to 112–24Gy [55] and is sometimes combined with fiducial marker implantation for enhanced target visualization [56, 57]. Based on our own institutional clinical experience lymph node oligometastases are poorly visible on CBCT in about 30% of all cases. Poor target visibility will require larger treatment margins to prevent under-dosage and may thereby be more limited by dose tolerance levels of surrounding OARs. The combination of small soft-tissue targets, high dose levels and steep dose gradients may therefore benefit from MR-guided online adaptive radiotherapy. The improved soft tissue contrast allows for online delineation of the target and OARs and to use these daily delineations for online adaptive treatment planning to get a more accurate treatment plan.

Thesis Outline

The aim of this thesis is to investigate novel treatment planning strategies for radiotherapy treatment planning and MR-guided online plan adaptation. The chapters in this thesis cover automated treatment planning (Chapter 2), MR-guided online plan adaptation possibilities for the 1.5T MR-linac (Chapter 3) and simulation, implementation and dosimetric evaluation of MR-guided treatment of lymph node oligometastases (Chapter 4-7).

Chapter 2 describes the development and clinical introduction of an automated treatment planning. A two-phased planning and optimization workflow was developed to automatically generate 77Gy 5-field simultaneously integrated boost intensity modulated radiation therapy (SIB-IMRT) plans for prostate cancer treatment. Moreover, a retrospective planning study was performed in which automatically and manually generated treatment plans were compared.

The promise of the MR-linac is that one can visualize all anatomical changes during the course of radiotherapy and hence adapt the treatment plan in order to always have the optimal treatment. Yet, there is a trade-off to be made between the time spent for adapting the treatment plan against the plan quality, which expires over time. In Chapter 3 the various daily plan adaptation methods will be presented and applied on five cases with varying levels of inter-fraction motion, regions of interest and target sizes: prostate, rectum, esophagus and lymph node oligometastases (single and multiple target). The plans were evaluated based on the clinical dose constraints and the optimization time was measured to give an insight of the plan adaptation possibilities of the 1.5T MR-linac and the previously described trade-off.

In Chapter 4 the dosimetric impact of online replanning as a method to correct for inter-fraction anatomical changes for SBRT of lymph node oligometastases on the 1.5T MR-linac is investigated. Pre-treatment plans were created with 3 and 8mm PTV margins reflecting our clinical practice for lymph nodes with good and poor visibility on CBCT. The dose–volume parameters of the pre-treatment plans were evaluated on daily anatomy as visible on the repeated MRIs and compared to online replanning.

Because the previous chapter showed beneficial dosimetric parameters of online replanning, Chapter 5 focuses on determining the optimal plan adaptation approach for MR-guided SBRT treatment of lymph node oligometastases on the 1.5T MR-linac. Using pre-treatment CT and repeated MR data, six different methods of plan adaptation were performed on the daily MRI and contours. To

determine the optimal plan adaptation approach, the adapted plans were evaluated using clinical dose criteria and the time required for performing the plan adaptation.

Chapter 6 and 7 describe the evaluation of the clinical treatments. In Chapter 6 the dosimetric differences between the first clinical treatments of lymph node oligometastases on the 1.5T MR-linac in which a completely new plan was generated based on the daily patient anatomy and contours compared to only correcting for the daily position of the patient are described. Additionally the PTV margin needed for adequate target-coverage was re-evaluated. The GTV coverage for the plans was evaluated by comparing the dose on both the online planning MRI, acquired at the start of the treatment fraction, as well as the post-delivery MRI, acquired after dose delivery. In Chapter 7 a target coverage and dose criteria based evaluation of the clinically delivered online adaptive radiotherapy treatment compared with conventional CBCT-linac plans was performed. The clinically delivered MR-linac plans were compared with the, otherwise given, conventional treatment by calculation of the CBCT-linac plans on the daily patient anatomy.

Finally, Chapter 8 presents a summary of the work conducted in this thesis and a general discussion regarding automated treatment planning, MR-guided online adaptive radiotherapy, treatment of lymph node oligometastases on the 1.5T MR-linac and future perspectives.

Chapter 2

Development and clinical introduction of automated radiotherapy treatment planning for prostate cancer

The following chapter is based on:

Dennis Winkel, Gijsbert H. Bol, Bram van Asselen, Jochem Hes, Vincent Scholten, Linda G.W. Kerkmeijer, Bas W. Raaymakers

Physics in Medicine & Biology (2016) Vol. 61, p.8587-8595

Abstract

To develop an automated radiotherapy treatment planning and optimization workflow to efficiently create patient specifically optimized clinical grade treatment plans for prostate cancer and to implement it in clinical practice a two-phased planning and optimization workflow was developed to automatically generate 77Gy 5-field simultaneously integrated boost intensity modulated radiation therapy (SIB-IMRT) plans for prostate cancer treatment. A retrospective planning study (n=100) was performed in which automatically and manually generated treatment plans were compared. A clinical pilot (n=21) was performed to investigate the usability of our method. Operator time for the planning process was reduced to<5min. The retrospective planning study showed that 98 plans met all clinical constraints. Significant improvements were made in the volume receiving 72Gy (V_{72Gy}) for the bladder and rectum and the mean dose of the bladder and the body. A reduced plan variance was observed. During the clinical pilot 20 automatically generated plans met all constraints and 17 plans were selected for treatment. The automated radiotherapy treatment planning and optimization workflow is capable of efficiently generating patient specifically optimized and improved clinical grade plans. It has now been adopted as the current standard workflow in our clinic to generate treatment plans for prostate cancer.

Introduction

In western countries, intensity modulated radiation therapy (IMRT) [58] is a frequently applied form of external beam radiation therapy to treat patients with prostate cancer. IMRT enables accurate dose delivery by a cumulative dose distribution, while sparing the adjacent healthy tissue. The main parameters that have to be taken into account for IMRT to create suitable treatment plans are the number of beams, their geometrical orientation and the intensity modulation. Because there always is a trade-off between target coverage and sparing of the surrounding tissues and organs at risk (OAR), radiotherapy treatment planning is a multicriterial optimization problem. In practice the problem is more subtle than just meeting the target coverage constraints and sparing of the OAR's as some structures are more sensitive to radiation than others and sparing of one OAR may be more important than another.

Having control over multiple aspects such as the number and configuration of beams, optimizer settings and cost functions, dosimetrists aim to create the most optimal plan with regard to clinical objectives and constraints. One of the most difficult challenges in treatment planning is that good solutions heavily depend on these objectives and constraints. In clinical practice, optimization of objectives and constraints is often a time-consuming task based on trial-and-error. Although plan generation often starts with a generic template, patient specific tailoring is required. This yields a plan which meets the clinical objectives and constraints, but there can exist a variation between the quality of these plans and the process is operator dependent [59, 60]. A part of these variations may be related to differences in knowledge and experience of dosimetrists. Another part can be caused by a lack of human or technological resources, which limits the time available for treatment planning or prevent new treatment techniques to be implemented.

We hypothesize that introducing automated radiotherapy treatment planning will increase consistency, improve plan quality and reduce workload. This means that operators have more time to work on more demanding IMRT plans. As prostate cancer has the highest incidence of all types of cancer in male patients, a high gain in efficiency can be achieved by reducing the time required for plan creation. Automated treatment planning is a strong tool to use for offline or online plan adaptation. It is also a requirement to make optimal use of novelty techniques such as the MR-linac [61–63].

In this study an automated radiotherapy treatment and optimization workflow was developed to provide an efficient and consistent solution for the creation of radiotherapy plans. The automated treatment planning and optimization workflow was applied to prostate cancer. Plan viability was retrospectively evaluated

and a clinical pilot was run to investigate the value of our automated radiotherapy treatment and optimization workflow in clinical practice.

Methods and materials

Automated treatment planning workflow

An automated radiotherapy treatment planning workflow was developed based on the treatment planning system Monaco by Elekta AB (Stockholm, Sweden) with the use of Elekta's research automation toolkit which functions as an API enabling our software to communicate with the Monaco user interface. This new framework is able to generate radiotherapy treatment plans without any user interaction using patient specific optimization (Figure 2.1). During phase one, the fluence and weights are optimized to get an optimal dose distribution. Phase two focuses on finding optimal field shapes and takes into account accelerator restrictions such as the multi leaf collimator (MLC) and gantry movements. After each phase, the current state is evaluated and, if dose requirements are not met, constraints are changed. The constraints are changed by using fixed predetermined step sizes. By varying these step sizes among the different target volumes and OAR, priority can be given to reach more sparing of certain structures.

The goal of phase one is to meet a guaranteed coverage of the target volumes. An initial phase one optimization is run, after which the dosimetric values are evaluated. If the target coverage does not meet set requirements, both target volume cost functions are tightened and OAR cost functions are loosened and phase one re-optimization occurs. As soon as the requirements are met or when the maximum amount of iterations is reached, an initial phase two optimization is performed. The goal of phase two is to reach optimal sparing of the OAR, while maintaining an acceptable coverage of the target volumes. This is done iteratively by tightening the cost functions for the organs at risk, based on dose-volume histogram (DVH) values, and re-optimizing phase two. This loop will attempt multiple different solutions and will continue until the maximum amount of iterations has been reached. By using this loop in combination with small step-sizes, a lot of different options are explored and the best plan can be selected for treatment. A graphical representation of this workflow is depicted in Figure 2.1.

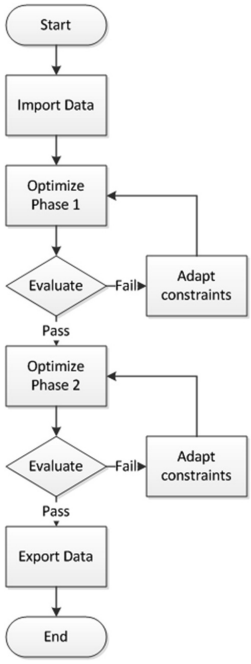

Figure 2.1: Graphical representation of the automated treatment planning workflow.

Retrospective planning study

To investigate the viability of automated treatment plans for prostate cancer, a retrospective planning study (n=100) was performed. Included were patients which were treated with a prescribed dose of 70Gy to the planning target volume (PTV), which includes the corpus of the prostate, the seminal vesicles and the GTV, with an 8mm margin. A simultaneous integrated boost (SIB) of 77Gy was given to the extended boost volume (EBV). The EBV consists of the corpus of the prostate and the gross tumour volume (GTV) with an 8mm margin in ventral, right, left and caudal direction with full exclusion of the rectum and bladder. Delineated OARs were the rectum, bladder, femoral heads and sphincter. To make a reliable comparison, the same dose criteria were maintained for automated treatment planning (Table 2.1). All plans were generated using 5 evenly spaced beams (Table 2.2). The maximum amount of segments was kept at 60. All other sequencing settings and parameters were also kept the same.

Table 2.1: Clinical dose criteria for SIB-IMRT prostate plans as used in the evaluation of the automatically generated and clinical treatment plans.

Structure	Constraint
EBV	$V_{73.15Gy}$>99%
PTV	$V_{66.5Gy}$>99%
Rectum	V_{72Gy}<5%
	V_{50Gy}<50%
Bladder	V_{72Gy}<10%
Sphincter	D_{mean}<37Gy
Femoral heads	D_{max}<50Gy

Table 2.2: Beam orientations used for both automatically and manually generated treatment plans.

Beam	Gantry (deg)	Collimator (deg)
1	40	0
2	100	3
3	180	6
4	260	354
5	320	357

Plan generation and evaluation

For all 100 cases an automated treatment plan was generated retrospectively and evaluated to see if the dose criteria were met. The same was done for the clinical treatment plans. The most important dosimetric measures were compared between the automatically generated and clinical plans. The time needed for manual treatment plan generation was measured to indicate the gain in time efficiency by planning automatically. All automated treatment plans were based on the same set of beam angles and sequencing settings. No alterations were made for any case. The maximum amount of loops was set to 15 for both phase one and two.

Clinical pilot

A prospective pilot study (n=21) was conducted in our clinic, in which the dosimetrist started the automatic planning process. If a plan was considered as an optimal plan, it was proposed for treatment. If not, an additional manual plan was made by the dosimetrist. The decision to make an additional manual plan was based on the knowledge and experience of the dosimetrist whether improvement was possible. Both plans were then reviewed by the radiation oncologist and clinical physicist and the most optimal clinical plan was selected for

treatment (Figure 2.2). The radiation oncologist and clinical physicist were aware which plan was automatically generated and which was created manually.

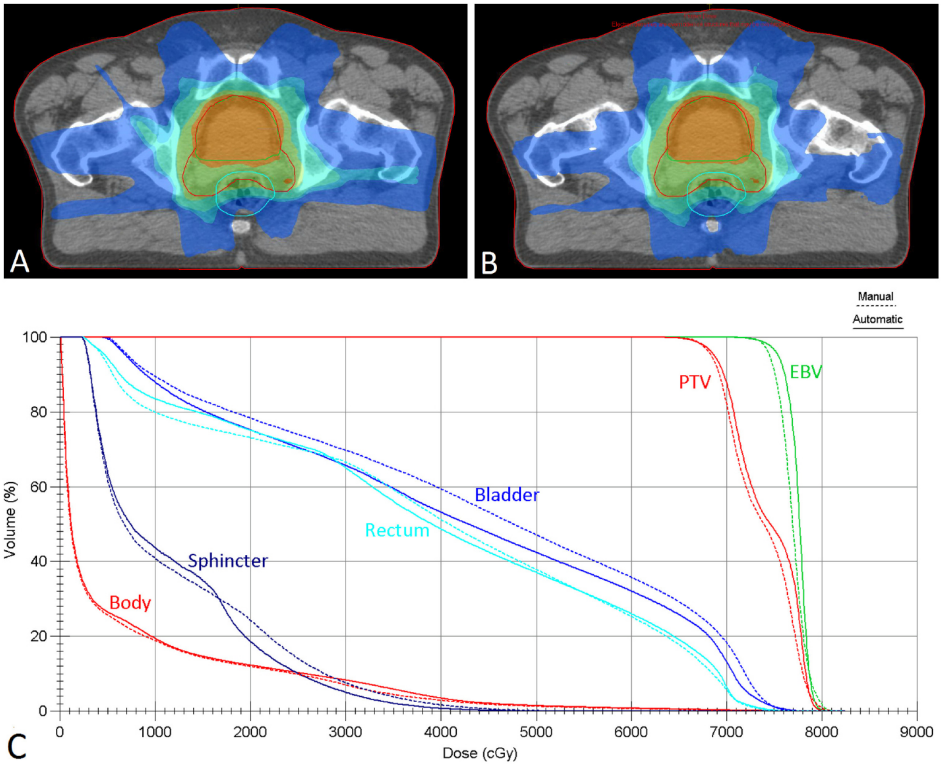

Figure 2.2: (A) Dose distribution in transversal plane of an automatic plan and (B) a manual plan. (C) The dose-volume histograms of these dose distributions.

Results

Retrospective planning study

The individual results for each of the 100 retrospectively performed automatic plans show that for 98 plans (98%) all clinical dose constraints are met. For the two plans that violated the clinical dose constraints, the constraints for the V_{72Gy} and V_{50Gy} of the rectum were not met. The target coverage was always reached. The dose constraints for the bladder, sphincter and femoral heads were not violated.

From the manually planned treatment plans, 86 met the clinical dose constraints. For two plans the V_{72Gy} constraint on the rectum was not met. In two plans the V_{50Gy} constraint on the rectum was not met and for one plan both rectum constraints were not met. In five plans the constraints set for a minimum target coverage of the EBV and PTV were not met. The remaining four plans that violated the dose criteria failed on a combination of one or more of the target coverage constraints and the V_{72Gy} and V_{50Gy} constraints for the rectum. The two patients of which the automated plan did not meet all dose criteria, the manual plans also did not meet all dose criteria.

Dosimetric comparison of automated plans and clinical plans

A comparison of the dosimetric values of both automatically generated plans and manually generated plans from the clinic show that on average the automatically generated plans yield significantly better sparing of the OARs (Table 2.3). Both the target coverage, maximum dose and mean for the EBV and PTV are similar for both types of plans. Significant improvements are observed in the V_{72Gy} of the rectum and bladder. Automatically generated plans also show a reduced mean dose for the bladder and the body (Figure 2.3). Automatically generated plans also show a lower variance.

Table 2.3: Dosimetric values for both the automatically and manually generated treatment plans (n=100). p-value obtained with paired t-test.

Structure	Parameter	Autoplanning	Clinic	p-value
	Maximum dose (Gy)	80.9±0.4	81.6±0.9	<0.001
	Mean dose (Gy)	77.4±0.1	77.2±0.2	<0.001
	$V_{73.15Gy}$ (%)	99.4±0.2	99.2±0.3	<0.001
PTV	$V_{66.5Gy}$ (%)	99.2±0.1	99.2±0.3	0.304
Rectum	Mean dose (Gy)	37.2±5.2	37.5±5.6	0.177
	V_{72Gy} (%)	1.8±1.2	2.7±1.3	<0.001
	V_{50Gy} (%)	31.4±9.1	31.4±9.2	0.735
Sphincter	Mean dose (Gy)	19.6±9.8	20.6±9.5	0.005
Bladder	Mean dose (Gy)	35.1±8.9	37.1±9.5	<0.001
	V_{72Gy} (%)	2.8±1.6	4.6±2.4	<0.001
Body	Mean dose (Gy)	6.4±1.1	6.7±1.1	<0.001

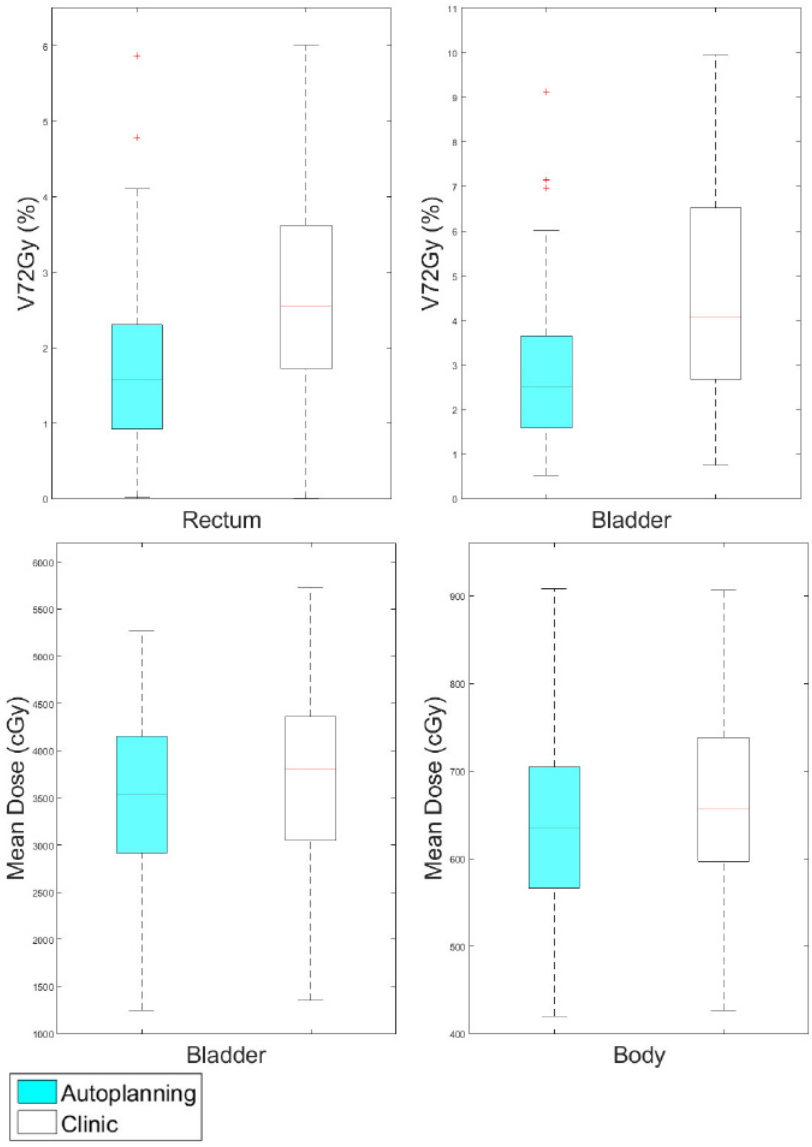

Figure 2.3: Graphical representation of the most relevant dosimetric results. Each figure represents a comparison between both the automatically generated plan and the manual plan.

Clinical pilot

Out of the 21 automatically generated treatment plans, 20 met all clinical dose constraints. For 12 cases an additional manual plan was created. In 17 cases the

radiation oncologist and clinical physicist selected the automatically generated plan for treatment. In the 4 cases where the manual plan was preferred, there were only small differences between the automatically and manually generated plans.

Planning-time comparison

The average time required to manually create a treatment plan is 2hours. With automated treatment planning the required operator time for plan generation has reduced to 5min, as the dosimetrist is only required to start the automated planning process and evaluate the resulting plan. The average time for automated plan generation is 90.1±19.2min. These measurements have been performed on our clinical workstations. Comparable measurements on more dated hardware has shown that the hardware capacity has significant influence on the speed of our automated treatment planning system. The calculation time for both the phase 1 and the phase 2 optimization loops scale linearly with the number of loops that are required. Moreover, the complexity of the patient anatomy and the amount of weight put on the cost functions will also influence the calculation time.

Discussion

In the present study we showed that automatically generating radiotherapy treatment plans for prostate cancer is feasible. Almost all automatically generated plans meet the clinical dose constraints and are therefore suitable for treatment. Because of the systematic approach the resulting plans show a lower variance and a higher plan consistency can be achieved, eliminating the inter- and intra-dosimetrist variability. This means that the automatically generated plans are more consistent than manually generated plans. The systematic approach used during automated treatment planning and optimization eliminates the variability as a result of differences in knowledge and experience of dosimetrists. The large reduction in manual interaction also greatly increases efficiency.

The plans that do not meet clinical dose constraints are close to a clinically acceptable plan, which will make them useable for warm start optimization, in which a dosimetrist can make adjustments to the plan using the current state as starting point. Making use of warm start optimization planning techniques will also be more time efficient compared to starting from scratch.

As in any treatment planning process there is trade-off between target coverage and dose to the OARs. There is however also a trade-off between the dose in one

organ at risk, with respect to the other. In prostate planning specifically, a lower dose to the rectum can be achieved by allowing more dose to the bladder and vice-versa. In current practice this is a choice which is often made implicitly by dosimetrists. For automated planning however, it is very important to make these choices beforehand, as well as getting a complete set of requirements which a final plan must meet, including soft constraints. To reach these requirements patient specific optimization is performed via the phase 1 and 2 iterations. The better the requirements are formulated, the more satisfactory the resulting treatment plans will be. Criteria must be set explicitly and may not be dependent of radiation oncologist's preference.

This study is focused on prostate cancer and shows that this method of automated treatment planning and optimization is suitable for clinical practice. While keeping in mind that prostate is a relatively simple tumour site in terms of anatomy, there is a potential of expanding this technique to other tumour sites. Non-cylindrical tumour sites, such as the breasts, or tumour sites with a large number of organs at risk, such as head-and-neck, will likely be a more complex challenge. Head and neck [16, 18, 19], breast [20, 21], prostate [17] and other tumour sites [64–66] have been previously investigated using a large variety of automated treatment planning techniques. Expanding automated treatment planning towards tumour sites with a large patient population will benefit efficiency and might as well increase plan quality and consistency. Exploring automated treatment planning for bone metastases or the bladder has already shown promising results.

Our experiments showed that often phase 1 passes on the first iteration. Increasing the amount of iterations in phase two to more than 15 did not result in any significant improvement in plan quality, but does increase the runtime. This is however expected to be site specific. The small step size and systematic approach used during optimization means that a lot of different plan options are explored. While running through the phase two optimization loop, the initial phase 2 plan is saved and is compared against every new plan resulting from following iterations. If the new plan is better, it will be saved and used as the current best plan. This way the best plan will be kept, regardless of the amount of iterations that are used.

In addition to being an asset for clinical use, increasing the efficiency and plan quality, automated treatment planning can also be of great use for research purposes. Planning studies comparing different beam setup, delivery methods such as volumetric modulated arc therapy (VMAT) or other parameters can be performed on large study sets, while not being extremely labour-intensive. By using

automatic plan generation more reliable comparisons can be made.

Considering the delivery efficiency of VMAT compared with that of IMRT, VMAT may be the preferred delivery technique for treating prostate cancer [67]. This study was performed based on IMRT plan delivery to make a fair comparison with the clinical workflow. Our automated planning and optimization workflow is however also capable of automatically generating VMAT plans and initial plans look promising.

For novel techniques such as the MR-Linac, which can track the patient's anatomy during radiation, real-time automated plan adaptation is necessary to take full advantage of its capabilities. The automated planning and optimization workflow presented in this study can generate new plans on demand, however our results show that it currently takes too long to use for full online replanning where ideally new plans should be generated within minutes. It can however, having diagnostic quality patient anatomy data available daily, be used for inter-fractional plan adaptation which can lead to a significant reduction in dose to the organs at risk [68]. Online adaptation methods are commercially available which are feasible for routine clinical practice [34]. Future plans include expansion of our current automated planning and optimization workflow with online adaptation to be able to perform this automatically.

Conclusion

An automated radiotherapy treatment planning and optimization workflow was developed to create patient specifically optimized treatment plans for prostate cancer which are suitable for clinical treatment. Treatment plans are more consistent, are associated with a lower dose to the OAR for most parameters and a large gain in time efficiency has been achieved. Automated treatment plan generation has now been adopted as the current standard workflow in our clinic to generate treatment plans for prostate cancer. Future work will include expanding our automated treatment planning to other tumour sites and develop other automated radiotherapy workflows, as well as reducing the time for automated plan generation.

Chapter 2

Chapter 3

Adaptive radiotherapy: the Elekta Unity MR-linac concept

The following chapter is based on:

Dennis Winkel, Gijsbert H. Bol, Petra S. Kroon, Bram van Asselen, Sara S. Hackett, Anita M. Werensteijn-Honingh, Martijn P.W. Intven, Wietse S.C. Eppinga, Rob H.N. Tijssen, Linda G.W. Kerkmeijer, Hans C.J. de Boer, Stella Mook, Gert J. Meijer, Jochem Hes, Mirjam Willemsen-Bosman, Eline N. de Groot-van Breugel, Ina M. Jürgenliemk-Schulz, Bas W. Raaymakers

Clinical and Translational Radiation Oncology (2019) Vol. 18, p.54-59

Abstract

Background and purpose
The promise of the MR-linac is that one can visualize all anatomical changes during the course of radiotherapy and hence adapt the treatment plan in order to always have the optimal treatment. Yet, there is a trade-off to be made between the time spent for adapting the treatment plan against the dosimetric gain. In this work, the various daily plan adaptation methods will be presented and applied on a variety of tumour sites. The aim is to provide an insight in the behavior of the state-of-the-art 1.5T MRI guided on-line adaptive radiotherapy methods.

Materials and methods
To explore the different available plan adaptation workflows and methods, we have simulated online plan adaptation for five cases with varying levels of inter-fraction motion, regions of interest and target sizes: prostate, rectum, esophagus and lymph node oligometastases (single and multiple target). The plans were evaluated based on the clinical dose constraints and the optimization time was measured.

Results
The time needed for plan adaptation ranged between 17 and 485 seconds. More advanced plan adaptation methods generally resulted in more plans that met the clinical dose criteria. Violations were often caused by insufficient PTV coverage or, for the multiple lymph node case, a too high dose to OAR in the vicinity of the PTV. With full online replanning it was possible to create plans that met all clinical dose constraints for all cases.

Conclusions
Daily full online replanning is the most robust adaptive planning method for Unity. It is feasible for specific sites in clinically acceptable times. Faster methods are available, but before applying these, the specific use cases should be explored dosimetrically.

Introduction

In the UMC Utrecht, together with Elekta AB. (Stockholm, Sweden) and Philips (Best, The Netherlands) a hybrid 1.5T MRI linac (MR-linac) has been developed, built and clinically introduced [62, 36, 63]. This system has evolved to the Elekta Unity system and has been clinically introduced with the treatment of oligometastatic lymph nodes in 2018 [69].

The MR-linac design is a linear accelerator with integrated 1.5T MRI functionality, the proof of concept of this system is presented in Raaymakers et al. (2009) [63]. The goal of such integration is to enable soft-tissue contrast MR imaging directly from the treatment table to visualize all anatomical changes during the course of radiotherapy. MRI can be used to capture both inter-fraction motion but also intra-fraction motion [70]. These data can be applied in many ways as input for adaptive radiotherapy. Daily MRI can be used for soft-tissue based position verification or daily replanning, beam-on MRI can be used for time resolved dose accumulation [71] or real-time replanning [72].Finally, repeated anatomical and functional MRI can be used for treatment response assessment [73, 74].

Using repeated MRI data for adaptive radiotherapy requires to interpret it, which typically means propagating the contours from the (pre-treatment) reference data to the latest timepoint by image registration. This image registration is often an ill-posed problem which requires tumour site specific quality assurance to warrant realistic results [75]. The first release of Unity provides different means for daily adaptive, MRI based radiotherapy, as the treatment is initialized daily, manual inspection is used to validate the contouring. Also, the concept of Unity is that every treatment fraction requires a treatment plan adaptation, so for every treatment fraction, a choice between the various adaptation modes has to be made. The treatment plan adaptation strategies will be detailed below in the methods section. They can be divided into two main categories, being 'adapt-to-position' (ATP) and 'adapt-to-shape' (ATS). For ATP no daily delineation is needed nor possible, only the (isocenter) position is updated in the pre-treatment CT, while for ATS the daily MRI can be re-contoured to be used for adapting the treatment plan.

The promise of the MR-linac is that one can visualize all anatomical changes during the course of radiotherapy and hence adapt the treatment plan in order to always have the optimal treatment. This should lead to better target conformality and lower normal tissue involvement. Yet, there is a trade-off to be made between the time spent for adapting the treatment plan against the dosimetric gain. In this work, the various daily plan adaptation methods will be presented and applied on a variety of tumour sites. Both the dosimetric consequences as well as the

time such adaptation takes will be reported. The aim is to provide an insight in the current behavior of the state-of-the-art 1.5T MRI guided on-line adaptive radiotherapy methods.

Methods

Pre-treatment preparation

Prior to treatment on the 1.5T MR-linac a pre-treatment CT and MRI were acquired. A special table overlay was used for CT scan acquisition, to enable reproducible positioning of the RF coil and approximative patient set-up using specific couch index points. The target and organs at risk were contoured by a radiation oncologist on the pre-treatment imaging data. A pre-treatment plan is then generated using the Monaco 5.4 (Elekta AB, Stockholm, Sweden) treatment planning system (TPS).

Adaptive treatment planning

Each treatment fraction starts with the acquisition of an online MRI. The pre-treatment CT, contours and plan, together with the online MRI are used as input to adapt the plan for that specific session. Performing plan adaptation on the Unity system can be performed through two different workflows using the Monaco TPS: adapt to position (ATP) and adapt to shape (ATS) (Figure 3.1).

The ATP workflow allows for plan adaptation based on the online patient position. The pre-treatment CT is matched with the online MRI through rigid registration. Based on this rigid registration, the isocenter position in the reference data is updated. The pre-treatment plan is then recalculated or reoptimized to reproduce or improve the target coverage from the pre-treatment plan through one of the available plan adaptation methods. Recalculating or reoptimizing the plan is performed on the pre-treatment CT and contours. This implies, no contours need (and can) be edited, as the original contours will be used for the adapted plan.

The second workflow, adapt to shape (ATS), allows for plan adaptation based on the new patient anatomy and the plan is optimized on the daily MRI and adapted contours. Again, the first step is that the pre-treatment CT and online planning MRI are registered. The pre-treatment contours are then automatically propagated by deformable registration onto the online planning MRI. If deemed necessary, contours are edited by a radiation oncologist. Electron densities (ED)

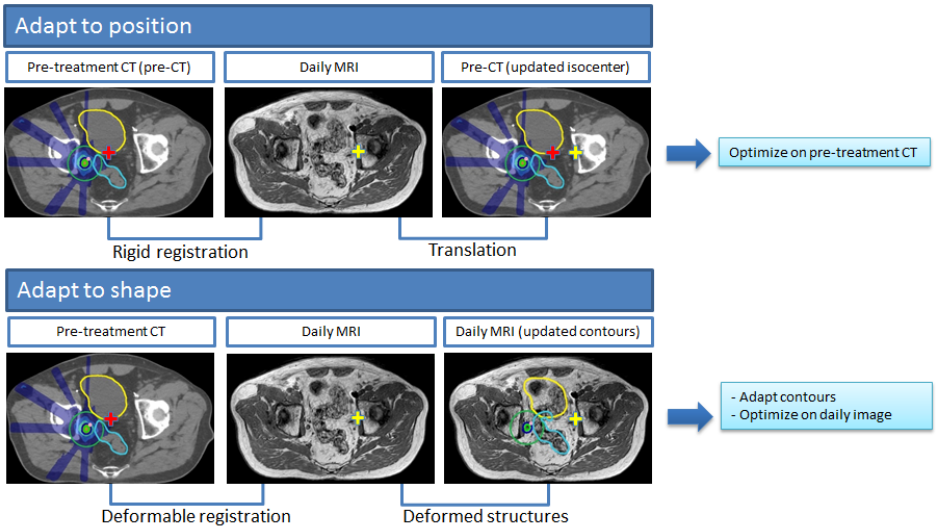

Figure 3.1: Schematic overview of the differences between the MR-linac Unity "adapt to shape" method in which online plan adaptation is performed on the new patient anatomy and optimized on the daily MRI and adapted contours, and the "adapt to position" method in which online plan adaptation is performed based on the new patient position and optimized on the pre-treatment CT and contours. Using the "adapt to position" method, rigid registration can be performed on the entire image sets, or using a clipbox around a region of interest.

were assigned per structure based on the average electron density value of the corresponding contour on the pre-treatment CT. This last step is important, because the plan is then recalculated or reoptimized on the online planning MRI and adjusted contours. Optimization in the ATS workflow is performed based on the pre-treatment planning objectives. Similar to ATP, the ATS workflow offers multiple options for plan recalculation or reoptimization.

Calculation and optimization methods

Overall, online MR-guided adaptive treatment planning on the 1.5T MR-linac allows for six different plan adaptation methods:

A Original Segments

B Adapt Segments

C Optimize Weights from segments

D Optimize Weights from fluence

E Optimize Weights and Shapes from segments

F Optimize Weights and Shapes from fluence

The Original Segments (A) method makes use of the segments and monitor units (MUs) from the pre-treatment plan. Herewith, the original plan is calculated on the pre-treatment CT (ATP) or daily MRI (ATS). The Adapt Segments (B) method shifts the segments from the pre-treatment plan relative to the isocenter, based on the registration between the pre-treatment and online images, using Segment Aperture Morphing (SAM) [10]. Using the resulting segments and the original segment weights, the dose is then recalculated. Both Optimize Weights (C,D) methods are based on optimizing the weights of the segments for the new patient position or daily anatomy by adjusting the amount of MUs. Method C optimizes the weights, using the set of segments from the pre-treatment plan after SAM. With method D the segments from the pre-treatment plan are discarded. The fluence is first reoptimized and a new set of segments is created. The new set of segments is then further optimized using segment weight optimization. The same distinction applies for both Weights and Shapes (E,F) methods. Either the pre-treatment segments are used (after SAM) for weight and shape optimization (method E), or the pre-treatment segments are discarded a dose fluence reoptimization is performed. The adjusted or new set of segments is then reoptimized for the new patient position or daily anatomy situation using both segment weight optimization. This method optimizes the amount of MUs per segment and further optimizes the segment shapes.

In general this means that for methods A, B, C and E, the segments from the pre-treatment plan are used for input (Figure 3.2). For method D and F, a new set of segments is created based on the reoptimized fluence. Method F, in which first the fluence is reoptimized and segmented and after which segment weight and shape optimization is performed, is equal to full online replanning. The ATP workflow does not offer the option to start with a fluence optimization. This implies that the ATP workflow only offers methods A, B, C and E. Again, note that for ATP, the plan adaptation is done on the pre-treatment CT, i.e. for E the plan on the original CT with the original contours is reoptimized solely for the updated isocenter position.

Plan exploration

To explore the different available plan adaptation workflows and methods, we have simulated online plan adaptation using the clinical system for five cases

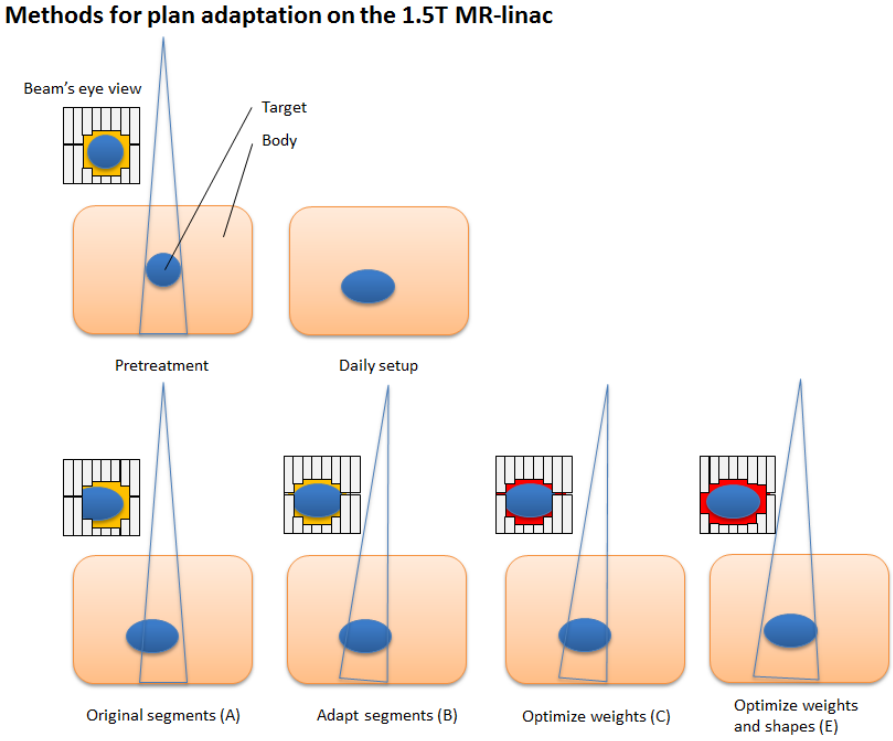

Figure 3.2: Schematic overview of the segment changes for the different plan recalculation and reoptimization methods available in the treatment planning software for the 1.5T MR-linac. A different background color (e.g. red or yellow) in the Beam's eye view (BEV) indicates a different segment weighting. When performing plan adaptation methods using optimize weights (method D) or optimize weights and shapes (method F) starting with full fluence optimization, the original segments are discarded and new initial plan segmentation is performed.

with varying levels of inter-fraction motion, regions of interest and target sizes: prostate, rectum, esophagus and lymph node (LN) oligometastases (single and multiple target). A pre-treatment CT and clinical plan were used to adapt the plan to the daily anatomy, as visible on MR-imaging. The datasets were registered to each other through rigid registration using a clipbox around the PTV. For the ATP workflow the optimization method to reproduce goal dose was used. The resulting plans were recalculated on the daily anatomy as visible on the online planning MRI. For the ATS workflow, the patient contours were manually corrected by a radiation oncologist. The plans were evaluated based on the clinical dose constraints and the optimization time was measured.

Results

The time needed for reoptimization using the available methods in the ATP workflow ranged between the 18 and 376 seconds (Table 3.1). Generally, a more complex patient anatomy led to longer reoptimization times. Method A and B did not result in plans that met the clinical dose constraints, see Table 3.1. With method C, only for the single LN case the adapted plan met all dose criteria. For the rectum case, the criteria were met when evaluating on the pre-treatment contours, but after recalculating the dose on the daily anatomy, violations were observed. For method E, the rectum and esophagus plans also met all dose criteria when evaluating on the pre-treatment contours, but showed violations after recalculation on the daily MR anatomy. The single LN plan met all dose criteria.

Table 3.1: Optimization time required for online plan optimization for the 1.5T MR-linac. A red background indicates one or more dose constraints were violated. Orange depicts all criteria were met on the pre-treatment data, but not when evaluating on the daily anatomy. Green depicts all criteria were met. Method A – F describe: A the original segments, B adapt segments, C optimize weights from segments, D optimize weights from fluence, E optimize weights and shapes from segments and F optimize weights and shapes from fluence, respectively.

	Adapt to position (ATP)				Adapt to shape (ATS)					
Method	**A**	**B**	**C**	**E**	**A**	**B**	**C**	**D**	**E**	**F**
	Time (s)	Time (s)	Time (s)	Time (s)	Time (s)	Time (s)	Time (s)	Time (s)	Time (s)	Time (s)
Prostate	23	23	35	117	21	21	37	50	217	213
Rectum	48	36	46	94	36	36	46	118	304	470
Esophagus	26	25	41	190	23	23	35	64	117	235
LN single	18	17	44	125	17	26	36	57	227	229
LN multiple	37	37	70	376	37	39	81	97	481	485

With the ATS workflow, reoptimization time was longer than for ATP and ranged between 17 and 485 seconds (Figure 3.3). Method A did not result in any plans that met the clinical dose criteria. Using method B, C and D, it was possible to create plans that met all clinical dose criteria for the single LN case, but not for prostate, rectum, esophagus and the multiple LN case. Using method E it was possible to create plans that met all criteria for rectum, esophagus and the single LN case. With method F, which is essentially full online replanning, it was possible to create plans that met all clinical dose constraints for all cases used in this study. Violations for other methods were often caused by insufficient PTV coverage or, for the multiple lymph node case, a too high dose to OAR in the vicinity of the PTV. In Figure 3.4 the dose distributions for the various adaptive modi are shown for the prostate case. It can be seen that, looking at the 80% dose-level, each results in different dose distributions.

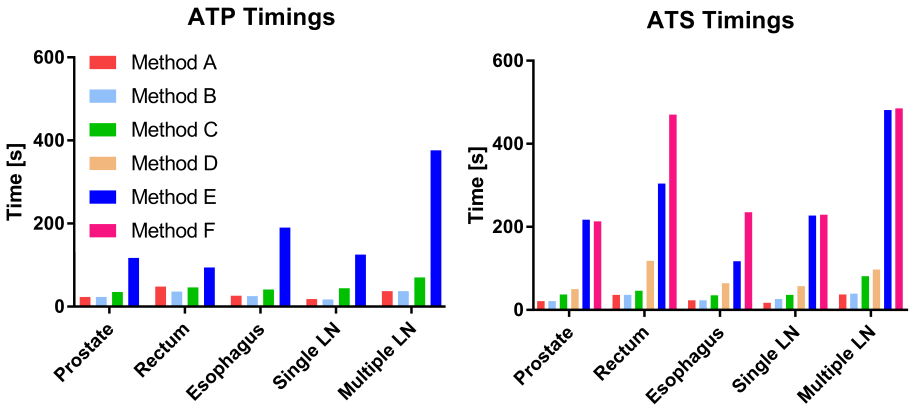

Figure 3.3: Recalculation or optimization time required for plan adaptation for the methods available in the adapt to position (ATP) and adapt to shape (ATS) workflows. Method A – F describe: A the original segments, B adapt segments, C optimize weights from segments, D optimize weights from fluence, E optimize weights and shapes from segments and F optimize weights and shapes from fluence, respectively.

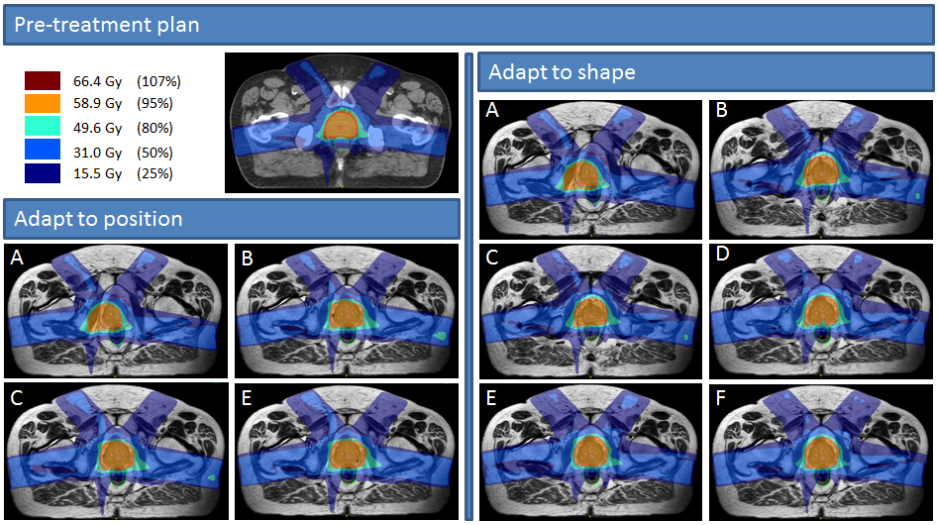

Figure 3.4: Prostate case with the resulting dose distributions for the adapt to position (ATP) and adapt to shape (ATS) workflows. Method A – F describe: A the original segments, B adapt segments, C optimize weights from segments, D optimize weights from fluence, E optimize weights and shapes from segments and F optimize weights and shapes from fluence, respectively.

Discussion

The ATP based plan adaptations are faster than ATS based methods. However, the ATP methods lack target coverage, even for small anatomical variations. For

this study we have used the current clinical CBCT-linac PTV margins. Using smaller margins, target coverage after ATP based plan adaptation is expected to be further reduced. Moreover, the ATP results are standardly presented by calculations on the pre-treatment reference data and this might not be representative for the actual anatomy as can be seen for the rectum and esophagus examples by the orange boxes in (Table 3.1); the ATP may report agreement with treatment planning constraints but when recalculating on the daily MRI, violations are seen.

The only method that passed all treatment planning constraints on the daily MRI was method F in the ATS workflow. This result was expected as this equals daily full replanning. One conclusion is that if the time for this method is considered acceptable, ATS with method F is the most robust adaptation. Yet, this approach requires on-line contour review or online contour editing which further adds to the overall required time. When only small anatomical changes are expected or relatively large intra-fraction motion could be induced by the increased initialization time, ATP might be preferred. Given the dosimetric results for the examples in this work, and the difference in time spent on method C, i.e. segment weight optimization, relative to A and B, ATP plus method C seems the minimal adaptation mode to use.

The choice between method C and E for ATP, i.e. reoptimizing just segment weights or also reoptimizing the segment shapes, depends on the tolerance for errors. Errors induced by any method can be quantified by recalculation using the daily MRI. If the error is too large, an offline replanning could be considered in order to mitigate, or at least minimize, the overall treatment dose violation. This approach might be acceptable for hyper-fractionated treatments. For hypo-fractionated treatments the investment into full daily replanning is better justified.

Within the Unity workflow, it is also possible to combine ATS and ATP. For instance, the treatment is initialized using full replanning, i.e. ATS using method F, but prior to beam delivery, a second MRI is acquired and if the anatomy is changed during the preparation, ATP is used to quickly adapt to the (probably small) anatomical change. In UMC Utrecht, this is the approach for our prostate treatments on Unity: ATS using method F is potentially followed by ATP with segment weight optimization if the prostate has shifted. Again, offline dose reconstruction can be done to verify accuracy of this approach.

A small disadvantage of ATS is that its MRI based reoptimization is done using bulk densities. However, this does not significantly influence the dose calculation accuracy when adequate bulk assignments are made [76]. For several cases this

might have a larger effect in which case electron densities assignment should be considered more carefully. In particular structures with high densities or air cavities with the influence of the electron return effect [77, 78].

The examples in this work are quite heterogeneous to show the mechanisms of the various workflows and adaptation methods. Before introducing a new patient category with a specific fractionation scheme on the Unity, a careful evaluation of the various options has to be made to choose the appropriate trade-off. For oligometastatic lymph node treatments with 5x 7 Gy, this is done in Winkel et al. (2019) [79, 80].

Future work is on intra-fraction plan adaptation, where the ultimate goal is to get to real-time plan adaptation while accounting for the dose delivered so far. Kontaxis et al. [81] presented a loop that enables such continuous reoptimization during beam delivery. Basically the approach mentioned above, where dosimetric errors are revealed by offline recalculation are a first, very simple, yet feasible, implementation of such loop. A next step could be to also allow, for instance, intra-fraction ATP.

The computational time associated with the different methods will decrease with increasing computer power and smarter algorithms. In a research setting, full replanning can already be done in approximately 1 minute [82]. Solid contour propagation and reliable quality assurance for this are key to speed up full replanning approaches [83].

Conclusion

Daily full online replanning is the most robust adaptive planning method for Unity. It is for specific sites feasible in clinically acceptable times. Faster methods are available, but before applying these, the specific use case should be explored dosimetrically.

Chapter 4

Simulated dosimetric impact of online replanning for stereotactic body radiation therapy of lymph node oligometastases on the 1.5T MR-linac

The following chapter is based on:

Dennis Winkel, Petra S. Kroon, Anita M. Werensteijn-Honingh, Gijsbert H. Bol, Bas W. Raaymakers, Ina M. Jürgenliemk-Schulz

Acta Oncologica (2018) Vol. 57, p.1705-1712

Abstract

Purpose
Online 1.5T MR imaging on the MR-linac gives better target visualization compared to CBCT and facilitates online adaptive treatment strategies including daily replanning. In this simulation study the dosimetric impact of online replanning was investigated for SBRT of lymph node oligometastases as a method for correcting for inter-fraction anatomical changes.

Methods
Pre-treatment plans were created for 17 pelvic and para-aortic lymph nodes, with 3mm and 8mm PTV margins reflecting our clinical practice for lymph nodes with good and poor visibility on CBCT. The dose-volume parameters of the pre-treatment plans were evaluated on daily anatomy as visible on the repeated MRIs and compared to online replanning.

Results
With online MRI-based replanning significant dosimetric improvements are obtained for the rectum, bladder, bowel and sigmoid without compromising the target dose. The amount of unintended violations of the dose constraints for target and surrounding organs could be reduced by 75% for 8mm and 66% for 3mm PTV margins.

Conclusions
The use of online replanning based on the actual anatomy as seen on repeated MRI compared to online position correction for lymph node oligometastases SBRT gives beneficial dosimetric outcomes and reduces the amount of unplanned violations of dose constraints.

Introduction

Image-guided radiation therapy (IGRT) has become increasingly important in modern radiotherapy to reduce the effect of treatment variations, such as setup errors and geometric variations of the target volume and organs at risk (OAR). Currently most modern radiotherapy treatment systems are equipped with cone-beam computed tomography (CBCT) to visualize the tumour [84]. CBCT has greatly contributed to precision radiotherapy for sites in which the tumour is clearly visible on CBCT, however it yields relatively poor soft tissue contrast. The lack of soft tissue contrast can make it difficult to accurately identify the target and surrounding OARs for soft tissue targets; therefore bony anatomy or artificial markers are frequently used as a surrogate for position verification [33, 31,32]. These procedures still result in quite large planning target volume (PTV) margins [46] or are invasive with additional burden for the patient.

Magnetic resonance imaging (MRI) guided radiotherapy treatment systems are commercially available and used in clinical practice and allow improving plan quality through online adaption [35, 34, 85]. With the 1.5T MR-linac [61], diagnostic quality images are available of the actual patient anatomy during treatment and MR-guided online adaptive workflows can be used [36]. Based on our institutional clinical experience, lymph node oligometastases are often small with mean gross tumour volumes (GTV) of < 3 cc, (as defined by expert radiation oncologists) and are poorly visible on CBCT in about 30% of all cases. The superior soft tissue contrast of online MR-images gives a better visibility of the target and surrounding OAR when compared to CBCT [37] which will potentially help to reduce the PTV margins.

For treatment of lymph node oligometastases, stereotactic body radiation therapy (SBRT) [86,40,87] is an often applied technique in which a relatively high amount of dose is delivered in few fractions with a very steep dose gradient [43]. In current clinical practice of SBRT for these targets inter-fraction motion is accounted for by online couch translation and (sometimes) small table rotations. Online couch translations account for rigid motion of the target, but do not deal with non-rigid changes of the PTV such as changes in size or shape. Differences between the planned and delivered dose after position corrections can also occur because of changes in the physical path and changes in tissue attenuation relative to the original plan [88]. When treating these tumours on the MR-linac, one can account for geometric variations of the target and OARs, as well as changes in the physical path and tissue attenuation. To accomplish this for external beam radiotherapy, online replanning is the optimal approach to fully incorporate all available anatomical data provided on the MR-linac and to deliver a highly conformal dose

to the tumour, while optimally sparing the OARs.

A recent study on SBRT for the treatment of oligometastatic disease of the abdomen and central thorax has shown that a combination of high dose, few fractions and a steep dose gradient improves with adaptive treatment on MR guided radiotherapy systems in terms of precise and conformal dose delivery and preventing potentially toxic violations of dose constraints [89]. Similar benefits could potentially be achieved with full online replanning of lymph node oligometastases for the pelvic and para-aortic region. By performing full online replanning a new plan is created on the daily anatomy while the patient is on the table, without making use of a pretreatment plan. Further dosimetric benefits could potentially be gained by a reduction of the PTV, because of better target visualization when treating on an MR-linac for lymph node oligometastases with poor visibility on CBCT. MRI guidance is already commonly applied in brachytherapy to minimize dose differences, which can occur between planning and irradiations [90].

This study is a R-IDEAL [91] stage 0 study in preparation of a clinical workflow for the treatment of lymph node oligometastases on the 1.5T MR-linac.R-IDEAL is a framework for systematic clinical evaluation of technical innovations in radiation oncology such as the MR-linac. Stage 0 covers all preparatory work needed before the innovation is ready for clinical use. In this study we investigate whether online replanning for SBRT of lymph node oligometastases on the 1.5T MR-linac yields beneficial dosimetric values compared to online position correction as performed on CBCT-linacs in current clinical practice.

Methods

Patient data characteristics

For this simulation study 17 pelvic and para-aortic pathological lymph nodes were included from 5 female patients with locally advanced cervical cancer. The patients had 2, 2, 4, 8 and 1 pathologic lymph nodes, respectively. The lymph node locations are spread relative to each other and are representative for lymph node oligometastases as treated in our clinic. All patients gave written informed consent for the use of their scans for research purposes. All patients had undergone pre-treatment and repeated MR imaging, suitable for radiotherapy, on a 1.5T Philips Ingenia (Best, The Netherlands) before and during the first three weeks of curative chemo-radiotherapy treatment. During imaging acquisition the rectum was required to be as empty as possible. In case of a significant presence of gas and faeces with a rectum diameter $>$ 4cm the patient was asked to empty the

rectum, or the rectum was deflated using a rectal cannula. For each patient, pre-treatment data and one inter-fraction dataset obtained during the course of EBRT were used with MRI-based delineations of lymph node GTV(s) and surrounding OAR (bladder, rectum, bowel bag, sigmoid, cauda equina and femoral bones). The mean GTV (in this case also demarcating the clinical target volume) of the lymph nodes was 2.5 ± 2.8cc (range, 0.4 – 15.8cc), based on expert delineations. There were no exclusion criteria.

Plan generation

For each lymph node five plans were generated to simulate the different treatment approaches: 1) pre-treatment plan with a 3 mm PTV margin and 2) calculated on daily anatomy after position correction, 3) pre-treatment plan with a 8 mm PTV margin and 4) calculated on daily anatomy after position correction, and 5) complete new plan generated on the daily anatomy (full online replanning). By means of these five plans the dosimetric situation of the current CBCT-linac treatment can be estimated (comparisons plan 1 and 2; or plan 3 and 4). In addition, the potential dosimetric benefit of a MR-linac treatment can be evaluated using plan 2 and 5, and using plan 4 and 5.

All plans were generated with a prescribed dose of 5x 7Gy to 95% of the PTV using the Monaco treatment planning software (TPS) research version 5.19.03d by Elekta AB (Stockholm, Sweden). To do a clean comparison of our technique we have eliminated differences in machine characteristics by creating all plans with the 7MV FFF beam model of the Elekta MR-linac and the 1.5T magnetic field in superior-inferior patient direction which is present when treating patients on the MR-linac. The dose constraints (Table 4.1) used for the OAR are considered hard dose constraints. OAR dose was attempted to be as low as possible, while maintaining adequate target coverage. Plan quality was evaluated by a multi-disciplinary SBRT oligo lymph node clinical team consisting of a radiation therapist, physicist and physician. Seven non-uniform beam orientations were used for these plans and were selected individually for each PTV to optimally account for patient anatomy and the location of the PTV. Unfavourable beam angles due to couch characteristics or the location of the cryostat were avoided. The statistical uncertainty for the Monte Carlo dose calculations was 3% per control point and the calculation grid size was 3mm. The maximum amount of segments per plan was 45 with a minimum area of 1.5cm^2 and width of 0.5cm.

Table 4.1: Clinically dose criteria for SBRT lymph node oligometastases treatment plans used for plan evaluation.

Structure	Constraint
PTV	$V_{35Gy} > 95\%$
	$D_{max} < 135\%$
Bladder[1,2]	$V_{38Gy} < 0.5$ cc
	$V_{18.3Gy} < 15$ cc
Bowel[1]	$V_{35Gy} < 0.5$ cc
	$V_{25Gy} < 10$ cc
Rectum[3]	$D_{max} < 40$ Gy
	$V_{35Gy} < 1$ cc
Sigmoid[3]	$D_{max} < 40$ Gy
	$V_{35Gy} < 1$ cc

1. UK SABR consortium guidelines 2016
2. Grim et al, 2011 [92]
3. In-house clinical constraints

Generation of pre-treatment plans on the planning CT

Two pre-treatment plans were created for each lymph node, with a 3mm as well as with a 8mm PTV margin and a prescription dose of 5x 7Gy to 95% of the PTV. The center of the PTV was set as plan isocenter. Using these margins we simulate cases of both good and poor visibility. In our current clinical protocol a CBCT simulation is performed in the pre-treatment preparation phase. A physician determines whether the lymph node oligometastases is well visible or not. A PTV margin of 8 mm is used for poorly visible lymph nodes (Figure 4.1) and 3 mm for visible lymph nodes. Using a vacuum cushion for immobilization, these PTV margins are considered to be sufficient to handle patient setup, intra-fraction motion and machine related uncertainties [93, 94, 55, 95].

Generation of plans by recalculating on the daily anatomy

As a simulation of current clinical practice, we calculated daily dose-volume histogram (DVH) parameters twice for each lymph node by calculating the dose of the pre-treatment plans with 3mm and 8mm PTV margins on the daily anatomy. To simulate the daily anatomy, a MRI dataset (Philips Ingenia, 1.5T, mDIXON 3D FFE T1W, flip angle 10°, TE1/TE2 = 1.6/3.9ms, TR = 5.7ms, reconstructed voxel 1.05·1.05·2.5mm^3, FOV 552·552·300mm^3) obtained at least one week into treatment was used. The target and the OARs were manually contoured. Electron density information was taken into account by matching and deforming the initial planning CT to the MRI data (Figure 4.2). In our clinic CBCT-based

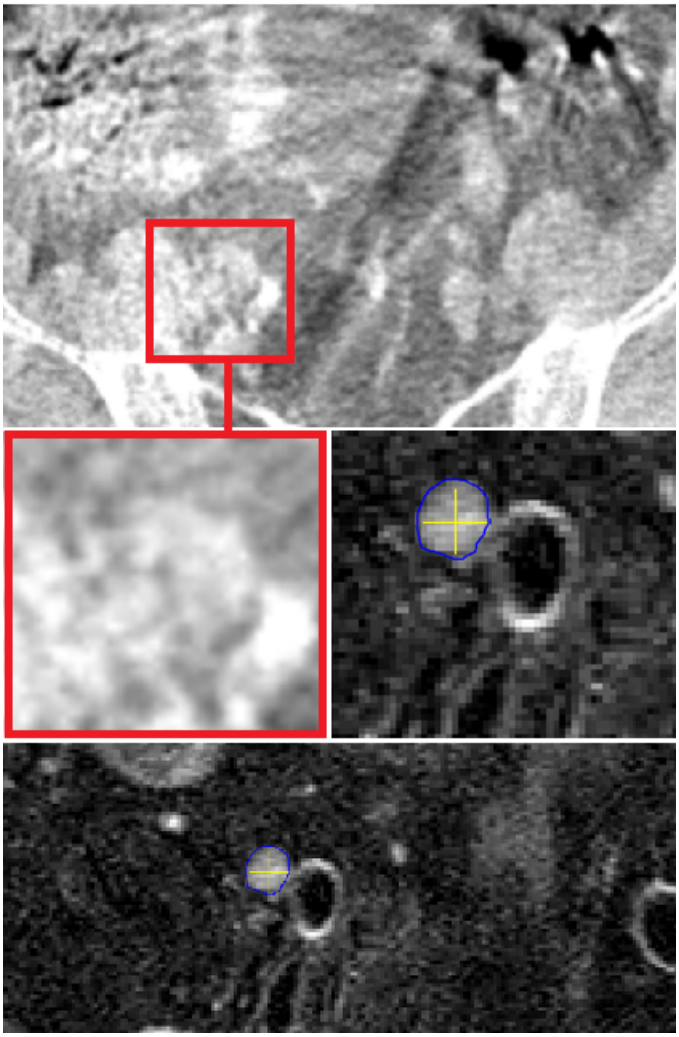

Figure 4.1: Transversal CBCT image (top and left) and a transversal T2-weighted mDIXON water image (bottom and right) of the same patient. The lymph node in the left iliac region is poorly visible on the CBCT and would therefore be treated with a 8mm PTV margin to sufficiently incorporate uncertainties, especially position verification.

online correction is performed by matching using a 0.5cm mask around the GTV or a clipbox with nearby structures for lymph nodes with good or poor visibility respectively. To simulate the online correction protocol we assumed that the reference point of this correction is equal to the center of the PTV and placed the plan isocenter at the center of the PTV according to the daily anatomy.

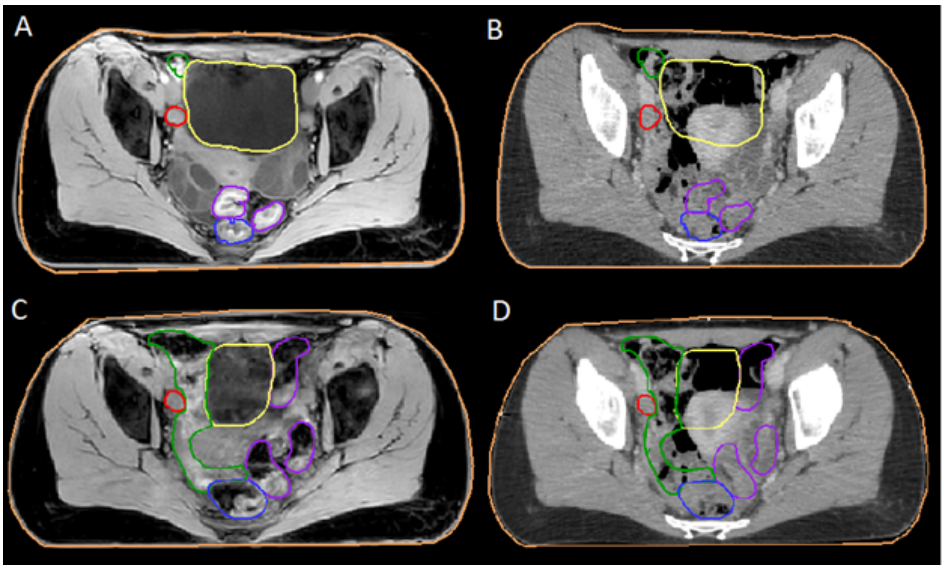

Figure 4.2: Pre-treatment T1-weighted mDIXON water MRI (A) and pre-treatment CT (B) data. MRI data obtained in-between fractions (C) and a deformed CT (D) based on the MRI data used to simulate daily patient anatomy. The target lymph node is visible in red. Large inter-fraction differences can be observed with regards to the location of large bowel (green contours), bladder (yellow contours), rectum (blue contours) and sigmoid (purple contours).

Generation of a new plan on the daily anatomy

To simulate replanning in a full-online workflow for the MR-linac, one new fully optimized treatment plans was created for each lymph node using daily target and OAR definitions based on the simulated daily patient anatomy. The used beam angles for online replanning were equal to those in the pre-treatment plan. For these plans a PTV margin of 3mm was applied, simulating the good visibility of lymph nodes on MRI. As the 1.5T MR-linac only allows for movement in superior-inferior direction, the isocenter is fixed in the center of the bore for the other directions. The isocenter position in the superior-inferior direction is set as close to center of the PTV as possible.

Evaluation

To estimate the dosimetric situation of the current CBCT-linac treatment and to evaluate the dosimetric impact of online replanning for the MR-linac all plans were evaluated using the target and OAR dose criteria. The plans with 8mm and 3mm PTV margins were both compared with online replanning using a 3mm PTV

margin, simulating treatment with good visibility of lymph nodes on the MR-linac. The DVH parameters for the PTV, rectum, bladder, bowel and sigmoid were compared between the initial plans simulated on the daily anatomy and the online plans. The PTV was evaluated using the PTV margin as was used during planning. The reference plans were evaluated using the original pre-treatment contours. The simulation plans using online translation or full-online replanning were evaluated using the contours from the simulated daily anatomy. Significance of these differences was determined using Wilcoxon matched-pairs signed rank tests. Results were considered significant with a p-value < 0.05.

Results

When a 3mm PTV margin was taken, it was possible to create pre-treatment plans that met clinical dose criteria for all 17 lymph nodes: all plans had adequate target coverage and did not violate OAR dose constraints. When the pre-treatment plans were evaluated after rigid table correction using daily anatomical contours from the repeated MRIs, 6 plans failed to meet all criteria. In 2 plans the V35Gy of the bowel was violated with 2.1 and 9.1cc. In one plan the V25Gy of the bowel was violated with 21.9cc. In 1 plan the V35Gy and Dmax (highest measured dose in a voxel) of the sigmoid were violated with 1.8cc and 44.7Gy respectively. PTV coverage was insufficient in 3 plans with a V100% in the range of 86.2-94.0% (should be $> 95\%$). GTV coverage was sufficient for all plans.

When a 8mm PTV margin was used, 12 of the 17 created pre-treatment plans met all dose criteria. When evaluating these plans on the anatomy as visible on the repeated MRIs this amount decreased to 8. Of these cases, 2 both violated dose constraints for the OARs and had insufficient PTV coverage with 89.7 and 94.8% of the prescribed dose instead of $> 95\%$ as intended. Two plans violated both the V_{35Gy} and V_{25Gy} of the bowel with 24.6 and 48.4cc for one plan and 7.9 and 16.9cc for the other plan. The V_{35Gy} of the bowel was violated with 0.9cc for one plan. For one plan the $V_{18.3Gy}$ of the bladder was violated with 17.5cc. Two plans violated both the V_{35Gy} and D_{max} of the sigmoid with 1.1cc and 43.0Gy for one plan and with 2.5cc and 43.8Gy for the other plan. The V_{35Gy} of the sigmoid was violated with 6.1cc for one plan. One plan did not have adequate PTV coverage with 89.9%. GTV coverage was sufficient for all plans. The dosimetric violations occurred in 4 out of 5 patients.

Full online replanning, simulating MR-linac treatment, resulted in a reduction of violations to the OARs. The number of instances of violation was reduced from 6 to 2 (66%) and 8 to 2 (75%) for lymph node oligometastases with a 3mm and 8mm margin, respectively. The two plans that did not meet requirements during

replanning violated the V_{35Gy} of the bowel with 0.5 and 1cc (Figure 4.3). In these cases the target position was closer to the bowel for the simulated daily anatomy compared to the situation at initial treatment planning, which caused large overlap between the rectum and PTV.

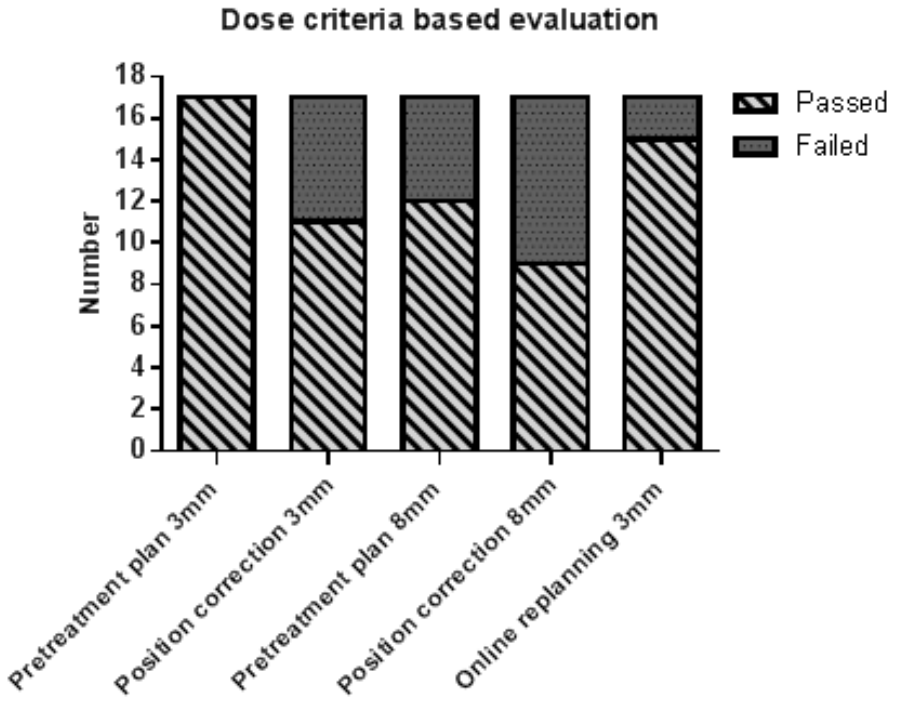

Figure 4.3: Number of plans (N=17) that passed or failed based on dose criteria for the initial plan, the initial plan calculated on the daily anatomy and full online replanning (simulating MR-linac treatment).

A comparison of DVH parameters between pre-treatment plans calculated on the simulated repeated MRI anatomy and online replanned plans shows that online replanning yields significant dosimetric benefits for OAR dose (Figure 4.4). For the pre-treatment plans made with a 3mm PTV margin, the mean dose was significantly reduced for the bladder, bowel, rectum and sigmoid (Table 4.2). The maximum dose and D_{2cc} of the bladder and the D_{2cc} of the rectum were also significantly reduced. For pre-treatment plans made with a 8mm PTV margin, online replanning shows additional dosimetric benefits apart from the significant reductions already present with the 3mm PTV margin (Table 4.3). The V_{25gy} for the bowel was significantly reduced. The maximum dose and D_{2cc} for the bowel

and sigmoid was also significantly lower.

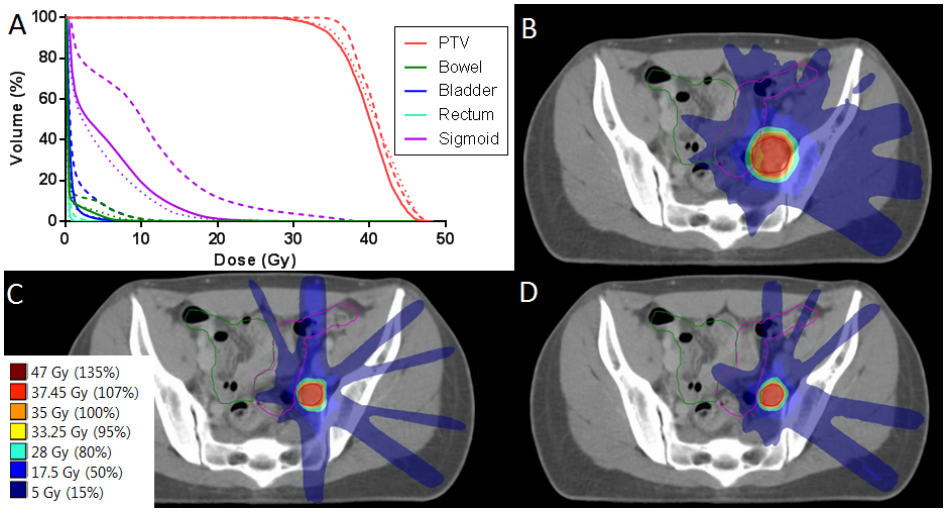

Figure 4.4: Sample DVH (A) and dose distributions of 8mm PTV (B/dashed line) and 3mm PTV (C/solid line) reference plans on the daily anatomy after position correction and full online replanning (D/dotted line). Anatomical contours are shown for PTV (red), large bowel (green) and sigmoid (purple).

Discussion

Inter-fraction motion of pelvic lymph nodes can occur with translations ranging between 7-30 mm based on pre-treatment CT imaging and CT imaging during treatment [96]. The current clinical protocol in which online correction is performed based on CBCT images is sufficient to correct for translations. It does not however account for changes in size and shape of the target and OARs, which can vary significantly over the course of treatment [97]. A correlation is found between volume changes of organs at risk and target shifts [98]. This can result in rotations of the targets which, when ellipse-shaped, can largely differentiate from the pre-treatment situation. In current clinical practice rotations are not often corrected for. In Figure 4.2 a substantial discrepancy can be seen between the state of the internal organs on the pre-treatment MRI and the pre-treatment CT. This example emphasizes the advantage of correcting for inter-fraction organ motion; also in other studies daily plan adaptation has been shown to improve dose volume parameters [99–103]. With the use of online replanning a completely new daily treatment plan can be created, which accounts for deformations of the PTV, as well as the actual OAR location.

Table 4.2: Dosimetric outcomes for lymph node oligometastases with a 3mm CTV-PTV margin.

Structure	Parameter	$\text{Plan}_{\text{PT3mm}}$	$\text{Plan}_{\text{PC3mm}}$	Plan_{MRL}	p-value
PTV	V35Gy (%)	98.0 [95.1 – 100]	96.6 [86.2 – 100]	97.8 [92.5 – 100]	0.82
Bladder	V38Gy (cc)	0.0 [0 – 0.1]	0.0 [0 – 0.1]	0	>0.99
	V18.3Gy (cc)	0.9 [0 – 5.8]	0.4 [0 – 5.1]	0.1 [0 – 0.9]	0.50
	Dmean (Gy)	1.2 [0.2- 3.4]	1.0 [0.2 – 3.6]	0.6 [0.1 – 2.7]	<0.01*
	Dmax (Gy)	13.1 [0.4 – 40.7]	10.5 [0.5 – 40.3]	9.0 [0.2 – 37.4]	<0.01*
	D2cc (Gy)	7.2 [0.5 – 24.5]	5.9 [0.4 – 23.6]	4.9 [0.1 – 22.0]	0.02*
Bowel	V35Gy (cc)	0.0 [0 – 0.1]	0.7 [0 – 9.1]	0.1 [0 – 1.0]	0.50
	V25Gy (cc)	0.2 [0 – 1.9]	1.7 [0 – 22.0]	0.6 [0 – 6.4]	0.13
	Dmean (Gy)	0.6 [0.2 – 19.3]	1.2 [0.1 – 5.0]	0.7 [0.1 – 1.6]	<0.01*
	Dmax (Gy)	22.9 [9.1 – 36.7]	19.3 [0.7 – 46.2]	18.0 [0.8 – 39.5]	0.35
	D2cc (Gy)	14.9 [5.7 – 24.9]	13.2 [0.4 – 41.7]	11.8 [0.3 – 37.3]	0.22
Rectum	V35Gy (cc)	0	0	0	-
	Dmean (Gy)	0.8 [0.2 – 2.2]	0.6 [0.1 – 1.6]	0.4 [0.1 – 2.0]	0.01*
	Dmax (Gy)	5.1 [0.4 – 14.4]	4.7 [0.2 – 16.8]	3.9 [0.3 – 10.3]	0.74
	D2cc (Gy)	3.7 [0.4 – 12.2]	3.2 [0.2 – 11.9]	2.0 [0.2 – 9.6]	0.02*
Sigmoid	V35Gy (cc)	0.0 [0 – 0.1]	0.1 [0 – 1.8]	0.0 [0 – 0.5]	0.13
	Dmean (Gy)	3.0 [0.4 – 10.2]	2.8 [0.6 – 5.5]	2.1 [0.5 – 5.3]	<0.01*
	Dmax (Gy)	13.1 [1.0 – 36.7]	21.0 [6.7 – 44.7]	19.2 [6.7 – 38.4]	0.05
	D2cc (Gy)	7.5 [0.7 – 16.6]	13.1 [4.8 – 34.4]	12.4 [3.7 – 32.2]	0.15

Dosimetric outcomes (mean and range) for the pre-treatment plans (PT) for lymph node oligometastases with a 3mm CTV-PTV margin, their respective simulations on daily anatomy after online position correction (PC) and replanning on the MR-linac (MRL). p-value obtained using Wilcoxon matched-pairs signed rank tests ($p < 0.05$ is significant and denoted with an asterix).

Online replanning reduces the amount of unplanned violations to the OARs. When moving from online position correction to online replanning, the number of instances of violation to the OARs can be significantly reduced, both for lymph nodes with good and poor visibility on CBCT. It can therefore be advocated to use online replanning to take non-rigid anatomical changes into account. The largest benefit is reached for lymph nodes that are poorly visible on CBCT. The superior soft tissue contrast on the MR-linac will allow for a considerable reduction of the PTV margin (i.e. reduction from 8 to 3mm in this particular situation), which importantly reduces the overlap between PTV and OARs.

A large variety of dose and fractionation schemes are currently being used for SBRT treatment of lymph node oligometastases varying between 5x 5Gy and 1x 24Gy [55]. A smaller PTV margin, as well as full-online replanning may allow for dose escalation and hypofractionation. Dose escalation is regarded to be desirable, in order to achieve improved and durable local control [104, 105]. On

Table 4.3: Dosimetric outcomes for lymph node oligometastases with a 8mm CTV-PTV margin.

Structure	Parameter	$\text{Plan}_{\text{PT8mm}}$	$\text{Plan}_{\text{PC8mm}}$	Plan_{MRL}	p-value
PTV	V35Gy (%)	98.2 [96.5 – 100]	97.4 [89.0 – 100]	97.8 [92.5 – 100]	0.67
Bladder	V38Gy (cc)	0	0.0 [0 – 0.4]	0	0.50
	V18.3Gy (cc)	3.69 [0 – 18.27]	2.2 [0 – 21.3]	0.1 [0 – 0.9]	0.13
	Dmean (Gy)	1.8 [0.2 – 6.4]	1.6 [0.2 – 6.9]	0.6 [0.1 – 2.7]	<0.01*
	Dmax (Gy)	14.8 [0.4 – 38.0]	13.3 [0.5 – 39.1]	9.0 [0.2 – 37.4]	<0.01*
	D2cc (Gy)	11.6 [0.3 – 35.5]	9.4 [0.4 – 36.0]	4.9 [0.1 – 22.0]	<0.01*
Bowel	V35Gy (cc)	0.4 [0 – 4.0]	2.0 [0 – 24.7]	0.1 [0 – 1.0]	0.13
	V25Gy (cc)	2.4 [0 – 19.4]	4.2 [0 – 48.4]	0.6 [0 – 6.4]	0.03*
	Dmean (Gy)	0.8 [0.3 – 3.0]	1.7 [0.1 – 7.1]	0.7 [0.1 – 1.6]	<0.01*
	Dmax (Gy)	29.8 [16.0 – 40.1]	23.1 [1.2 – 45.5]	18.0 [0.8 – 39.5]	<0.01*
	D2cc (Gy)	21.1 [11.8 – 36.8]	16.2 [0.6 – 41.5]	11.8 [0.3 – 37.3]	<0.01*
Rectum	V35Gy (cc)	0	0	0	-
	Dmean (Gy)	1.3 [0.2 – 4.2]	1.1 [0.1 – 4.5]	0.4 [0.1 – 2.0]	<0.01*
	Dmax (Gy)	6.4 [0.5 – 17.4]	5.6 [0.3 – 16.8]	3.9 [0.3 – 10.3]	0.03*
	D2cc (Gy)	4.5 [0.5 – 13.2]	3.7 [0.2 – 13.4]	2.0 [0.2 – 9.6]	<0.01*
Sigmoid	V35Gy (cc)	0.1 [0 – 0.9]	0.6 [0 – 6.1]	0.0 [0 – 0.5]	0.06
	Dmean (Gy)	4.7 [0.8 – 20.4]	4.4 [1.4 – 10.2]	2.1 [0.5 – 5.3]	<0.01*
	Dmax (Gy)	15.3 [3.7 – 40.3]	26.4 [12.2 – 43.8]	19.2 [6.7 – 38.4]	<0.01*
	D2cc (Gy)	10.9 [2.1 – 31.5]	17.9 [3.9 – 36.8]	12.4 [3.7 – 32.2]	<0.01*

Dosimetric outcomes (mean and range) for the pre-treatment plans (PT) for lymph node oligometastases with a 8mm CTV-PTV margin, their respective simulations on daily anatomy after online position correction (PC) and replanning on the MR-linac (MRL). p-value obtained using Wilcoxon matched-pairs signed rank tests ($p < 0.05$ is significant and denoted with an asterix).

the interfraction CBCTs the visibility of the target and OARs are not sufficient to perform these analyses. The improved target structure visibility with the MR-linac, combined with online replanning could also provide opportunities for hypofractionation, without the need for invasive marker placement procedures, compared with hypofractionated SBRT using the CyberKnife [106, 56]. Future clinical trials must show whether dose escalation and hypofractionation is possible and whether this results in clinically relevant endpoints. SBRT treatment of lymph node oligometastases on the MR-linac using online replanning therefore opens up possibilities for dose escalation, without increasing the risk on OAR dose constraint violations.

For the purpose of this study we have only simulated online replanning on daily anatomy for one fraction, for which it yields significantly better dosimetric values. This shows that online replanning for high dose single-fraction SBRT of oligo lymph nodes is required to achieve a lower dose to the OARs while maintaining

adequate target coverage. The exact benefit for treatment with multiple fractions is yet to be investigated for lymph node oligometastases. Dosimetric benefits are however expected during the whole course of treatment as the daily anatomy is optimally taken into account with daily online replanning or similar daily plan adaptation approaches [107, 108]. Based on these promising results, a clinical workflow for the 1.5T MR-linac is being developed for treatment of lymph node oligometastases in the near future.

For our simulations we have considered each pathological lymph node as an individual target with an individual treatment plan. Based on clinical experience about 25% of all patients present with multiple lymph node oligometastases which are mostly treated simultaneously using one treatment plan [109]. Independent inter-fraction motion between multiple lymph node targets can occur [110]. When multiple lymph node oligometastases are treated simultaneously, the inter-fraction motion of the targets relative to each other cannot always be accurately corrected for by translations. The dosimetric benefit of online replanning for this group is therefore expected to be even larger than in the current study. Future studies are necessary to determine the exact dosimetric benefit.

The amount of patients included in this study is limited because of the field-of-view of the MRI-datasets. More data would be beneficial to obtain more robust results. However we do believe that our study shows clear qualitative findings and gives us confidence to apply our proposed methodology in R-IDEAL stage 1/2a studies in which expected outcomes are proof of concept, technical improvements, feasibility and safety. After these studies we aim to work towards single-fraction radiotherapy treatment of these targets.

This study solely focuses on the application of online replanning for SBRT of lymph node oligometastases in the pelvic and para-aortic region. However, these results could also be indicative for other tumour sites, which present with inter-fraction variability of target size, shape and location of OARs in the proximity of the target. As PTVs were very small within this study, with an average PTV is 4.4 2.7cc (range, 1.6 – 10.3cc), and a smilar workflow was used as in the first-in-man study [36], online replanning based on the Monaco TPS could be performed in a timely manner suitable for online treatment. Full online replanning is the preferred method, as it optimally takes daily anatomy information into account. For larger PTVs it might not be possible to perform online replanning in a timeframe suitable for online adaptive treatment therefore other adaptation techniques will be needed such as virtual couch shift (VCS) which corrects for translations and rotations [111]. Further research will be performed to investigate opportunities for dose escalation and hypofractionation, as well as online replanning for multiple

targets.

Conclusion

The use of online replanning for SBRT of lymph node oligometastases on the MR-linac yields beneficial dosimetric values compared to CBCT-based online position correction using couch translations. Online replanning reduces the number of unplanned violations of dose constraints for surrounding OARs. The proposed method for online replanning is most beneficial for lymph nodes poorly visible on CBCT, as for these targets both margin reduction and online replanning are applied, however dosimetric improvements remain present for lymph nodes with good visibility on CBCT.

Chapter 5

Evaluation of plan adaptation strategies for stereotactic radiotherapy of lymph node oligometastases using online magnetic resonance image guidance

The following chapter is based on:

Dennis Winkel, Gijsbert H. Bol, Anita M. Werensteijn-Honingh, Ilse H. Kiekebosch, Bram van Asselen, Martijn P.W. Intven, Wietse S.C. Eppinga, Bas W. Raaymakers, Ina M. Jürgenliemk-Schulz, Petra S. Kroon

Physics and Imaging in Radiation Oncology (2019) Vol. 9, p.58-64

Abstract

Background and purpose
Recent studies have shown that the use of magnetic resonance (MR) guided online plan adaptation yields beneficial dosimetric values and reduces unplanned violations of the dose constraints for stereotactic body radiation therapy (SBRT) of lymph node oligometastases. The purpose of this R-IDEAL stage 0 study was to determine the optimal plan adaptation approach for MR-guided SBRT treatment of lymph node oligometastases.

Materials and methods
Using pre-treatment computed tomography (CT) and repeated MR data from five patients with in total 17 pathological lymph nodes, six different methods of plan adaptation were performed on the daily MRI and contours. To determine the optimal plan adaptation approach for treatment of lymph node oligometastases, the adapted plans were evaluated using clinical dose criteria and the time required for performing the plan adaptation.

Results
The average time needed for the different plan adaptation methods ranged between 11 and 119 seconds. More advanced adaptation methods resulted in more plans that met the clinical dose criteria [range, 0-16 out of 17 plans]. The results show a large difference between target coverage achieved by the different plan adaptation methods.

Conclusions
Results suggested that multiple plan adaptation methods, based on plan adaptation on the daily anatomy, were feasible for MR-guided SBRT treatment of lymph node oligometastases. The most advanced method, in which a full online replanning was performed by segment shape and weight optimization after fluence optimization, yielded the most favourable dosimetric values and could be performed within a time-frame acceptable (< 5 minutes) for MR-guided treatment.

Introduction

Image-guided radiation therapy (IGRT) [29] has vastly developed over the past decades and is currently indispensible in modern radiation therapy to reduce the effect of setup errors and geometrical variations of the target volume and organs at risk (OARs). To visualize the target volume and surrounding tissues prior to treatment, techniques such as portal imaging and cone-beam computed tomography (CBCT) are often used [84, 112]. These techniques have greatly contributed towards precision radiotherapy, but yield relatively poor soft tissue contrast which can make it challenging to accurately identify the target. To resolve this problem bony anatomy or implanted fiducial markers are often used as surrogate for position verification of the target [31, 33, 32].

Magnetic resonance (MR) guided radiotherapy systems are becoming increasingly available and are introduced in clinical practice [34–36]. Compared to linear accelerators with CBCT, these MR-guided systems provide a better soft tissue contrast which allows incorporation of more detailed patient anatomical information in the radiotherapy treatment plan [38, 37]. One of these MR-guided systems is the 1.5T MR-linac, which is able to provide diagnostic quality imaging of the patient anatomy during radiation therapy [113]. This enables accurate identification of the target volume, as well as the OARs and other surrounding tissues, and offers opportunities for online plan adaptation using the actual patient anatomy [39]. However, to be able to perform plan adaptation on the actual patient anatomy, multiple additional, and potentially time-consuming, steps are required. After obtaining online imaging, it must be registered with pre-treatment imaging. Deformable image registration is required to propagate the contours, after which they must be evaluated and potentially corrected. Because a new plan is created, plan quality assurance (QA) should be performed prior to delivery [36, 114].

Local treatment of lymph node oligometastases is commonly performed using stereotactic body radiation therapy (SBRT) [46, 115, 116]. In SBRT a relatively high irradiation dose is delivered in a limited number of fractions to the target in a highly conformal manner with steep dose gradients to achieve good sparing of the OARs [42, 43]. To keep treatment volumes as small as possible and minimize the amount of normal tissue that is irradiated, good target visualization during treatment is necessary in SBRT [117]. When using SBRT for the treatment of lymph node oligometastases good online target visualisation is needed to deal with inter-fraction changes in shape and size of the target and OARs and different positions of the target relative to OARs [97]. MR-guided online adaptive radiotherapy is clinically deliverable and safe and allows for dose escalation and OARs sparing compared to non-adaptive abdominal SBRT [118].

Recent studies have shown that the use of MR-guided online plan adaptation, taking daily anatomical variations into account, yields beneficial dosimetric values and reduces the amount of unplanned violations of the dose constraints [117, 89]. While the dosimetric benefit is already shown, there are multiple approaches for MR-guided online plan adaptation, based on contours generated on the daily anatomy, to be explored.

Although it is evident that a high plan quality is always preferred, time is also a limiting factor to keep total treatment time within 45 minutes, which is considered acceptable. With this in mind, online plan adaptation should preferably be performed within five minutes. The purpose of this R-IDEAL stage 0 [91] study was to evaluate different plan adaptation strategies to determine the optimal plan adaptation approach for MR-guided SBRT treatment of lymph node oligometastases.

Materials and Methods

Patient data

Pre-treatment computed tomography (CT) and sequential magnetic resonance imaging (MRI) data from five female patients with locally advanced cervical cancer with in total 17 pelvic and para-aortic pathological lymph nodes was used. All patients were treated with chemoradiation with curative intention and an additional MRI was acquired during the first three weeks of treatment. This patient data, which was used as a test case, did not contain real oligometastatic state. Because of the palliative intent of this treatment, we don't want to place any additional load on patients with lymph node oligometastases with additional imaging. It is expected for lymph nodes and surrounding OARs to behave similar in oligometastatic state. MRI was acquired on a 1.5T Philips Ingenia using a mDIXON 3D FFE T1W sequence (flip angle 10°, TE1/TE2 = 1.6/3.9ms, TR = 5.7ms, reconstructed voxel $1.05 \cdot 1.05 \cdot 2.5 mm^3$, FOV $552 \cdot 552 \cdot 300 mm^3$) during free breathing and was used for delineation. Patient preparation and motion management was equal for all image acquisition. The acquisition time (approximately six minutes) and image quality of these scans are comparable to the 1.5T MR-linac (Unity, Elekta AB, Stockholm, Sweden). All lymph node metastases and OARs on the pre-treatment CT and MRI scans were delineated by an experienced radiation oncologist treating lymph node oligometastases. The mean gross target volume (GTV) of the lymph nodes was 2.5 ± 2.8 cm^3 (1 SD) [range, 0.4 – 15.8 cm^3]. All patients gave written informed consent.

Pre-treatment plan generation

A pre-treatment plan for each of the 17 individual lymph nodes was generated on the pre-treatment CT with a prescribed dose of 5x7Gy to the target, using a 3mm isotropic planning target volume (PTV) margin which will be used in our clinical protocol. Using a vacuum cushion for immobilization, these PTV margins are considered to be sufficient to handle patient setup, intra-fraction motion and machine related uncertainties [36, 95, 94, 55, 93, 119]. All plans were generated using Monaco (Version 5.40.00 build 19, Elekta AB, Sweden) treatment planning software (TPS) with the MR-linac machine model and a 1.5T magnetic field in superior-inferior patient direction. The hardware used consists of an Intel Xeon E5-2960 CPU, 128GB RAM and two Nvidia Quadro GP100 GPU's. OAR dose was lowered as much as possible, while maintaining a sufficient PTV coverage of $V_{35Gy} > 95\%$. Clinical dose criteria for the OARs were based on the UK SABR consortium guidelines (2016) (Table 5.1). The plans were generated for intensity modulated radiotherapy (IMRT) with a maximum of 45 segments and a minimum of five monitor units per segment. Seven gantry angles were selected depending on the location of the target [120]. For left sided targets, the following gantry angles were used: 0°, 30°, 60°, 90°, 114°, 144° and 174°. For right sided targets, the used gantry angles were mirrored: 0°, 330°, 300°, 270°, 246°, 216° and 186°. All dose calculation was performed using the GPUMCD [121] dose engine available in Monaco TPS with a statistical uncertainty of 3% per control point. A calculation grid size of 3mm was used to increase optimization speed, which was resampled by the TPS to a grid size of 1mm for accurate dosimetric evaluation after optimization.

Table 5.1: Clinical dose criteria for SBRT lymph node oligometastases plans for 5 fractions as used in the evaluation of the treatment plans, based on the UK SABR consortium guidelines (2016).

Structure	Constraint
Planning target volume	$V_{35Gy} > 95\%$
	$D_{max} < 47.25$ Gy
Bladder	$V_{38Gy} < 0.5$ cm^3
	$V_{18.3Gy} < 15$ cm^3
Bowel, rectum, sigmoid	$V_{35Gy} < 0.5$ cm^3
	$V_{25Gy} < 10$ cm^3

Plan adaptation strategies

Plan adaptation was performed using the plan from the pre-treatment CT and daily MRI and contours. Both data sets were automatically registered with each other by rigid registration based on mutual information [122] and the contours were automatically propagated by deformable registration using the Monaco TPS. Electron densities were assigned per structure based on the average ED value of the corresponding contour on the pre-treatment CT. No overrides were used for structures for either the pre-treatment CT and daily MR. After these steps it was possible to perform plan adaptation on the new anatomy using one of the following six plan adaptation methods available in the adapt to shape workflow, which enables online plan adaptation on daily contours (Figure 5.1):

A Original Segments

B Adapt Segments

C Optimize Weights from segments

D Optimize Weights from fluence

E Optimize Weights and Shapes from segments

F Optimize Weights and Shapes from fluence

The Original Segments (A) method makes use of the segments and monitor units (MUs) from the pre-treatment plan, and only the plan isocenter is modified. Herewith, the original plan is calculated on the daily anatomy. The Adapt Segments (B) method shifts the segments from the pre-treatment plan relative to the isocenter, based on the registration between the pre-treatment and online images, using Segment Aperture Morphing (SAM) [75]. Using the resulting segments, the dose is calculated on the daily anatomy. Both Optimize Weights (C,D) methods are based on optimizing the weights of the segments for the daily anatomy by adjusting the amount of MUs. Method C optimizes the weights, using the set of segments from the pre-treatment plan after SAM. With method D the fluence is first re-optimized and a new set of segments is created. The new set of segments is then further optimized using segment weight optimization. The same distinction applies for both Weights and Shapes (E,F) methods. Either the pre-treatment segments are used (after SAM) for weight and shape optimization (method E), or a fluence re-optimization is performed and the new set of segments is optimized for the daily anatomy situation using both segment weight optimization, adjusting the amount of MUs, and segment shape optimization. So for method A, B, C and E, the segments from the pre-treatment plan are used for input and for method

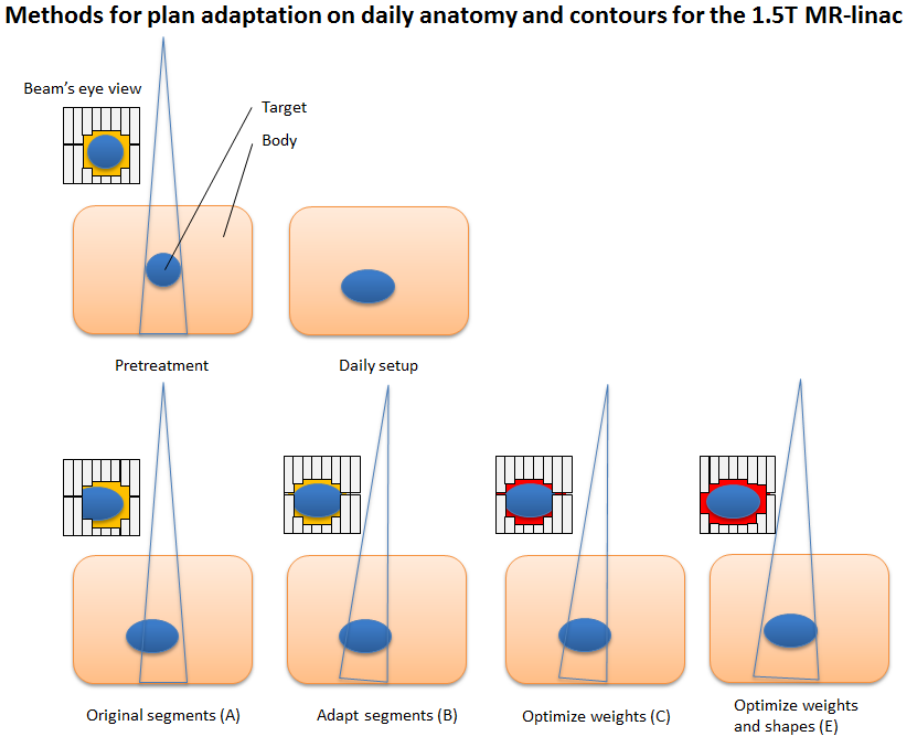

Figure 5.1: Schematic overview of the segment changes for the different plan adaptation methods available in the treatment planning software for the 1.5T MR-linac for plan adaptation on the daily anatomy and contours. A different background color (e.g. red or yellow) in the Beam's eye view (BEV) indicates a different segment weighting. When performing plan adaptation methods using optimize weights (method D) or optimize weights and shapes (method F) starting with full fluence optimization, the original segments are discarded and new initial plan segmentation is performed.

D and F, a new set of segments is created based on the re-optimized fluence. Method F, in which first the fluence is re-optimized and segmented and afterwards segment weight and shape optimization is performed, is equal to full online replanning. The plan is optimized towards the original planning constraints. No additional manual planning was performed.

Evaluation

To determine the optimal plan adaptation approach, the plans were evaluated based on the optimization time required for the plan adaptation and the clinical dose criteria (Table 5.1) for the PTV coverage and surrounding OARs: bladder,

bowel, rectum and sigmoid. The average time required for plan adaptation will be reported with one standard deviation (SDV).

Results

The median PTV on the daily MR was 99% [range, 90% - 105%] of the PTV on the pre-treatment CT. The average calculation time needed for the different plan adaptation methods ranged between 11 and 119 seconds. More advanced adaptation methods resulted in more plans that met the clinical dose criteria [range, 0-16 out of 17 plans](Figure 5.2). The results showed a difference between target coverage achieved by the different plan adaptation methods (Figure 5.3). Differences in dose to the OARs between the pre-treatment plan and different plan adaptation methods occurred. The largest differences occurred using method A. Methods B-F showed large similarities (Figure 5.4). Finally, the times for plan adaptation increased when more complex plan adaptation methods were used (Figure 5.5).

For the pre-treatment plans 16 out of 17 (94%) met all clinical dose criteria. For one plan it was not possible to achieve sufficient target coverage, without violating dose criteria for the OARs. This particular plan resulted in a PTV V_{35Gy} of 84%. The median PTV V_{35Gy} for all pre-treatment plans was 99% [84 – 100%].

Plan adaptation using method A: the Original Segments method did not result in any plans that met clinical dose criteria. The target coverage was poor with a median PTV V_{35Gy} of 32 [0 – 77%]. In addition, violations to the OARs were present. One plan had violations of both the D0.5 cm^3 and D15 cm^3 of the bladder with 38.2Gy and 18.7Gy, respectively. The same plan also had a violation of the D0.5cm^3 of the sigmoid with a value of 36.3Gy. Two other plans had a violation of the D0.5 cm^3 of the bowel with values of 36.5Gy in one plan and 36.2Gy in the other plan. Performing plan adaptation using this method took on average 11 $\pm$ 3s.

Using the Adapt Segments method (method B) did not result in any plans that had sufficient target coverage, however the coverage was higher compared to the previously described Original Segments method with a median PTV V_{35Gy} of 92% [71 – 95%]. Although target coverage was insufficient in all plans, 11/17 (65%) of the plans had a PTV V_{35Gy} of $> 90\%$ and were thereby close to an acceptable target coverage of $> 95\%$. The clinical dose criteria for the OARs were met in all 17 plans. Using this method plan adaptation took 11 $\pm$ 2s on average.

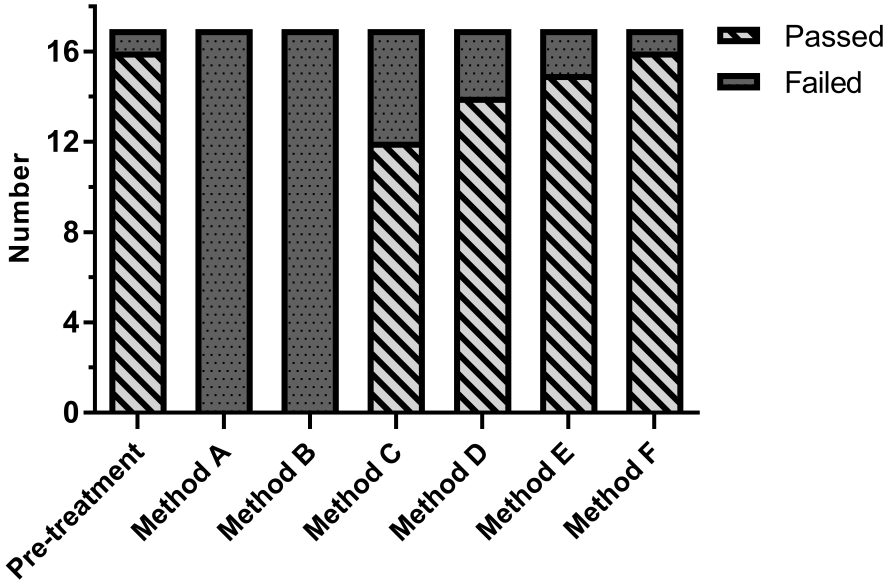

Figure 5.2: Number of plans (N=17 lymph nodes) that met all dose criteria based on the UK SABR consortium guidelines and a prescribed dose of $V_{35Gy} > 95\%$ for plan adaptation on the daily anatomy and contours for the 1.5T MR-linac. Method A – F describe: A the original segments, B adapt segments, C optimize weights from segments, D optimize weights from fluence, E optimize weights and shapes from segments and F optimize weights and shapes from fluence, respectively.

The Optimize Weights from segments method (method C) resulted in 12/17 (71%) plans that met all clinical dose criteria. In four plans the PTV V_{35Gy} was insufficient with values of 80%, 90%, 92% and 94%. One of these plans also had a violation of the D0.5cm^3 of the bowel with a value of 35.6Gy. The remaining plan that did not meet the clinical dose criteria had a violation of the maximum dose in the PTV which was 47.7Gy. The average time for plan adaptation using this method was 19 $\pm$ 3s.

With method D, the Optimize Weights from fluence method, 14/17 (82%) plans met all clinical dose criteria. Three plans violated the dose criteria with regards to the target coverage with a PTV V_{35Gy} of 71%, 91% and 93%. The clinical dose constraints for the OARs were not violated. Using this method for plan adaptation took 25 $\pm$ 5s on average.

Plan adaptation with the optimize weights and shapes method (method E), using the original segments, resulted in 15/17 (88%) plans that met all clinical dose

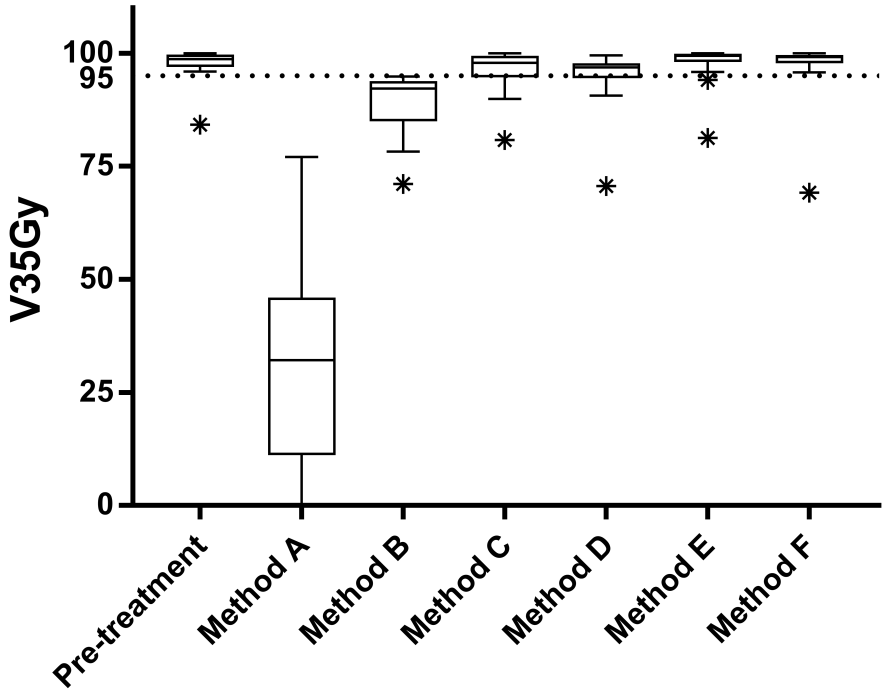

Figure 5.3: Boxplot of the target dose coverage (N=17 lymph nodes) described as planning target volume (PTV) V_{35Gy} in % for plan adaptation on the daily anatomy and contours for the 1.5T MR-linac. The 95% line depicts the minimum target coverage following the clinical dose constraints. The bars show the upper and lower quartiles. The whiskers show the minimum and maximum values, excluding outliers which are denoted with an asterisk. Method A – F describe: A the original segments, B adapt segments, C optimize weights from segments, D optimize weights from fluence, E optimize weights and shapes from segments and F optimize weights and shapes from fluence, respectively.

criteria. The two plans that did not meet the clinical dose criteria had insufficient target coverage with a PTV V_{35Gy} of 81% and 94%. As for the previous method, no violations of the clinical dose constraints for the OARs were found. Plan adaptation using this method took 112 ± 26s on average.

Using the optimize weights and shapes method (method F), after full fluence re-optimization, 16/17 (94%) of all plans met clinical dose criteria. One plan, which did also not meet sufficient target coverage during pre-treatment planning, did not meet the constraint for the PTV V_{35Gy} with a value of 69%. Using this method, which is a full online replanning, optimization took 119 ± 22s on average.

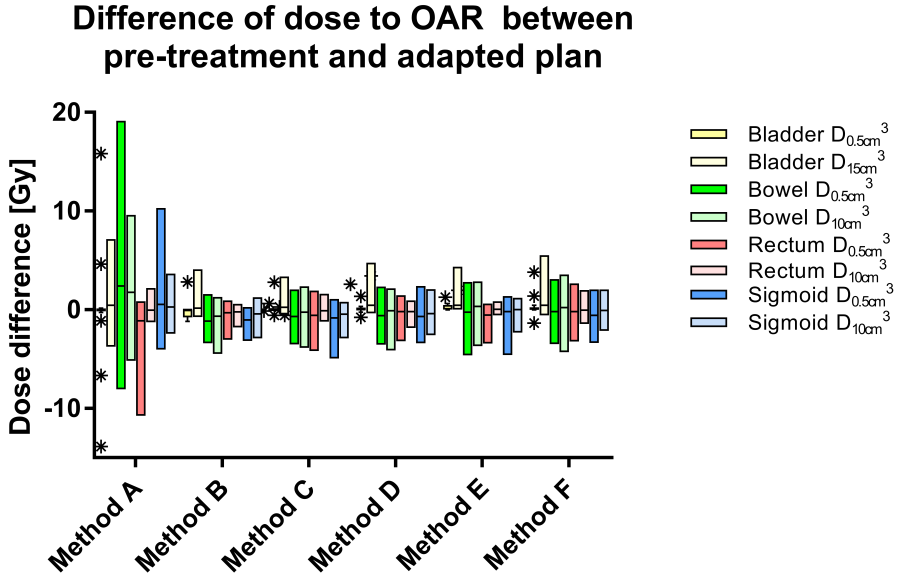

Figure 5.4: Boxplot of the dose difference between pre-treatment and adapted plan on the 1.5T MR-linac based on daily anatomy for each method (N=17 lymph nodes). The bars show the upper and lower quartiles. The whiskers show the minimum and maximum values, excluding outliers which are denoted with an asterisk. Method A – F describe: A the original segments, B adapt segments, C optimize weights from segments, D optimize weights from fluence, E optimize weights and shapes from segments and F optimize weights and shapes from fluence, respectively.

Discussion

This study shows that it is feasible to perform online plan adaptation for MR-guided SBRT treatment of lymph node oligometastases using different plan adaptation methods. The Original Segments method (method A) did not result in suitable plans, which was expected because even the slightest positioning error or inter-fraction motion with regards to the pre-treatment plan would mean that the treatment plan would no longer correctly align with the PTV. The Adapt Segments method (method B) did yield improved target coverage compared to the Original Segments method, however for all cases this was below clinical criteria. This can be explained by changes in target size and shape, which for small targets can have a large impact on relative target coverage. These methods could however perform well enough for treatment sites with little inter-fraction motion and in which the patient can be accurately positioned to limit systematic error. Regardless, random error will remain and may influence the performance.

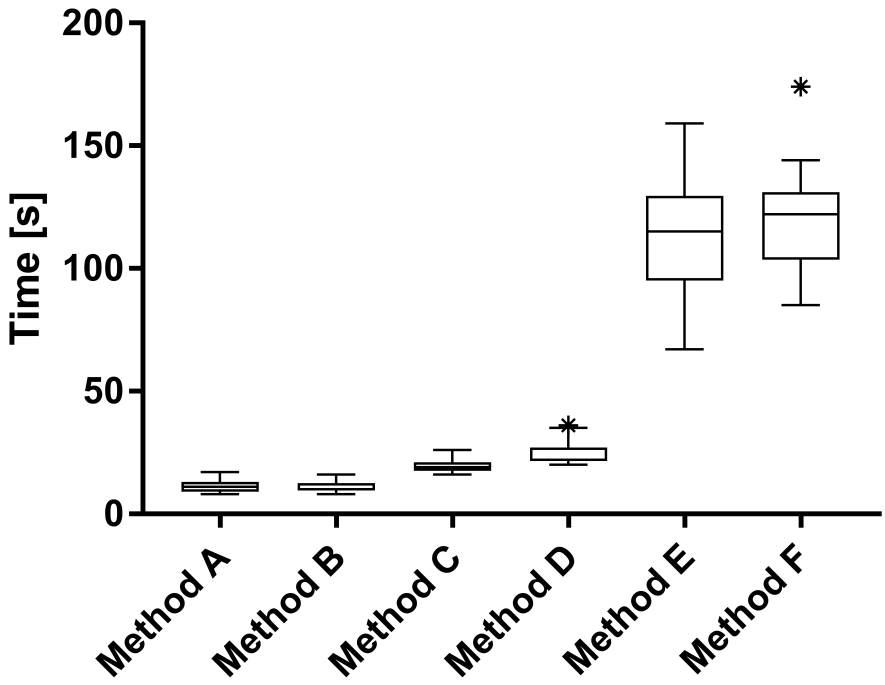

Figure 5.5: Boxplot of the measured time in seconds for each different plan adaptation method (N=17 lymph nodes) for plan adaptation on the daily anatomy and contours for the 1.5T MR-linac. The bars show the upper and lower quartiles. The whiskers show the minimum and maximum values, excluding outliers which are denoted with an asterisk. Method A – F describe: A the original segments, B adapt segments, C optimize weights from segments, D optimize weights from fluence, E optimize weights and shapes from segments and F optimize weights and shapes from fluence, respectively.

Both weight optimization and weight and shape optimization allow the use of the original segments (method C and E), or to re-optimize the fluence and perform an initial segmentation prior to these optimizations (method D and F). Comparing these options show that using a fluence re-optimization results in more favourable dosimetric values. This was expected as with this method it is possible to more accurately incorporate the daily target definition.

Using weight optimization could be suitable for treatment sites with little inter-fraction motion and large treatment volumes in which more advanced methods take too long. As this method does not alter the shape of the segments, changes in size and shape of the target are not accounted for. Therefore it might be less

suitable for tumor sites in which large inter-fraction changes can occur such as cervix [98] or prostate [123]. Plan adaptation using segment shape and weight optimization yields the best results.

Method F is equal to a full online replanning on the actual anatomy which was also done during the 1.5T MR-linac first-in-man study [36]. Full online replanning, in which a completely new plan is generated on the daily anatomy without taking pre-treatment data into account, is the preferred method, as it optimally takes daily anatomy information into account. Although this method takes relatively long (on average two minutes) compared to the first four methods described in this study, applying this strategy for daily online replanning of lymph node oligometastases is feasible time-wise when comparing to implementations of online adaptive radiotherapy by other institutions [114]. It is important to reduce the time between daily image acquisition and start of the treatment as organ motion may increase over time [124] and to ensure patient comfort.

For one particular plan it was not possible to meet the clinical dose criteria during pre-treatment planning. It was not able to obtain sufficient PTV coverage, due to overlap of the PTV and OAR adjacent to the target. Performing plan adaptation for this particular situation did also not result in acceptable treatment plans, this resulting in the outliers presented in Figure 5.3. The close vicinity of OAR relative to the target, and therewith inability to create an acceptable treatment plan, may be indicative for the inability to create acceptable plans during online adaptive treatment.

The main challenge of plan adaptation for lymph node oligometastases is to achieve sufficient PTV coverage, which was not always possible using the faster plan adaptation methods. For treatment of lymph node oligometastases, in which the targets are relatively small, this can be explained as even a slight misalignment between the treatment plan and the target will have a relatively large impact. For other sites with larger target volumes, this is expected to be less problematic, and the faster plan adaptation methods might perform sufficiently. This will need to be investigated in tumour site specific studies.

A limitation of this study is that the patient data consisted only of female patients who underwent chemo-radiotherapy. The chemo-radiotherapy might result in larger changes of the target volume and shape between pre-treatment and online imaging compared to patients which are being treated for oligo metastatic disease in our clinic. However, the latter patient group does not receive additional imaging. Because of the palliative intent of this treatment, we do not want to place any additional load on these patients. Regardless, the positive treated lymph nodes of the patient group we used is representative for the position of lymph node

oligometastases in the pelvic area as treated in our clinic. As it is expected for lymph nodes and surrounding OARs to behave similar in oligometastatic state we believe that the data is suitable to perform this analysis and gives us confidence to further implement this in our clinical workflow.

The clinical dose criteria for the OARs used in this study primarily focus on high dose regions, where most toxicity occurs [114]. Looking more closely at the pre-treatment and adapted plans, it can be seen that due to steep dose gradients, high dose regions only occur in the close vicinity of the target. For this reason it appears sufficient to limit the online re-contouring to a small region, as has been observed and proposed in several recent studies [125, 126]. Such an approach can lead to a reduction in total treatment time or may free up additional time for other processes such as plan adaptation and allow for fast adaptive replanning [85]. Limiting the online re-contouring of OAR to a small region requires the use of absolute dose constraints.

Recent studies have shown initial benefits and feasibility of MR-guided online adaptive radiotherapy. A case study by Tyran et al. showed the necessity of online plan adaptation for all fractions because of inter-fraction motion of the stomach [127]. A phase I trial on MR-guided online adaptive radiotherapy for the treatment of oligometastatic or unresectable primary malignancies of the abdomen resulted in online adaptive replanning for 81/97 fractions to due to initial plan violation of OAR constraints (61/97) or opportunity for PTV dose escalation (20/97) [118].

For specific tumour sites in which plan adaptation has to be performed on larger target volumes, calculation time will increase, dependant on which plan adaptation method is used. This could potentially mean that the methods which include segment shape optimization will no longer be feasible within a time-span suitable for online adaptive treatment and that therefore another method must be used. Increasing optimization time potentially increases temporally dependant intra-fraction motion, requiring either larger treatment margins, motion mitigation protocols or additional plan adaptation [128, 129]. A combination of large deforming target volumes, OARs in the vicinity of the target and the presence of inter-fraction motion might therefore be challenging. The most suitable methods and limitations for online plan adaptation are best investigated per treatment type. Ideally, a combination of real-time intra-fraction MRI, automatic contouring, tracking and real-time adaptive replanning should be utilized to fully benefit from MR guidance [130, 72].

In conclusion, multiple plan adaptation methods, based on plan adaptation on the daily anatomy, are feasible for MR-guided SBRT of lymph node oligometastases.

The most advanced method, in which a full online replanning is performed by segment shape and weight optimization after a full fluence optimization, performs as good as pre-treatment planning, yields the most favourable dosimetric values and can be performed within a time-frame acceptable for MR-guided treatment.

Appendix

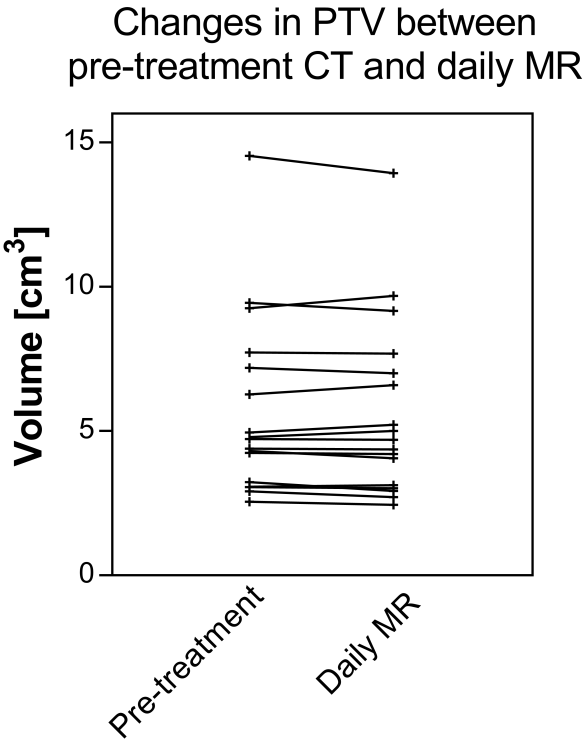

Supplementary Figure 5.1: Overview of the planning target volume (PTV) in cm^3 on the pre-treatment and the online imaging. The PTV on the online imaging was on average 99 $\pm$ 4% [range, 90 - 105%] of the PTV on the pre-treatment imaging.

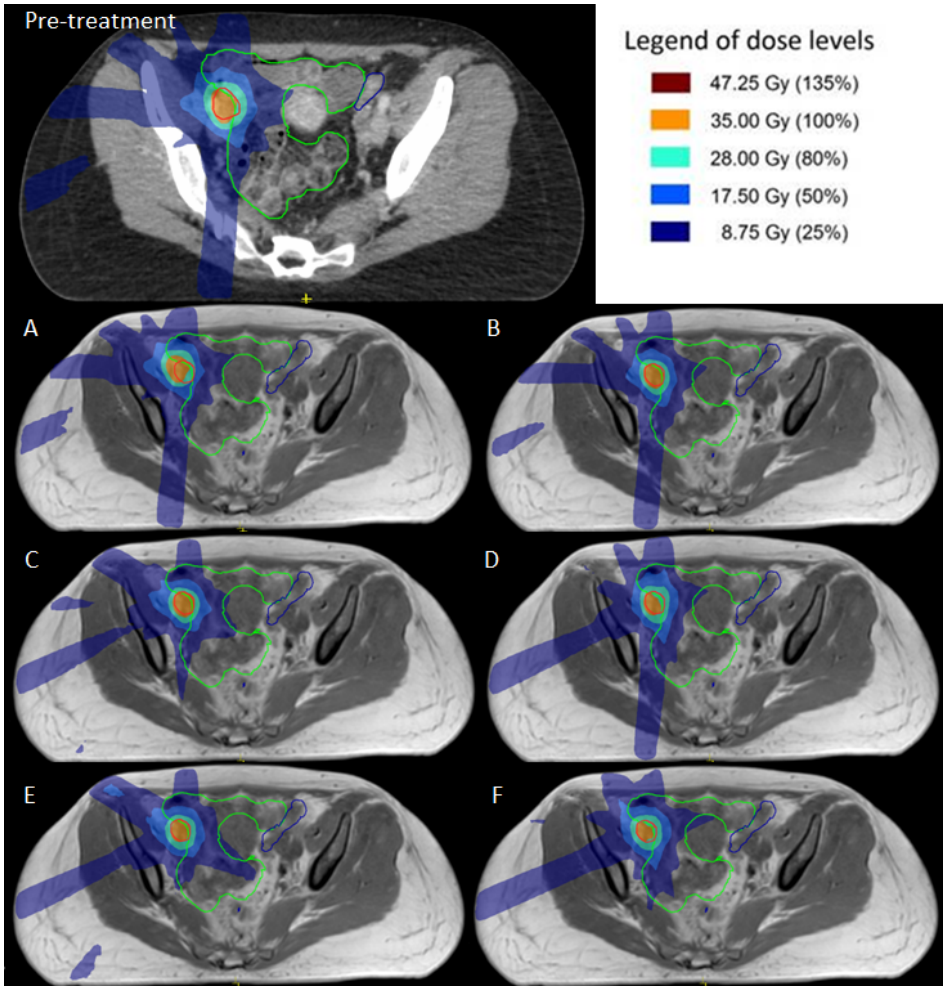

Supplementary Figure 5.2: Sample dose distributions of the pre-treatment plan and adapted plans using methods A – F for the case in which it was not possible to satisfy clinical dose criteria. Anatomical contours are shown for the PTV (red), bowel (green) and sigmoid (blue). Method A – F describe: A the original segments, B adapt segments, C optimize weights from segments, D optimize weights from fluence, E optimize weights and shapes from segments and F optimize weights and shapes from fluence, respectively.

Chapter 6

Individual Lymph Nodes: "See it and Zap it"

The following chapter is based on:

Dennis Winkel, Anita M. Werensteijn-Honingh, Petra S. Kroon, Wietse S.C. Eppinga, Gijsbert H. Bol, Martijn P.W. Intven, Hans C.J. de Boer, Louk M.W. Snoeren, Jochem Hes, Bas W. Raaymakers, Ina M. Jürgenliemk-Schulz

Clinical and Translational Radiation Oncology (2019) Vol. 18, p.46-53

Abstract

Background and purpose
With magnetic resonance imaging (MRI)-guided radiotherapy systems such as the 1.5T MR-linac the daily anatomy can be visualized before, during and after radiation delivery. With these treatment systems, seeing metastatic nodes with MRI and zapping them with stereotactic body radiotherapy (SBRT) comes into reach. The purpose of this study is to investigate different online treatment planning strategies and to determine the planning target volume (PTV) margin needed for adequate target coverage when treating lymph node oligometastases with SBRT on the 1.5T MR-linac.

Materials and methods
Ten patients were treated for single pelvic or para-aortic lymph node metastases on the 1.5T MR-linac with a prescribed dose of 5x7Gy with a 3mm isotropic GTV- PTV margin. Based on the daily MRI and actual contours, a completely new treatment plan was generated for each session (adapt to shape, ATS). These were compared with plans optimized on pre-treatment CT contours after correcting for the online target position (adapt to position, ATP). At the end of each treatment session, a post-radiation delivery MRI was acquired on which the GTV was delineated to evaluate the GTV coverage and PTV margins.

Results
The median PTV V_{35Gy} was 99.9% [90.7-100%] for the clinically delivered ATS plans compared to 93.6% [76.3-99.7%] when using ATP. The median GTV V_{35Gy} during radiotherapy delivery was 100% [98-100%] on the online planning and post-delivery MRIs for ATS and 100% [93.9-100%] for ATP, respectively. The applied 3mm isotropic PTV margin is considered adequate.

Conclusions
For pelvic and para-aortic metastatic lymph nodes, online MRI-guided adaptive treatment planning results in adequate PTV and GTV coverage when taking the actual patient anatomy into account (ATS). Generally, GTV coverage remained adequate throughout the treatment session for both adaptive planning strategies. "Seeing and zapping" metastatic lymph nodes comes within reach for MRI-guided SBRT.

Introduction

In recent years, stereotactic body radiotherapy (SBRT) has developed into standard clinical care for patients with oligometastases in many centers [51, 131, 132]. Based on the oligometastatic disease paradigm [133], treatment of individual metastatic lesions is being used to treat patients with limited metastatic disease to postpone the start of systemic therapies and ideally improve the progression-free survival or overall survival without compromising the quality of life [51–53, 134].

Experience with minimally invasive therapies such as stereotactic body radiotherapy (SBRT) as alternative to surgery has mainly been gained for inoperable patients with liver and lung oligometastases [135–140]. However, SBRT has since been incorporated in standard clinical care for lymph node and bone oligometastases [141–143] and is also being used for oligometastases located in adrenal glands [144, 145]. The minimally invasive nature of SBRT can be an advantage compared with surgical resection [51, 135], especially for small target structures such as metastatic lymph nodes.

With prostate specific membrane antigen positron emission tomography (PSMA-PET) small metastatic nodes can be detected in a very early stage with less than 10 mm and even less than 5 mm short axis diameter [146]. In the majority of patients treated with SBRT for oligometastatic lymph nodes, the affected nodes originate from prostate cancer and like the primary tumors, have a low alpha/beta ratio [50]. This is considered one of the reasons for responding very well to SBRT, with local control being achieved in 98.1% of patients in a pooled analysis [55]. For oligometastases from other origins, a biological effective dose >100Gy is also thought to be beneficial for achieving local control [51], but this will require a higher dose per fraction. In general, toxicity for SBRT of lymph node oligometastases is reported being mild, with on average 3% acute grade 2, 1% late grade 2, 0.3% acute grade 3 and 0.4% late grade 3 toxicity [131]. For prostate cancer oligometastases, SBRT can delay the start of androgen deprivation therapy (ADT) with approximately 8 – 13 months [52, 141], thereby hopefully maintaining the patient's quality of life and avoiding the side effects of ADT such as sexual dysfunction [54].

SBRT for oligometastases has mainly been applied with cone beam computed tomography (CBCT) linear accelerators (linacs) or CyberKnife, with fractionation schedules ranging from 5x 5-10 Gy to 1x 12-24 Gy [55]. Single fraction SBRT has been used in some centers, in several cases aided by fiducial marker implantation [56, 57, 147–149]. To our knowledge, peer reviewed reports on the accuracy of lymph node targeting with CBCT are lacking. However, in our own clinical routine about 30% of metastatic lymph node (as detected by diagnostic PET-CT

and MRI) are poorly visible on CBCT [117]. Compared to CBCT, magnetic resonance imaging (MRI) provides superior visualization of soft tissue targets with metastatic lymph nodes being one example [37].

The combination of online MRI for target and organ at risk (OAR) delineation, full online treatment planning and MRI for position verification is realized in the 1.5T MR-linac (combined 1.5T MR scanner and linear accelerator, Unity, Elekta AB, Stockholm, Sweden) [36,69]. New treatment plans based on the actual anatomy as depicted on MRI can be generated for every treatment fraction and online position verification is based on MRI information. The anatomy can be visualized during radiotherapy delivery (beam-on MRI) and after radiation delivery. With these facilities on board seeing the metastatic nodes with MRI and zapping them with SBRT comes into reach, as does high dose single fraction SBRT without fiducial markers. Furthermore, the daily anatomy of nearby OAR can easily be taken into account for daily treatment planning [69], which may decrease treatment related toxicity and increase the number of patients eligible for single fraction treatments [117, 150, 89].

However, despite the expected gain there are still uncertainties with regard to 1.5T MR-linac treatments in general and for lymph node metastases SBRT in particular. The clinically used PTV margin is still based on experiences at CBCT-linac, intra-fraction analyses using diagnostic MRIs and MR-linac commissioning data. In addition, the quality of inter-fraction correction with the 1.5T MR-linac with the two distinct online planning workflows: 'adapt to position' (ATP) and 'adapt to shape' (ATS) has not been investigated based on clinical data. The dosimetric effects of these different planning strategies may significantly affect the treatment benefit of online MRI guidance.

The objective of this manuscript is to demonstrate how close we are to "see it and zap it" when treating lymph node oligometastases in the pelvis and para-aortic region with SBRT on the 1.5T MR-linac. Focus will be on 1) the suitability of ATS and ATP for correcting for inter-fraction motion and 2) the feasibility of delivering the dose adequately with ATS and ATP with a pre-defined PTV margin of 3 mm.

Methods

Patient characteristics

Ten patients were treated for single pelvic lymph node oligometastases on the 1.5T MR-linac (Unity, Elekta AB, Stockholm, Sweden) at our institute between August

2018 and February 2019. The metastatic lymph nodes were located in the pelvic region for seven patients, the other three patients had para-aortic lymph nodes (at the levels of L2-Th12 vertebral bodies). The patients with para-aortic lymph nodes received a 4D CT to assess whether the breathing induced target motion amplitude was within limits. For eight patients, the metastatic nodes originated from prostate cancer and were detected using Gallium-68 PSMA PET scans. The primary tumor was rectal or esophageal cancer for two patients, diagnosis of these lymph nodes was based on 2-deoxy-2-fluorine-18-fluoro-D-glucose PET ((18)FDG-PET). The metastatic lymph nodes were diagnosed within median 49 months [range 18 - 159] after initial diagnosis of the primary tumor. All patients have provided written informed consent for using their data as part of an ethics review board approved observational study. The median short-axis diameter of the metastatic lymph nodes was 7.5 mm [5.3 – 21.3 mm].

Clinical treatment

Pre-treatment preparation consisted of MR imaging followed by CT-based treatment planning using the anatomical information of the registered MRI. For pre-treatment CT scan acquisition a special table overlay was used to enable patient set-up using specific couch index points. By doing so the position of the patient along the length of the couch is known and reproducible between the CT scan and each MRI based treatment session [69]. To reduce eventual motion, patients with lymph node metastases in the pelvic region were immobilized using a vacuum mattress (BlueBAG, Elekta AB, Stockholm, Sweden) with both hands on the chest and the elbows along the body. The patients with affected nodes in the para-aortic region were treated whilst wearing an abdominal corset [10] with the arms along the body.

Nodal targets were treated with a GTV-PTV margin of 3 mm. For each patient, a seven-beam IMRT pre-treatment plan [120] was created using Monaco TPS (Elekta AB, Stockholm, Sweden), taking into account the presence of the 1.5T magnetic field. For patients treated with the arms along the body, beam angles were selected such that the beams would not traverse the arms. OAR dose was lowered as much as possible, while maintaining a sufficient PTV coverage of V_{35Gy}>95% and a Dmax between 120-135%. Clinical dose criteria for the OARs were based on the UK SABR consortium guidelines (2016) (Table 6.1).

With online MR imaging as provided in the 1.5T MRI-linac, the pre-treatment plan can be adapted by either 1) taking the new target position into account (adapt to position, ATP) and optimizing on the pre-treatment CT and contours

Table 6.1: Clinical dose criteria

Structure	Offline constraints (pre-treatment plan)	online constraints
Planning target volume	$V_{35Gy} > 95\%$ $D_{0.1\ cm^3} < 47.25$ Gy	$V_{35Gy} > 95\%$ $D_{0.1\ cm^3} < 47.25$ Gy
Aorta	$V_{53Gy} < 0.5\ cm^3$	$V_{53Gy} < 0.5\ cm^3$
Bladder	$V_{38Gy} < 0.5\ cm^3$ $V_{18.3Gy} < 15\ cm^3$	$V_{38Gy} < 0.5\ cm^3$
Bowel bag + colon	$V_{32Gy} < 0.5\ cm^3$ $V_{25Gy} < 10\ cm^3$	$V_{32Gy} < 0.5\ cm^3$
Duodenum + stomach	$V_{35Gy} < 0.5\ cm^3$ $V_{25Gy} < 10\ cm^3$	$V_{35Gy} < 0.5\ cm^3$
Esophagus	$V_{34Gy} < 0.5\ cm^3$ $V_{27.5Gy} < 5\ cm^3$	$V_{34Gy} < 0.5\ cm^3$
Kidney	$V_{16.8Gy} < 67\%$	$V_{16.8Gy} < 67\%$
Nerve root + sacral plexus	$V_{32Gy} < 0.1\ cm^3$	$V_{32Gy} < 0.1\ cm^3$
Rectum + sigmoid	$V_{32Gy} < 0.5\ cm^3$ $D_{max} < 40$ Gy	$V_{32Gy} < 0.5\ cm^3$
Spinal cord	$D_{max} < 28$ Gy	$D_{max} < 28$ Gy
Ureter	$D_{max} < 40$ Gy	$D_{max} < 40$ Gy

after a rigid registration and translation or 2) using the new patient anatomy (adapt to shape, ATS) and optimizing on the daily image and adapted contours (Figure 6.1). For our clinical treatments plan adaptation was performed using the ATS workflow. During each treatment session, a daily MRI was acquired. Contours were automatically deformed. If necessary, the contours of the target lymph node(s) and OARs within 2 cm of the PTV(s) were manually adapted by a radiation oncologist [69]. Based on the daily MRI and the adapted contours, a completely new treatment plan was generated using segment shape and weight optimization based on a newly optimized fluence [80]. Radiation delivery according to the new plan was performed after MRI based position verification by repeated MRI radiation delivery was performed.

After each treatment session offline assessment of the intra-fraction motion was performed by recalculating the GTV coverage on the actual anatomy as seen on the post-delivery MRI, which was acquired on average 31:03 ± 3:40 minutes after the online planning MRI. Contouring of the GTV on the post-delivery MRI was performed by a single observer. Inter-observer contouring variation is considered negligible for these small and well visible lesions.

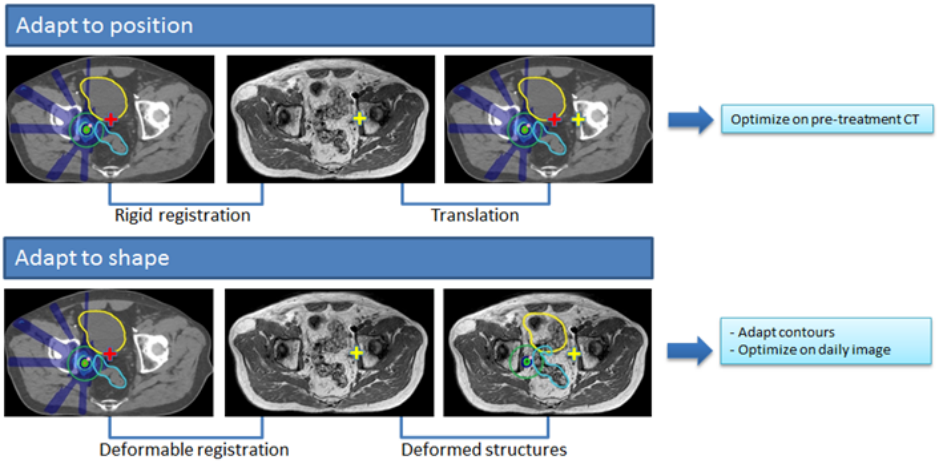

Figure 6.1: Schematic overview of the differences between the MR-linac Unity "adapt to shape" method in which online plan adaptation is performed on the new patient anatomy and optimized on the daily MRI and adapted contours, and the "adapt to position" method in which online plan adaptation is performed based on the new patient position and optimized on the pre-treatment CT and contours. Using the "adapt to position" method, rigid registration can be performed on the entire image sets, or using a clipbox around a region of interest [151].

Retrospective analyses

ATS versus ATP based plan adaptation

To investigate the suitability for correcting for inter-fraction motion the dosimetric impact of plan adaptation based on the new patient position (ATP) versus plan adaptation using the daily anatomic information and contours (ATS) was evaluated. An additional plan was retrospectively created for each treatment fraction using the ATP workflow with segment shape and weight optimization. Because the resulting dose-volume histogram parameters for an ATP plan are based on the pre-treatment CT contours and may essentially give a false representation of the actual situation, these plans have additionally been calculated on the daily MRI and contours. The GTV and PTV coverage was then compared for each of these 3 plans; the clinically delivered ATS plans, the ATP plans and the ATP plans calculated on the daily anatomy.

GTV target coverage analysis

To determine whether dose coverage was sufficient during treatment and if PTV margins were adequate, the GTV coverage for the clinically delivered (ATS) plans and the ATP plans was evaluated. This was done by evaluating the dose on both

the online planning MRI, acquired at the start of the treatment fraction, as well as the post-delivery MRI, acquired after dose delivery.

PTV margin determination

The PTV margin was re-evaluated using data of these first 10 patients with single lymph node metastases treated on the MR-linac. The margin M_{PTV} required to ensure a minimum dose to the GTV of 35 Gy for 90% of the patients was calculated using the Van Herk recipe [8] given by:

$$M_{PTV} = \alpha\Sigma + \beta\sigma - \beta\sigma_\rho \tag{6.1}$$

with $\alpha = 2.5$, $\beta = 0.84$ and $\sigma_\rho = 3.2$ mm. A β value of 0.84 was used assuming a stereotactic treatment with a plateau-prescription dose ratio of 1.25 and maximum short axis diameter of the GTV $> \sigma$. σ_ρ defines the standard deviation that describes the width of an idealized Gaussian penumbra for the total dose distribution in water, which was approximately valid because electron densities were assessed to electron density of water except for the bones [69]. $\sigma = \sqrt{\sigma_{intra}^2 + \sigma_\rho^2}$ defines the total random error and $\Sigma = \sqrt{\Sigma_{intra}^2 + \Sigma_{MV-MRI}^2 + \Sigma_{MRI}^2}$ the total systemic error. This recipe is still adequate for hypo-fractionated treatments when $\sigma_{intra} << \sigma_\rho$ [152] and the effective systematic and random errors are used [153]. Delineations errors were not taken into account assuming that the physician includes the GTV generously as had been decided by forehand. The different error sources were also assumed to be statistically independent and normally distributed.

Both Σ_{MV-MRI} and Σ_{MRI} were based on 3D vector measurements in our clinic. The contributions to the systematic errors were assumed isotrope. $\Sigma_{MV-MRI} = 0.3/\sqrt{3}$ mm was obtained from Raaymakers et al. [36] which defines the global error between the machine and MRI coordinate system. $\Sigma_{MRI} = 0.84/\sqrt{3}$ mm was determined during commissioning and describes the maximum residual geometric errors after gradient non-linearity correction within a 200 mm diameter spherical volume (DSV). This was measured on a large geometric fidelity phantom as described in Tijssen et al [154]. To obtain the systematic (Σ_{intra}) and random (σ_{intra}) group error due to intra-fraction motion, the distance in center of gravity of both GTV delineations, on the online MRI and post treatment MRI, was calculated for all five fractions of each patient. The intra-fraction deviations were then defined as the distance in center of gravity divided by two. The methodology given in Stroom and Heijmen. [155] was used to determine the group mean M (mean-of-means), systematic group error (defined as the standard deviation of the means) and random group error (defined as the root-mean-square of the

standard deviations). The effective systematic error and effective random error were equal to the derived systematic and random error because the errors due to intra-fraction motion were already based on only 5 fractions. In case the group mean M significantly differed from zero, M was added to margin

Results

ATS versus ATP plan adaptation

The clinically delivered ATS plans show the highest PTV coverage with a median V_{35Gy} of 99.9% [90.7-100%] and GTV coverage with a median V_{35Gy} of 100% [99.7-100%]. For 9 fractions, PTV coverage was reduced during online planning to meet OAR constraints. The ATP plans, evaluated on the pre-treatment CT, also show sufficient target coverage with a median PTV V_{35Gy} of 98.5% [91.0-99.9%] and GTV V_{35Gy} of 100% for all fractions. However, after calculating the ATP plans on the new MRI based anatomy and contours, the PTV coverage is significantly lower (p-value ¡0.01, Wilcoxon matched-pairs signed rank test) with a median PTV V_{35Gy} of 93.6% [76.3-99.7%] and a median GTV V_{35Gy} of 100% [93.9-100%]. Additionally, a larger variance between target coverage is observed (Figure 6.2). If an OAR dose constraint violation occurred, the violation was with a maximum of 2 Gy or 0.2 cc for both methods.

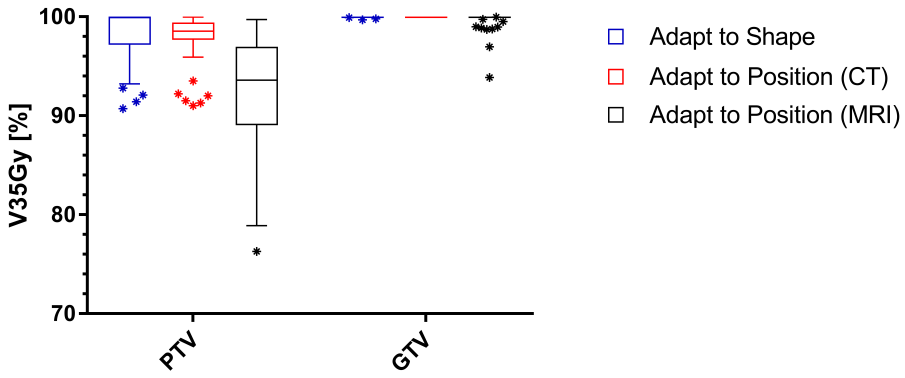

Figure 6.2: Boxplot of the target dose coverage (N = 50 fractions) described as planning target volume (PTV) and gross target volume (GTV) V35Gy in % for the adapted treatment plans. The bars show the upper and lower quartiles. The whiskers show the 5-95 percentiles. Outliers are denoted with an asterisk. The target coverage for the adapt to shape plans is evaluated on the daily MRI. The target coverage for the adapt to position (CT) plans is evaluated on the pre-treatment CT and the target coverage for the adapt to shape (MRI) plans is evaluated on the daily MRI.

GTV target coverage analysis

For the clinically delivered ATS plans the median GTV V_{35Gy} was 100% [99.7-100%] and the median GTV D_{mean} was 42.3 Gy [37.6-44.7 Gy] on the online planning MRI. On the post-radiation delivery MRI the median GTV V_{35Gy} was 100% [98.0-100%] and the median GTV D_{mean} was 42.2 Gy [37.9-44.7 Gy] (Figure 6.3). For 45 of the 50 fractions (90%) the GTV V_{35Gy} on the post-delivery MRI remained 100%. For one patient, a slight reduction of the GTV coverage was necessary during online treatment planning for 3 fractions due to the dose constraint for the sacral plexus in the vicinity of the target. For the ATP plans the median GTV V_{35Gy} was 100% [93.9-100%] and the median GTV D_{mean} was 41.6 Gy [39.0-43.6 Gy] on the online planning MRI. On the post-radiation delivery MRI the median GTV V_{35Gy} was 100% [93.4-100%] and the median GTV D_{mean} was 41.5 Gy [38.9-43.7 Gy]. For 35 of the 50 fractions (70%) the GTV V_{35Gy} was 100% on the post-delivery MRI. Figure 6.4 shows a visual example.

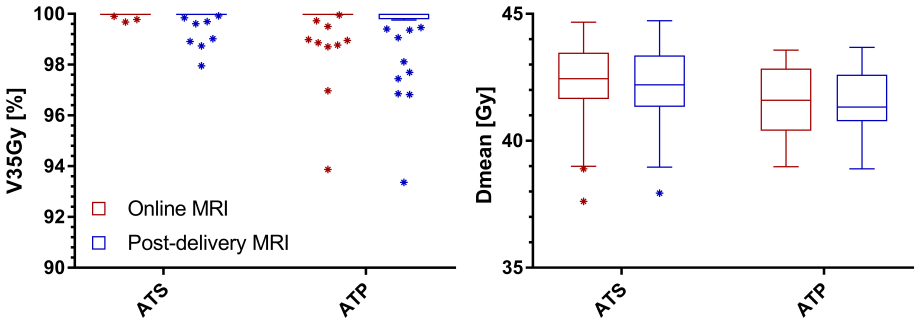

Figure 6.3: Boxplot graph of the GTV coverage (N = 50) described as V35Gy in % and Dmean in Gy for the clinically delivered (ATS) plans and the ATP plans. The bars show the upper and lower quartiles. The whiskers show the minimum and maximum values, excluding outliers (1.5 times the interquartile range) which are denoted with an asterisk. The coverage is evaluated on the daily MRI.

PTV margin analyses

The systematic and random intra-fraction displacement errors were respectively 0.31 and 0.27 mm in AP-direction, 0.54 and 0.23 mm in CC-direction and 0.22 and 0.33 mm in LR-direction. Only in AP-direction the group mean M (mean-of-mean) was significantly different from zero. The targets moved systematic in posterior direction during the individual MR-linac treatments. The group mean M was 0.33 mm in AP-direction, -0.07 mm in CC direction and 0.04 mm in LR-direction. The required PTV margin was estimated being 1.5 mm in LR-direction, 1.8 in AP-direction and 1.9 in CC-direction, respectively. Figure 6.5 shows two

examples of intra-fraction motion.

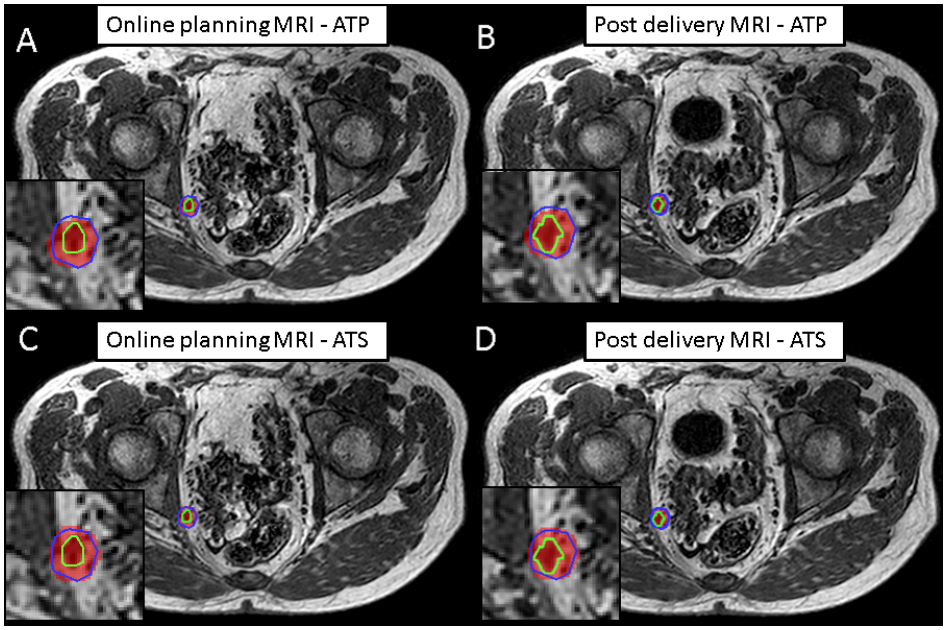

Figure 6.4: Sample case with intra-fraction expansion of the bladder due to increased filling. Visible are the 35 Gy dose level (red), the PTV (blue) and the actual location of the GTV (green) for the ATP plan on the online planning MRI (A) and the post-delivery MRI (B) and the ATS plan on the online planning MRI (C) and the post-delivery MRI (D). The GTV V35Gy remained 100% for the clinically delivered (ATS) plan. For this particular case the increasing bladder filling and GTV shift resulted in a small reduction of GTV V35Gy from 100% to 97.5% with the ATP plan.

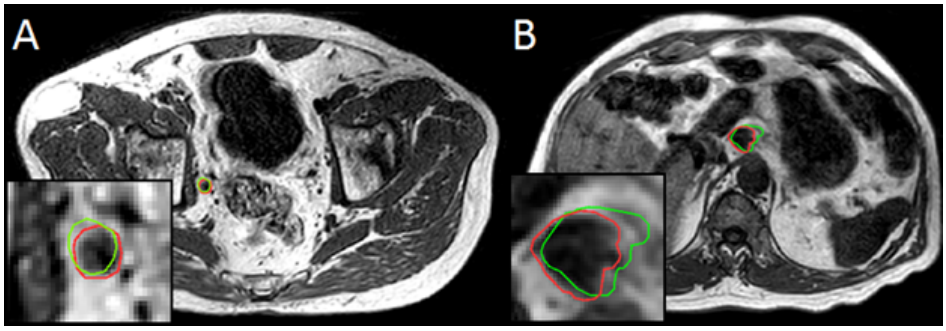

Figure 6.5: Example cases intra-fraction target motion of lymph node oligometastases in the pelvic (A) and para-aortic (B) region. Visible are the post-delivery MRIs with the online planning GTV (green) and the GTV as observed on the post-delivery MRI (red).

Discussion

MRI guided radiotherapy has been established during the last two decades. Broad clinical implementation has been realized for brachytherapy indications, mainly cervix and prostate [156–158]. Clinical gain of MRI guided brachytherapy in terms of local control and survival, not to the cost of treatment related morbidity, has been demonstrated for all stages of advanced cervical [159, 160] and for prostate cancer [161]. In parallel, MRI guidance has become clinically available for external beam radiotherapy (EBRT) in 2014 with the combination of a 0.3T MRI and 60 Cobalt radiotherapy device as realized in MRidian [162]. Since 2017 the combination of a 1.5T MRI and 7MV linear accelerator is available, bringing new opportunities for MRI guided high accuracy radiotherapy [36]. Since July 2018 this radiotherapy system is increasingly available for clinical routine treatments, starting in Europe and North-America with potential for global spread.

In our institute first clinical treatments on the 1.5T MR-linac were performed for patients with single oligometastatic lymph nodes in pelvis and para-aortic region. All nodes were well visible on the MRIs taken for treatment planning and position verification. The nodes were treated with SBRT (5x 7 Gy) and the ATS online planning option, which allows to correct for inter-fraction motion by full online treatment planning based on the actual anatomy. All treatment planning aims were met for 40 out of 50 fractions. For 10 fractions the PTV coverage had to be sacrificed slightly in order to meet the hard constraints for OAR adjacent to the nodes and in 3 of these fractions the GTV coverage of the online plan was slightly less than intended (minimum 99.7%). In case the ATP workflow had been used online optimization would have been performed on the pre-treatment patient anatomy. In this case our treatment planning aims would have been met for only 19 out of 50 fractions and the GTV V_{35Gy} was reduced to 93.9% in the worst case.

These clinical results show the additional dosimetric benefit of adaptive MRI-guided radiotherapy with online treatment planning based on the actual patient anatomy. In case of (hypo)-fractionated treatment approaches eventual inter-fraction anatomical changes can be accounted for. Because the ATS workflow is relatively labour-intensive compared to ATP, future studies will aim at predicting for which patients ATS would be most beneficial, and for whom ATP would also provide sufficient target coverage.

When evaluating the dose distributions of the online treatment plan on the anatomy of the post-treatment anatomy the chosen isotropic PTV margin of 3 mm turned out being adequate for treating single lymph nodes in the pelvis and para-aortic region on the MR-linac with the ATS treatment planning option. A

limitation of this method is that potential system errors (e.g. MV-MR misalignments) are not accounted for. The PTV margin has to account for system errors as well as intra-fraction target motions and was therefore re-evaluated. Based on the Van Herk recipe [8] an isotropic PTV margin of 2 mm would have been adequate in all three directions in our series. However, noting the limitations of the recipe for SBRT treatments, very small tumors and higher density structures [152, 163] we will still use a PTV margin of 3 mm for this particular indication in further treatments.

Within the group of oligometastatic nodal disease gain in terms of PTV margin reduction and less dose to the surrounding is especially expected for multiple metastatic lesions. In this situation daily treatment planning according to the daily anatomy might attenuate the effect of relative position shifts of the individual nodes relative to each other due to the changes of surrounding organs. Position shifts of pelvic lymph nodes are caused by movements and volume changes of the surrounding organs [93] and are not comparable to the intra-fraction motions of thoracic and abdominal lymph nodes, which are mainly affected by breathing [164, 165]. Dosimetric gain of 1.5T MR-linac treatments is also expected in other tumor sites with potentially large inter and intra-fraction motion and substantial deformations such as prostate [166], cervix [167], and rectum [168].

A factor with potential impact on the PTV-margin is the time needed for an entire MR-linac treatment procedure. On-couch time for single lymph node SBRT is currently between 30-45 minutes in our clinical routine. The majority of this time is occupied by treatment planning and radiation delivery with IMRT, which is considerably longer than the few minutes being needed to deliver a VMAT plan as available for CBCT machines. However, when comparing the CBCT-linac single plan option for all treatment fractions with the daily treatment plan option of the 1.5T MR-linac we see dosimetric gain for target and/or OARs [151]. Further PTV margin reduction and dosimetric gain of MR-linac treatments is to be expected with intended machine and software updates. Less time consuming MRI protocols and treatment planning algorithms, VMAT instead of IMRT, tumor tracking during irradiation are among the options currently being developed.

Gain for our patients will include improved comfort through further hypo-fractionation with single fraction treatments on the MR-linac being aimed at as final goal. Due to the excellent soft tissue contrast of MRI treatment margins can be small, fiducial marker implantation as applied by others for position verification purposes can be avoided [56, 57]. Clinical gain in terms of tumor related outcome such as local control, prolonged survival, later onset of systemic treatment as well as morbidity and quality of life is yet to be established.

Our study is limited by the relatively low number of cases available for the retrospective evaluation of ATS and ATP planning approaches and the margin analysis. The nodes, which are mainly originating from prostate cancer were detected by PSMA-PET, reflect small volume targets and essential volume reductions during the course of treatment are not expected [97]. Regardless of these limitations, the here presented findings correspond to earlier reported pre-clinical investigations [117, 80] and validate our current treatment approach.

In conclusion, metastatic lymph nodes in the pelvis and para-aortic region can be treated on the 1.5T MR-linac within an acceptable time frame for the whole treatment procedure. We can effectively perform MRI based online treatment planning taking into account the actual patient anatomy and deliver the intended dose to the targets using small but adequate treatment margins. We feel that we are close to "See it and Zap it" with single fraction treatments including MRI based tumor tracking as final goal.

Chapter 6

Chapter 7

Target coverage and dose criteria based evaluation of the first clinical 1.5T MR-linac SBRT treatments of lymph node oligometastases compared with conventional CBCT-linac treatment

The following chapter is based on:

Dennis Winkel, Gijsbert H. Bol, Anita M. Werensteijn-Honingh, Martijn P.W. Intven, Wietse S.C. Eppinga, Jochem Hes, Louk M.W. Snoeren, Gonda G. Sikkes, Christa G. M. Gadellaa-van Hooijdonk, Bas W. Raaymakers, Ina M. Jürgenliemk-Schulz, Petra S. Kroon

Radiotherapy and Oncology (2019) *Submitted*

Abstract

Background and purpose
Patients were treated at our institute for single and multiple lymph node oligometastases on the 1.5T MR-linac since August 2018. The superior soft-tissue contrast and additional software features of the MR-linac compared to CBCT-lincas allow for online adaptive treatment planning. The purpose of this study was to perform a target coverage and dose criteria based evaluation of the clinically delivered online adaptive radiotherapy treatment compared with conventional CBCT-linac plans.

Materials and methods
Patient data was used from 14 patients with single lymph node oligometastases and 6 patients with multiple (2-3) metastases. All patients were treated on the 1.5T MR-linac with a prescribed dose of 5x7Gy to 95% of the PTV and a CBCT-linac plan was created for each patient. The difference in target coverage between these plans was compared and plans were evaluated based on dose criteria for each fraction after calculating the CBCT-plan on the daily anatomy. The GTV coverage was evaluated based on the online planning MRI and the post-delivery MRI.

Results
For both single and multiple lymph node oligometastases the GTV V_{35Gy} had a median value of 100% for both the MR-linac plans and CBCT-plans pre- and post-delivery and did not significantly differ. The percentage of plans that met all dose constraints was improved from 19% to 84% and 20% to 67% for single and multiple lymph node cases, respectively.

Conclusions
Target coverage and dose criteria based evaluation of the first clinical 1.5T MR-linac SBRT treatments of lymph node oligometastases compared with conventional CBCT-linac treatment shows a smaller amount of unplanned violations of dose criteria. The GTV coverage was slightly, but not significantly, improved. Benefit is primarily gained in patients treated for multiple lymph node oligometastases: geometrical deformations are then accounted for, dose can be delivered in one plan and margins are reduced.

Introduction

In recent years stereotactic body radiation therapy (SBRT) has become the standard treatment option for the treatment of patients with lymph node oligometastases in many centers [51, 131]. SBRT allows for the delivery of a relatively high amount of dose in few fractions with a very steep dose gradient [43] and is often given to postpone the start of systematic therapy and improve progression-free or overall survival without compromising the quality of life [52, 53]. In the majority of the patients treated for lymph node oligometastases the affected nodes originate from prostate cancer and have a low alpha/beta ratio [50]. This means that, through SBRT, a high biologically effective dose ($>$ 100Gy) can be given which is associated with high local control [55].

For accurate dose delivery, image-guided radiotherapy (IGRT) has become increasingly important for target visualization

During SBRT of lymph node oligometastases on CBCT-linacs, inter-fraction motion is accounted for by couch translations and sometimes also for rotations. These translations and rotations can compensate for rigid target motion, but not for non-rigid changes of the target such as changes in size or shape. Additionally, it is not possible to account for anatomical changes in the location of the target and OARs, as well as path length changes and tissue attenuation. This can cause differences between the planned dose and delivered dose after position correction [88]. Therefore using position verification and correction procedures, but not optimally taking the new patient anatomy into account, may still result in unplanned violations of dose constraints [89, 117]. Additionally, it may result in underdosage of the PTV prior to delivery, which in turn can cause underdosage of the GTV due to intra-fraction motion.

Inter-fraction variations of soft tissue targets can be more optimally dealt with using MR-guided radiotherapy systems such as the 1.5T MR-linac (combined 1.5T MR scanner and linear accelerator, Unity, Elekta AB, Stockholm, Sweden) [36, 113]. This system provides diagnostic quality imaging of the patient anatomy before and during treatment, which allows for MR-guided online adaptive workflows [169]. In August 2018, SBRT of lymph node oligometastases on the 1.5T MR-linac has commenced within our institute using online MRI-based delineation of the target and OARs, full-online replanning and MRI based position verification [69].

A R-IDEAL [91] stage 0 study simulating the dosimetric impact of online replanning for SBRT of lymph node oligometastases on the 1.5T MR-linac compared

to online position correction showed beneficial dosimetric outcomes and a reduction of unplanned violations of dose constraints [117]. The purpose of this study was to perform a target coverage and dose criteria based evaluation of the clinically delivered online adaptive radiotherapy treatment compared with conventional CBCT-linac plans.

Methods

Patient characteristics

Patients were treated at our institute for single and multiple lymph node oligometastases on the 1.5T MR-linac (Unity, Elekta AB, Stockholm, Sweden) since August 2018. For this study, patient data was used from 14 patients with single lymph node oligometastases and 6 patients with multiple (2-3) metastases located in the pelvic and para-aortic region (Table 7.1).

Table 7.1: Patient data characteristics

Single lymph node oligometastases patients (N=14)		
	CBCT-linac	MR-linac
GTV [cc]	0.53 [range, 0.15 – 6.83]	
Δ GTV Pretreatment – Rx [cc]	0.01 [range -2.25 – 0.82]	
PTV margin [mm]	3 (N=10), 8 (N=4)	3 (N=14)

Multiple lymph node oligometastases patients (N=6)		
	CBCT-linac	MR-linac
GTV per patient [N]	2 (N=3), 3 (N=3)	
GTV [cc]	0.36 [range, 0.08 – 1.49]	
Δ GTV Pretreatment – Rx [cc]	0.01 [range, -1.04 – 0.29]	
PTV per patient [N]	1 (N=1), 2(N=4), 3 (N=1)	2 (N=3), 3 (N=3)
PTV margin [mm]	3 (N=8), 5 (N=2), 8 (N=3)	3 (N=15)
Treatment plans per patient (N)	1 (N=4), 2 (N=2)	1 (N=6)

Clinical treatment

Pre-treatment CT and MR imaging were acquired for each patient and registered. To provide reproducibility of the patient position along the length of the couch between the pre-treatment CT scan and each MRI based treatment session, the pre-treatment CT was acquired using a special table overlay to enable patient set-up using specific couch index points [69]. To reduce potential motion, patients

with lymph node metastases in the pelvic region were initially immobilized using a vacuum mattress (BlueBAG, Elekta AB, Stockholm, Sweden) with both hands on the chest and the elbows along the body. Two more recent patients were not treated in a vacuum mattress, due to a change in common practice. The patients with affected nodes in the para-aortic region were treated whilst wearing an abdominal corset with the arms along the body [10].

All patients were treated on the 1.5T MR-linac with a prescribed dose of 5 x 7Gy to 95% of the PTV. For each patient, a six-, seven- or ten-beam MR-linac IMRT pre-treatment plan was created with a GTV-PTV margin of 3mm using Monaco TPS (Elekta AB, Stockholm, Sweden), taking into account the presence of the 1.5T magnetic field. For patients treated with the arms along the body, beam angles were selected such that the beams would not traverse the arms. Additionally a CBCT-linac VMAT back-up plan was created for each patient. A radiation oncologist determined whether the lymph node oligometastases were well visible or not on CBCT. A PTV margin of 8mm was used for poorly visible lymph nodes and 3mm for visible lymph nodes [117]. For patients with multiple lymph node oligometastases, the plans consisted of one, two or three PTV's. For the CBCT-linac plans, a medical physicist and radiation oncologist decided on one or two separate plans, placement of the isocenter, depending on the specific anatomical situation of the patient and PTV margins. OAR dose was lowered as much as possible, while maintaining a sufficient PTV coverage of V_{35Gy} >95% and a D_{max} between 120-135%. Clinical dose criteria for the OARs were based on the UK SABR consortium guidelines (2016) (Table 7.2).

During each online treatment session the adapt to shape (ATS) workflow was followed to allow for adaptive treatment planning [169]. A daily MRI was acquired onto which the pre-treatment contours were automatically deformed. If necessary, the contours of the target lymph node(s) and OARs within 2 cm of the PTV(s) were manually adapted by a radiation oncologist [69]. Based on the daily MRI and adapted contours, a new plan was created [79]. Radiation delivery according to the new plan was performed after MRI based position verification. After each treatment session offline assessment of the intra-fraction motion was performed by recalculating the GTV coverage on the actual anatomy as seen on the post-delivery MRI. Contouring of the GTV on the post-delivery MRI was performed by multiple observers. Inter-observer contouring variation on MRI is considered negligible for these small and well visible lesions.

Table 7.2: Clinical dose criteria

Structure	Offline constraints (pre-treatment plan)	online constraints
Planning target volume	$V_{35Gy} > 95\%$ $D_{0.1\ cm^3} < 47.25$ Gy	$V_{35Gy} > 95\%$ $D_{0.1\ cm^3} < 47.25$ Gy
Aorta	$V_{53Gy} < 0.5\ cm^3$	$V_{53Gy} < 0.5\ cm^3$
Bladder	$V_{38Gy} < 0.5\ cm^3$ $V_{18.3Gy} < 15\ cm^3$	$V_{38Gy} < 0.5\ cm^3$
Bowel bag + colon	$V_{32Gy} < 0.5\ cm^3$ $V_{25Gy} < 10\ cm^3$	$V_{32Gy} < 0.5\ cm^3$
Duodenum + stomach	$V_{35Gy} < 0.5\ cm^3$ $V_{25Gy} < 10\ cm^3$	$V_{35Gy} < 0.5\ cm^3$
Esophagus	$V_{34Gy} < 0.5\ cm^3$ $V_{27.5Gy} < 5\ cm^3$	$V_{34Gy} < 0.5\ cm^3$
Kidney	$V_{16.8Gy} < 67\%$	$V_{16.8Gy} < 67\%$
Nerve root + sacral plexus	$V_{32Gy} < 0.1\ cm^3$	$V_{32Gy} < 0.1\ cm^3$
Rectum + sigmoid	$V_{32Gy} < 0.5\ cm^3$ $D_{max} < 40$ Gy	$V_{32Gy} < 0.5\ cm^3$
Spinal cord	$D_{max} < 28$ Gy	$D_{max} < 28$ Gy
Ureter	$D_{max} < 40$ Gy	$D_{max} < 40$ Gy

Retrospective analyses

Comparison of MR-linac and CBCT-linac plans

The differences in target coverage between the clinically delivered MR-linac and the CBCT-linac plans were compared for each treatment session. Additionally, the plans were evaluated based on the clinical dose criteria for the target coverage and OAR dose. The CBCT-linac plan was calculated on the daily MRI and contours from the online treatment. The electron density information was retained by matching and deforming the initial planning CT to the daily MRI data. In our clinic, CBCT-based online correction is performed by matching using a 0.5cm mask around the GTV or a clipbox with nearby structures for lymph nodes with good or poor visibility, respectively. To simulate the online correction protocol we assumed that the reference point of this correction is equal to the center of the PTV and placed the plan isocenter at the center of the PTV according to the daily anatomy. For multiple PTV's, the isocenter was placed as was done in the pre-treatment planning of the CBCT-linac plans. If CBCT-linac treatment would be performed with two plans, the doses were summed. The plans were evaluated using the clinical dose constraints and compared based on PTV and GTV coverage.

Intra-fraction GTV coverage analysis

To determine whether dose coverage was sufficient during treatment and if PTV margins were adequate, the GTV coverage for the clinically delivered (ATS) plans and the CBCT-linac plans were evaluated. This was done by evaluating the dose on both the online planning MRI, acquired at the start of the treatment fraction, as well as the post-delivery MRI, acquired after dose delivery.

Results

Pre-delivery target coverage comparison and dose constraint based evaluation

For single lymph node oligometastases the clinically delivered MR-linac plans had a median GTV V_{35Gy} value of 100% [99.7-100%] compared to 100% [98.7-100%] for the CBCT-linac plans. As could be expected, the PTV V_{35Gy} was significantly higher (p-value <0.01) with a median of 100% [90.7-100%] compared to 94.9% [47.7-100%] for the CBCT-linac plans. All dose criteria were met for the MR-linac plans in 59/70 (84%) fractions. Violations occurred with a maximum of 3Gy or a maximum PTV V_{35Gy} reduction of 4.3%. For the CBCT-plans all dose criteria were met in 13/70 (19%) fractions. Violations occurred with a maximum of 2.5Gy or 0.1cc for OARs and a maximum PTV V_{35Gy} reduction of 47.3%.

For multiple lymph node oligometastases the clinically delivered MR-linac plans had a median GTV V_{35Gy} value of 100% [100-100%] compared to 100% [8.9-100%] for the CBCT-linac plans. Also here the PTV V_{35Gy} was significantly higher (p-value <0.01) with a median of 100% [93.4-100%] compared to 94.7% [31.6-100%] for the CBCT-linac plans. All dose criteria were met for the MR-linac plans in 20/30 (67%) fractions. Violations occurred with a maximum of 0.5Gy or 0.1cc for OARs and a maximum PTV V_{35Gy} reduction of 1.6%. For the CBCT-plans all dose criteria were met in 6/30 (20%) fractions. Violations occurred with a maximum of 0.5Gy or 0.7cc for OARs and a maximum PTV V_{35Gy} and GTV V_{35Gy} reduction of 64.4% and 86.1%, respectively. These results are summarized in Figure 7.1.

GTV intra-fraction target coverage analysis

For the clinically delivered single lymph node oligometastases plans the median GTV V_{35Gy} was 100% [99.7–100%] and the median GTV D_{mean} was 43.0Gy

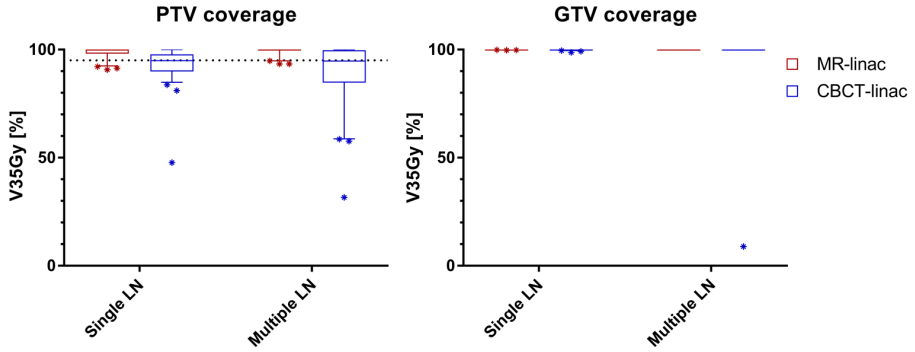

Figure 7.1: Boxplot of the target dose coverage described as planning target volume (PTV) and gross target volume (GTV) V_{35Gy} in % for the adapted treatment plans. The bars show the upper and lower quartiles. The whiskers show the 5-95 percentiles. Outliers are denoted with an asterisk. The dotted line for the PTV graph (left) denotes the minimal required coverage according to the dose constraints.

[37.6–46.1Gy] on the online planning MRI. On the post-radiation delivery MRI the median GTV V_{35Gy} was 100% [98.0–100%] and the median GTV D_{mean} was 42.9Gy [37.9–45.8Gy]. For 62 of the 70 fractions (89%) the GTV V_{35Gy} on the post-delivery MRI remained 100%. For one patient, a slight reduction of the GTV coverage was necessary during online treatment planning for 3 fractions due to the dose constraint for the sacral plexus in the vicinity of the target. For the CBCT-linac plans the median GTV V_{35Gy} was 100% [98.7–100%] and the median GTV D_{mean} was 44.5Gy [41.6–46.8Gy] on the online planning contours. On the post-radiation delivery contours the median GTV V_{35Gy} was 100% [72.4–100%] and the median GTV D_{mean} was 44.5Gy [37.2–46.2Gy]. For 56 of the 70 fractions (80%) the GTV V_{35Gy} was 100% on the post-delivery contours (Figure 7.2).

The clinically delivered multiple lymph node plans showed a median GTV V_{35Gy} of 100% [100–100%] and the median GTV D_{mean} was 43.5Gy [39.8–46.3Gy] on the online planning MRI. On the post-radiation delivery MRI the median GTV V_{35Gy} was 100% [57.7–100%] and the median GTV D_{mean} was 43.2Gy [35.8–46.1Gy]. For 63 of the 75 targets (84%) the GTV V_{35Gy} on the post-delivery MRI remained 100%. For the CBCT-linac plans the median GTV V_{35Gy} was 100% [8.9–100%] and the median GTV D_{mean} was 44.2Gy [33.4–46.7Gy] on the online planning contours. On the post-radiation delivery contours the median GTV V_{35Gy} was 100% [0–100%] and the median GTV D_{mean} was 43.7Gy [32.4–46.4Gy]. For 61 of the 75 targets (81%) the GTV V_{35Gy} was 100% on the post-delivery contours (Figure 7.3).

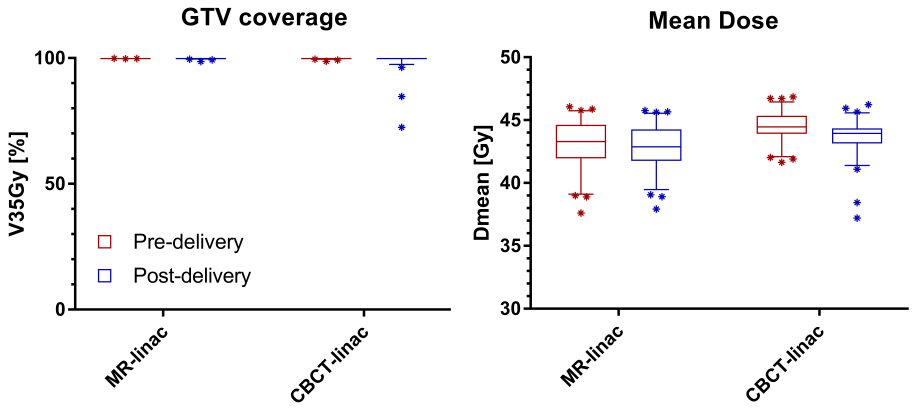

Figure 7.2: Boxplot graph of the GTV coverage and mean GTV dose of single lymph node oligometastases described as V_{35Gy} in % and D_{mean} in Gy for the clinically delivered MR-linac plans and the CBCT-linac evaluated on pre- and post-delivery contours. The bars show the upper and lower quartiles. The whiskers show the 5-95 percentiles. Outliers are denoted with an asterisk.

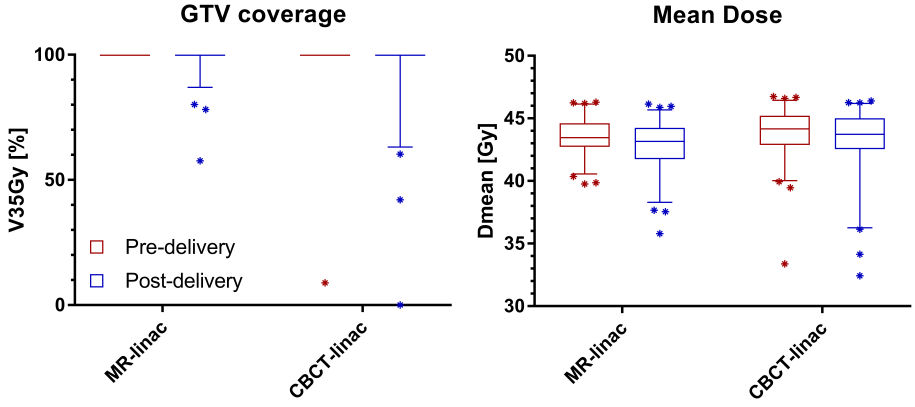

Figure 7.3: Boxplot graph of the GTV coverage and mean GTV dose of multiple lymph node oligometastases described as V_{35Gy} in % and D_{mean} in Gy for the clinically delivered MR-linac plans and the CBCT-linac evaluated on pre- and post-delivery contours. The bars show the upper and lower quartiles. The whiskers show the 5-95 percentiles. Outliers are denoted with an asterisk.

Discussion

Within this study we have compared the target coverage of the clinically delivered online adaptive radiotherapy treatment with the CBCT-linac VMAT plans for patients with both single or multiple lymph node oligometastases and evaluated the plans based on the clinical dose criteria. Our results show no significant

difference between the GTV coverage and mean GTV dose between the MR-linac and the CBCT-linac plans. Even though the PTV coverage was significantly higher for the MR-linac plans, which corresponded to earlier findings [117], the GTV remained adequately covered for most fractions. Because the post-delivery GTV coverage for the CBCT-linac plans was also evaluated on the post MR-linac delivery MRI, this potentially shows a worst-case scenario. The CBCT-linac plans are VMAT plans which have lower delivery times and less intra-fraction motion might be expected. In addition to the longer delivery times, the entire workflow for MR-linac treatment is also longer than CBCT-linac treatment. This means that the benefit with regards to improved GTV coverage for the group of single lymph node oligometastases for this particular seems limited. In cases where target coverage and OAR constraints are more demanding such as hypo-fractionated treatments, benefit could however be obtained.

A benefit for treatment of multiple lymph node oligometastases is present in cases with large deformation of the patient anatomy and can additionally be explained by independent inter-fraction motion of the targets, which may occur [110]. Position correction through couch translations may therefore not always be sufficient. This can be seen in particular for one fraction in a patient receiving simultaneous treatment of three lymph node metastases. While GTV coverage was adequate in four fractions with a V_{35Gy} of 100% for all targets, one target would receive only a GTV V_{35Gy} of 8.9% and 0% in one fraction in the pre- and post-delivery situation, respectively (Figure 5). This is caused by independent motion of the targets due to deformation of the patient anatomy. Roper et al. [170] have shown that in general, the risk of compromised coverage increased with decreasing target volume, increasing rotational error and increasing distance between targets. This also corresponds with the relatively large distance and distal position of this particular target to the other two targets for this particular case. Although in general excellent plan quality and clinical efficiency can be reached with single-isocenter treatment of multiple targets [171], rotational errors cannot be ignored for high precision treatment, especially when the distance between a target and the isocenter is large [172]. Treating multiple lymph node oligometastases on the 1.5T MR-linac means that the use of multiple plans and larger margins to account for rotational uncertainties are no longer required. The improved soft tissue contrast on MR also eliminates the need for larger PTV margins.

The possibility for accurate dose delivery using an online MR-guided adaptive workflow in which the patient anatomy is fully taken into account to mitigate for inter-fraction motion opens up further opportunities. One of such opportunities is improved patient comfort through hypo-fractionation and potentially single fraction treatment of lymph node oligometastases. While at this moment different

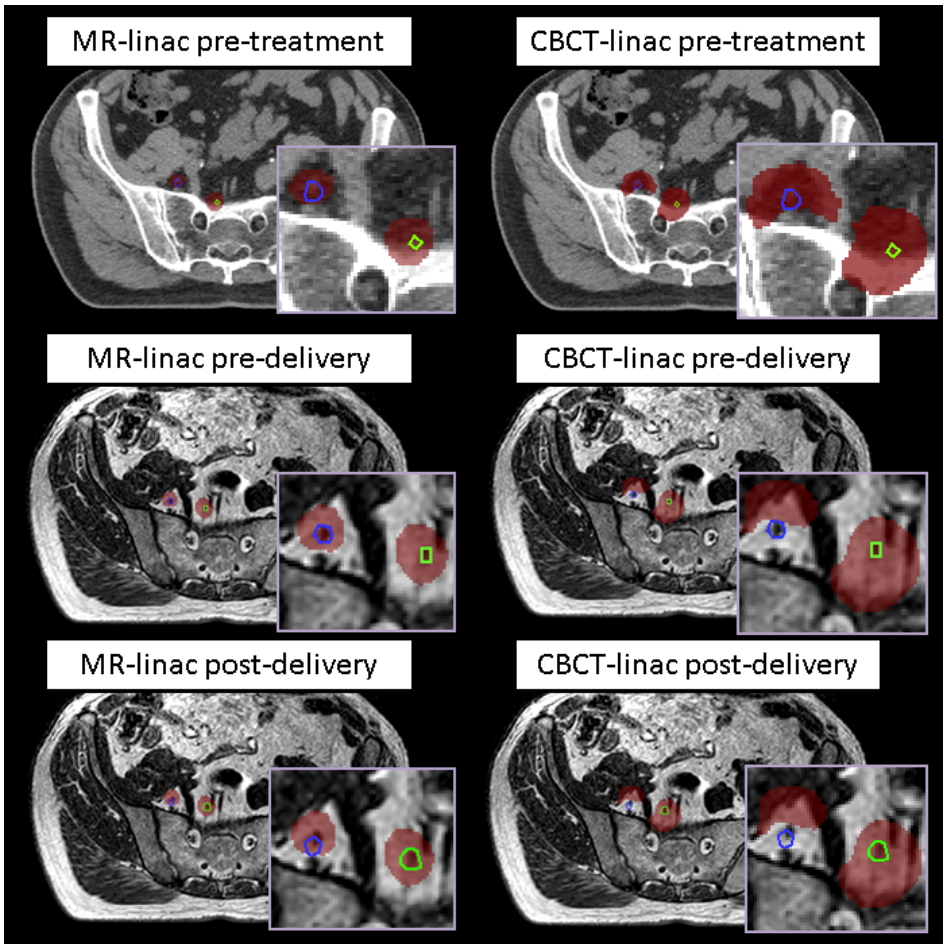

Figure 7.4: Pre-treatment, pre-delivery and post-delivery example of a multiple lymph node oligometastases case with three targets. Visible are the two most distal GTVs (blue and green) the 35Gy dose level (red). Geometrical variations would have led to under-dosage (V_{35Gy} of 8.9%) of the distal GTV (blue) when using the CBCT-linac plan in the pre-delivery situation and under-dosage (V_{35Gy} of 0%) in the post-delivery situation, regardless of the use of a 8mm PTV margin. GTV coverage remained adequate with a V_{35Gy} of 100% for the MR-linac plans, using 3mm PTV margins.

hypo-fractionated schemes are already being applied [55], this is sometimes done using fiducial marker implantation which is invasive for the patient [106, 56]. The superior soft-tissue contrast provided by MR-guidance might eliminate the need for such fiducial markers. Other opportunities for dosimetric improvements are expected in other tumor sites with the potential for large inter-fraction motion and anatomical deformations such as cervix [167], prostate [166] and rectum [168].

With online MR-guided adaptive radiotherapy being a relatively new technique, its distinct features already show to be able to effectively deal with day-to-day geometrical deformations of the target and surrounding OARs. Further research and technical improvements are expected to make this technique even more versatile and allow for various methods of dose delivery, intra-fraction plan adaptation [72] and adequate tissue tracking. Increased delivery speed will reduce the window of intra-fraction motion and may therefore also lead to further margin reduction. While it is currently possible to perform full online replanning in approximately one minute [82], computer power is also expected to grow over the years, decreasing computational time for some of these techniques. Additionally, it is important to have reliable quality assurance and contour propagation [83].These developments may further contribute towards precise and patient-specific treatments.

Our results also show that with the use of MR-linac online plan adaptation, the amount of unplanned violations of dose constraints can be reduced, which corresponds to earlier studies [117, 89, 118]. A limitation of this study, is that OARs were only evaluated based on the dose constraints. Further research should be conducted to investigate the impact of daily online adaptive replanning on the OAR dose more thoroughly. Additionally, clinical outcomes such as improved local control, prolonged survival and later onset of systemic treatment are yet to be determined.

Conclusion

Target coverage and dose criteria based evaluation of the first clinical 1.5T MR-linac SBRT treatments of lymph node oligometastases compared with conventional CBCT-linac treatment shows a smaller amount of unplanned violations of dose criteria. The GTV coverage was slightly, but not significantly, improved. Benefit is primarily gained in patients treated for multiple lymph node oligometastases: geometrical deformations are then accounted for, dose can be delivered in one plan and margins are reduced.

Chapter 8

Summary and general discussion

Summary

Treatment planning is an important aspect of radiotherapy to make sure adequate target coverage is achieved, without compromising tolerances of surrounding healthy tissue. Automated treatment planning has contributed to reduced variance and higher efficiency and plays a role in certain supporting aspects such as quality assurance and decision making. Image guided radiotherapy (IGRT) ensures accurate delivery of the treatment plan on the intended location. The introduction of MR-guidance in radiotherapy has shifted the paradigm and, compared to conventional radiotherapy treatment, opened up numerous opportunities for online treatment planning and plan adaptation based on the actual patient anatomy.

In Chapter 2 a two-phased planning and optimization workflow was developed to automatically generate 77Gy 5-field simultaneously integrated boost intensity modulated radiation therapy (SIB-IMRT) plans for prostate cancer treatment. A retrospective planning study (n=100) was performed in which automatically and manually generated treatment plans were compared. A clinical pilot (n=21) was performed to investigate the usability of our method. Operator time for the planning process was reduced to<5 min. The retrospective planning study showed that 98 plans met all clinical constraints. Significant improvements were made in the volume receiving 72Gy for the bladder and rectum and the mean dose of the bladder and the body. A reduced plan variance was observed. During the clinical pilot 20 automatically generated plans met all constraints and 17 plans were selected for treatment. The automated radiotherapy treatment planning and optimization workflow is capable of efficiently generating patient specific, optimized and improved clinical grade plans. It was adopted as the current standard workflow in our clinic to generate treatment plans for prostate cancer.

The promise of the MR-linac is that one can visualize all anatomical changes during the course of radiotherapy and hence adapt the treatment plan in order to always have the optimal treatment. Yet, there is a trade-off to be made between the time spent for adapting the treatment plan against the plan quality, which can expire over time. In Chapter 3, the various daily plan adaptation methods were presented and applied on five cases with varying levels of inter-fraction motion, regions of interest and target sizes: prostate, rectum, esophagus and lymph node oligometastases (single and multiple target). The plans were evaluated based on the clinical dose constraints and the optimization time was measured. The time needed for plan adaptation ranged between 17 and 485s. More advanced plan adaptation methods generally resulted in more plans that met the clinical dose criteria. Daily full online replanning is the most robust adaptive planning method for Unity. It is feasible for specific sites in clinically acceptable times. Faster methods are available, but before applying these, the specific use cases should be explored dosimetrically.

Chapter 4 investigated the dosimetric impact of online replanning for SBRT of lymph node oligometastases as a method for correcting for inter-fraction anatomical changes. Pre-treatment plans were created for 17 pelvic and para-aortic lymph nodes, with 3 and 8mm PTV margins reflecting our clinical practice for lymph nodes with good and poor visibility on CBCT, respectively. The dose–volume parameters of the pre-treatment plans were evaluated on the daily anatomy as visible on the repeated MRIs and compared to online replanning. With online MRI-based replanning significant dosimetric improvements are obtained for the rectum, bladder, bowel and sigmoid without compromising the target dose. The amount of unintended violations of the dose constraints for target and surrounding organs could be reduced by 75% for targets with a 8mm margin on a CBCT-linac and 66% for targets with a 3mm PTV margin on CBCT-linac when applying online replanning. The use of online replanning based on the actual anatomy as seen on repeated MRI compared to online position correction for lymph node oligometastases SBRT gives beneficial dosimetric outcomes and reduces the amount of unplanned violations of dose constraints.

In Chapter 5 we determined the optimal plan adaptation approach for MR-guided SBRT treatment of lymph node oligometastases. Using pre-treatment computed tomography (CT) and repeated MR data from five patients with in total 17 pathological lymph nodes, six different methods of plan adaptation were performed on the daily MRI and contours. To determine the optimal plan adaptation approach for treatment of lymph node oligometastases, the adapted plans were evaluated using clinical dose criteria and the time required for performing the plan adaptation. The average time needed for the different plan adaptation methods ranged

between 11 and 119s. More advanced adaptation methods resulted in more plans that met the clinical dose criteria [range, 0–16 out of 17 plans]. The results show a large difference between target coverage achieved by the different plan adaptation methods. Results suggested that multiple plan adaptation methods, based on plan adaptation on the daily anatomy, are feasible for MR-guided SBRT treatment of lymph node oligometastases. The most advanced method, in which a full online replanning was performed by segment shape and weight optimization after fluence optimization, yielded the most favorable dosimetric values and could be performed within a time-frame acceptable (<5 min) for MR-guided treatment.

Chapter 6 assesses the clinically applied adaptive planning strategy and the planning target volume (PTV) margin needed for adequate target coverage when treating lymph node oligometastases with SBRT on the 1.5T MR-linac. Also, the results are compared to a simpler patient position based plan adaptation method to show that incorporating daily patient anatomy is necessary. Ten patients were treated for single pelvic or para-aortic lymph node metastases on the 1.5T MR-linac with a prescribed dose of 5x7Gy with a 3mm isotropic GTV- PTV margin. Based on the daily MRI and actual contours, a completely new treatment plan was generated for each session (adapt to shape, ATS). These were compared with plans optimized on pre-treatment CT contours after correcting for the online target position (adapt to position, ATP). At the end of each treatment session, a post-radiation delivery MRI was acquired on which the GTV was delineated to evaluate the GTV coverage and PTV margins. The median PTV V_{35Gy} was 99.9% [90.7–100%] for the clinically delivered ATS plans compared to 93.6% [76.3–99.7%] when using ATP. The median GTV V_{35Gy} during radiotherapy delivery was 100% [98–100%] on the online planning and post-delivery MRIs for ATS and 100% [93.9–100%] for ATP, respectively. The applied 3mm isotropic PTV margin is considered adequate. For pelvic and para-aortic metastatic lymph nodes, online MRI-guided adaptive treatment planning results in adequate PTV and GTV coverage when taking the actual patient anatomy into account (ATS). Generally, GTV coverage remained adequate throughout the treatment session for both adaptive planning strategies. The ATS plans however, showed more cases in which the planning aims were met.

In Chapter 7 the target coverage and dose criteria of the rst 1.5T MR-linac SBRT treatments of single and multiple lymph node oligometastases were evaluated and compared to conventional CBCT-linac treatment. Patient data was used from 14 patients with single lymph node oligometastases and 6 patients with multiple (2-3) metastases. All patients were treated on the 1.5T MR-linac with a prescribed dose of 5x7Gy to 95% of the PTV and a CBCT-linac plan was created for each patient. The dosimetric differences between these plans were compared for each fraction

after calculating the CBCT-plan on the daily anatomy. The GTV coverage was evaluated based on the online planning MRI and the post-delivery MRI. For both single and multiple lymph node oligometastases the GTV V_{35Gy} had a median value of 100% for both the MR-linac plans and CBCT-plans pre- and post-delivery and did not signicantly dier. The percentage of plans that meet all dose constraints was improved from 19% to 84% and 20% to 67% for single and multiple lymph node cases, respectively. Target coverage and dose criteria based evaluation of the rst clinical 1.5T MR-linac SBRT treatments of lymph node oligometastases compared with conventional CBCT-linac treatment shows a smaller amount of unplanned violations of dose criteria. The GTV coverage was slightly, but not signicantly, improved. Benet is primarily gained in patients treated for multiple lymph node oligometastases: geometrical deformations are accounted for, dose can be delivered in one plan and margins are reduced.

Automated treatment planning and dierent MR-guided online plan adaptation strategies were discussed. The work conducted in this thesis also contains the introduction of SBRT of lymph node oligometastases on the 1.5T MR-linac by simulation of the potential dosimetric gain, determining the most appropriate plan adaptation strategy and by evaluating the treatments against the conventional CBCT-linac treatment and alternative strategies. Essentially, this thesis describes a possible blueprint for the introduction of new MR-guided online adaptive treatments on the 1.5T MR-linac.

General discussion

Automated treatment planning

Over the last few years, developments and innovations in the field of automated radiotherapy treatment planning has led to improved efficiency and quality of radiotherapy treatment planning [13,15,22]. The work presented in chapter 2 shows that automatically generating radiotherapy treatment plans for prostate cancer is feasible. Even though we have only focused on prostate cancer for this specific work, automated radiotherapy treatment planning is currently being performed in clinical practice for a wide array of treatment sites including more complex situations such as in head-and-neck [16, 18, 19], breast [20, 21] and prostate [17] radiotherapy. At this moment automated treatment planning is used in the UMC Utrecht to create a library of plans for bladder cancer.

Because of the systematic approach of automated treatment planning, a large benefit is that it will decrease inter- and intra-dosimetrist variability resulting

in a lower variance and a higher plan consistency. Almost all generated plans meet clinical dose constraints and in many cases can produce plans which are equal or better when compared to manually generated treatment plans [173, 174, 174–176, 64]. The automated nature of this process, greatly reducing operator time, strongly increases efficiency, which is a big driving force for these type of innovations. A challenge of the systemic approach of automated treatment planning comes in play when dealing with the trade-off between target coverage and dose to the surrounding OARs. In current practice it is often an implicit choice made by the dosimetrist to further reduce dose to a certain OAR, by in turn allowing additional dose in another OAR. For automated planning however, it is very important to objectify the plan requirements. The better the requirements are formulated, the more satisfactory the resulting treatment plans will be. It is crucial that the team of radiation oncologists involved comes to a consensus and describes objective and explicit criteria. A wish-list implementation such as used in iCycle is a good example of objectified plan requirements [64].

Because treatment planning is multi-objective, with a trade-off between target dose and OAR sparing, one should find a Pareto optimal solution in which neither of the objectives can be improved, without degrading the other. This principal that is also used in iCycle [64], is also inherently implemented in the automated treatment planning workflow presented in Chapter 2. The dose to the OARs is aimed to be lowered as much as possible, while maintaining adequate target coverage.

The reduced operator time in automated treatment planning also allows for efficient generation of a library of plans [23]. Multiple plans are generated based on expected variations in the patient anatomy and the best suitable plan can be selected based on online image guidance [24, 25]. Other than direct use for clinical purposes, automated radiotherapy treatment planning algorithms have also been applied to supportive tools such as plan quality assessment and verification or to predict what type of dose distribution can be achieved for a certain patient [24,25]. Being able to predict what type of dose distribution can be achieved, through techniques such as deep learning [177], may also function as a decision making support tool in selecting the most optimal treatment for a patient, e.g. photon or proton therapy [178], making automated treatment planning a versatile technology in clinical practice. In addition to benefits for clinical practice, automated radiotherapy treatment planning can also be used for research purposes. By automating certain aspects of the treatment planning process it is possible to efficiently and without bias compare different treatment planning approaches using large sets of patient data to get reliable results [16, 179, 180]. A potential use case for automated treatment planning in relation to new developments in

online MR-guided adaptive treatment planning is determining the most optimal plan adaptation strategy by trying many different methods on a large amount of patient data.

It is known that plan quality in manual treatment planning is highly dependent on the skill and experience of the dosimetrist, but one should realize that the implementation of automated treatment planning also requires a high level of knowledge regarding treatment planning and preferably site-specific planning experience to be able to optimally implement and configure the automated treatment planning system. This also applies to selecting the plan requirements and the order of priorities in wish-list type optimizations. A suboptimally functioning automated treatment planning solution will result in treatment plans that are inferior compared to manual planning and will essentially, because of the systematic approach, introduce additional systematic error in the treatments by producing plans that are of lesser quality than what could be achieved. Therefor it is important that the development, configuration and implementation of such automated treatment planning solutions is conducted in close collaboration with physicists, dosimetrists and physicians.

In the future, the amount of automated treatment planning solutions will likely increase. As the amount of manual planning work decreases, the dosimetrist might lose their skills and experience with regards to certain type of treatment plans. Dosimetrists will not become completely redundant, but their role will change. Instead of generating bulk treatment plans, they are likely to generate class solutions for automated planning. Then, automated treatment planning will most likely be applied to handle less complex and frequent types of treatment planning, freeing up the dosimetrists to spend more time on more complex and demanding cases. On the path towards frequent automated treatment planning, automated treatment planning can and will function as benchmark to increase overall plan quality and consistency.

MRI-guided radiotherapy

MRI guided radiotherapy has been established during the last two decades and since then broad clinical implementation for brachytherapy indications, mainly prostate and cervix [158,157,156], has been realized. In parallel, MRI guidance has become clinically available for EBRT in 2014 with the combination of a 0.35T MRI and 60 Cobalt radiotherapy device as realized in MRidian [162]. Since 2017 the combination of a 1.5T MRI and 7MV linear accelerator is available, bringing new opportunities for MRI guided high accuracy radiotherapy [36]. Since July 2018

this radiotherapy system is increasingly available for clinical routine treatments, starting in Europe and North-America with potential for global spread.

MRI guided radiotherapy has certainly introduced a new era in IGRT because of the many advantages offered by MRI guidance. Conventional IGRT methods are often used to match the patient to a previously acquired image of the anatomy prior to treatment and still heavily relies on effective patient immobilization. The superior soft tissue contrast of MRI compared to CBCT makes it possible to accurately identify and delineate target structures and OARS [37]. This will give major advantages in areas in which soft tissue is involved such as the abdomen. Additionally MRI can be used to quantify motion.

Being able to accurately identify and delineate target structures and OARs during treatment makes it possible to incorporate daily patient anatomy in online adaptive treatment planning, rather than matching the patient with a previously acquired image of the anatomy and a previously generated treatment plan. By fully incorporating the daily anatomy of the patient, inter-fraction motion can be dealt with efficiently. Good results have been achieved in terms of improved target coverage and a reduction of unplanned violations of dose criteria [89,118,127] as can also be seen in Chapter 7 of this thesis. Dealing with inter-fraction motion may also allow for PTV margin reduction which in its turn may allow for further dose escalation in specific treatment sites.

These novel MR-guided systems allow for imaging of the patient during beam delivery. By real-time monitoring of the patient anatomy it will be possible to react to unexpected events through exception gating and potentially supports tumor tracking. Gating can effectively deal with intra-fraction motion by only delivering the dose when the target position is within a pre-defined threshold [162,181–183]. With tumor tracking the radiation beam will essentially follow the target by shifting the MLC and make treatment times shorter than with gating [184,185]. These techniques should be further developed and are essential for hypo-fractionated treatments. Another big advantage of beam-on MRI is that currently offline dose reconstruction can be performed, which shall ultimately also become possible during delivery and be incorporated in real-time plan adaptation [72].

Another distinct advantage of MRI guidance is that it allows for functional imaging during the course of radiotherapy treatment. The future of MRI guidance combined with functional imaging may potentially allow incorporation of functional data to not only adapt the treatment plan based on anatomical changes, but also based on differences in treatment response [186]. For example the use of the apparent diffusion coefficient (ADC) which can be obtained diffusion-weighted imaging may provide both qualitative and quantitative information which can be

used to identify early treatment response and predict local recurrence [187, 188]. If this technique is combined with real-time adaptive plan optimization, it would open up a whole new level of precision and personalization in radiotherapy [189].

Even though the use of MRI guidance yields distinct advantages over other methods of IGRT, several challenges remain. MRI does not give electron density properties such as CT techniques. This can however be compensated for with the use of model based pseudo CT generation [190] or deep learning [191]. Fraction times for MR-guided treatment are relatively long, compared to CBCT-guided treatment. This is caused by additional steps in the online workflow such as delineating the online patient anatomy. Although this is largely done by automated deformable contour propagation, small edits by the physician are often required. To speed up this process, online re-contouring of the OAR is often limited to a small region around the target [125, 126]. This problem can be further addressed by robust contour propagation and reliable quality assurance [83]. Other time-costly factors include independent dose calculations or slower dose delivery because of lower dose rates or delivery techniques. Longer fraction times may cause additional challenges for tumor sites in which large intra-fraction motion may be expected [166–168]. With intra-fraction plan adaptation, this will not be a hurdle anymore, except for patient comfort.

Online plan adaptation

Based on pre-delivery MRI acquisition it is possible to perform online plan adaptation while the patient is on the treatment table, as described in Chapter 3. Several different planning strategies have been previously described such as the Virtual Couch Shift (VCS) method in which the dose is transformed to the daily anatomy based on the daily rigid transformation [111]. Plan adaptation on the 1.5T MR-linac is possible through two different approaches. In the first approach the treatment plan is adapted to the new patient position (adapt to position, ATP) and re-optimized on the pre-treatment imaging. The second method is done by incorporating the daily MRI and adapted contours (adapt to shape, ATS). The re-optimization is then performed on the daily MRI. In Chapter 3 it became apparent that there is a trade-off between the time needed for online plan adaptation against the plan quality, which expires over time due to intra-fraction motion. In particular, calculation times are longer for larger target volumes and more complex anatomies.

Although it might seem preferable to always incorporate as much daily information as possible, this might not always be viable. Using the ATS workflow requires

deformable contour propagation and potentially manual editing of the contours. Followed by full online replanning with segment shape and weight optimization, the time required might be of such length that for specific cases with large intra-fraction motion the anatomical situation between acquiring the daily MRI used for plan adaptation and the anatomy at the time of beam delivery might have significantly changed. Additionally, incorporating the daily anatomy might not even give a significant advantage over using the ATP workflow for treatment sites in which little inter-fraction variation is expected.

Daily online replanning seems feasible in clinically acceptable times, but one should investigate the most suitable approach per use case and will depend on several factors such as the complexity of the anatomy and the inter- and intra-fraction motion [166–168]. Additionally, it is also possible to look for hybrid plan adaptation solutions, where two steps of plan adaptation are being applied before dose delivery. A more time-consuming ATS workflow can be utilized to deal with larger inter-fraction motion, followed by an ATP step to account for the intra-fraction motion that occurred during the process of contour propagation, contour editing and re-optimization. Such approach is currently being applied within our institute for MR-linac prostate treatments. In practice the pre-treatment plan is used as input for the online plan adaptation. A first intra-fraction implementation could be to also allow, for instance, intra-fraction ATP, where based on the imaging acquired during dose delivery, the decision can be made to adapt the dose to a modified patient position. This can further be improved by warping the delivered dose of previous fractions and incorporate it in dose calculations for the subsequent fractions [81]. This however requires accurate dose reconstruction and accumulation. Also this is essential for intra-fraction plan adaptation, where the ultimate goal is to get to real-time plan adaptation while accounting for the dose delivered so far. Kontaxis et al. [81] presented a loop that enables such continuous re-optimization during beam delivery.

With online MR-guided plan adaptation being a relatively new technique, its distinct features already yield benefit. Nowadays it is possible to accurately deal with inter-fraction motion in a clinical setting by taking advantage of the superior soft-tissue contrast of MRI-guidance and the therefrom derived technical advantages and possibilities. Further research and technical improvements will make this technique even more versatile and allow for various methods of dose delivery, intra-fraction plan adaptation [72] and adequate tissue tracking. Real-time dose accumulation and reconstruction will be used as an input for further inter- and intra-fraction plan adaptation [72, 71]. Proof of concept has shown the viability of many of these advances. While it is essentially already possible to perform full online replanning in approximately one minute [82], computer power

is also expected to grow over the years, decreasing computational time even. Additionally, advances towards reliable quality assurance and contour propagation are being made [83]. This facilitates objective, and potentially, automated evaluation of contour propagation, such advancements are required to get to automated, real-time, adaptive radiotherapy.

MRI-guided SBRT of lymph node oligometastases

SBRT of lymph node oligometastases benefits from the superior soft-tissue contrast, which often forms a challenge in the lower abdominal region. In this thesis SBRT of lymph node oligometastases on the 1.5T MR-linac has showed improved target coverage and a reduction of unplanned violations of OARs. This benefit can be seen both for lymph nodes with good and poor visibility on CBCT. It can therefore be advocated to use online replanning to take non-rigid anatomical changes into account.

As investigated in Chapter 4, large benefit can be reached for lymph nodes that are poorly visible on CBCT. The superior soft tissue contrast on the MR-linac will allow for a considerable reduction of the PTV margin (i.e. reduction from 8 to 3mm in this particular situation), which importantly reduces the overlap between PTV and OARs. The improved target structure visibility with the MR-linac, combined with online replanning could also provide opportunities for hypofractionation, without the need for invasive marker placement procedures, compared with hypofractionated SBRT using the CyberKnife [56, 106]. SBRT treatment of lymph node oligometastases on the MR-linac using online replanning therefore opens up possibilities for dose escalation, without increasing the risk on OAR dose constraint violations. Further studies must be conducted to show whether dose escalation and hypofractionation are possible. Ultimately, this treatment is performed in a single fraction, but this still requires technical developments such as intra-fraction plan adaptation and faster dose delivery to either deal with the increased window for intra-fraction motion, or reduce the total treatment time. The latter must also be considered for patient comfort. While hypo-fractionated treatment improves patient comfort, longer-term clinical outcomes such as improved local control, prolonged survival and later onset of systemic treatment are yet to be determined.

Improved target coverage can already be observed for single target cases, however the benefit for multiple lymph node oligometastases is largest. This can potentially be explained by independent inter-fraction motion of the targets, which may occur [110]. Position correction through couch translations may therefore

not always be sufficient. This is caused by independent motion of the targets due to geometrical changes of surrounding organs. Roper et al. have shown that in general, the risk of compromised coverage increased with decreasing target volume, increasing rotational error and increasing distance between targets [170]. This also corresponds with the relatively large distance and distal position of this particular target to the other two targets for this particular case. Although that in many cases good plan quality and clinical efficiency can be reached with single-isocenter treatment of multiple targets [171, 109, 192], rotational errors cannot be ignored for high precision treatment, especially when the distance between a target and the isocenter is large [172]. More deformation of the patient relative to the pre-treatment situation, will result in insufficient target coverage as is presented in Chapter 7. This can however be adequately dealt with using MR-guided online adaptive planning strategies.

It is clear that for treatment sites in which large anatomical deformations can occur, such as multiple lymph node oligometastases, benefit is evident. The effect of online adaptive planning on the OAR dosis is still to be further investigated. The whole treatment can be performed within an acceptable time frame for the whole procedure [69]. MRI-guided plan adaptation has been efficiently performed taking into account the actual patient anatomy and deliver the intended dose to the targets using small but adequate treatment margins.

Overall conclusion

In conclusion, automated treatment planning and several methods of online plan adaptation to account for inter-fraction motion were discussed. The most suitable methods were explored for different type of treatment sites. Single lymph node oligometastases was a good starting point as these are typically relatively small and approximately rigid. This easens and speeds up the contour propagation and editing as well as on-line treatment planning. The first treatments showcased the clinical feasibility of true online, MRI guided radiotherapy to account for inter-fraction variability. Cases with multiple lymph node oligometastases have offered insights on more deforming targets. With future developments, lymph node oligometastases might be treated in 1 fraction with intra-fraction adaptive radiotherapy. This thesis is essentially a blueprint for the introduction of new and more complex treatment sites on the 1.5T MR-linac. Exciting times are ahead for technological and clinical advances in radiotherapy.

Chapter 9

Samenvatting

Ter voorbereiding van een radiotherapiebehandeling worden er CT en MRI beelden gemaakt van de patiënt, waarop het doelgebied en andere belangrijke weefsels worden ingetekend. Op basis hiervan wordt er een dosisplan gemaakt. Dosisplanning is een belangrijk aspect waarmee gezorgd wordt dat er voldoende dosis aan de tumor wordt gegeven zonder dosislimieten van gezonde weefsels rond de tumor te overschrijden. Automatische dosisplanning heeft bijgedragen aan een reductie in variantie en een hogere efficiëntie en speelt een ondersteunende rol in verschillende aspecten van de radiotherapie, zoals kwaliteitsbewaking en besluitvorming. Beeldgestuurde radiotherapie zorgt voor het nauwkeurig afstralen van de dosis op de juiste locatie. De introductie van MRI-gestuurde radiotherapie heeft gezorgd voor een verschuiving in de wereld van radiotherapie en biedt, vanwege verbeterd contrast tussen zachte weefels, vele nieuwe mogelijkheden voor online dosisplanning en planadaptatie gebaseerd op de actuele anatomie van de patiënt.

In hoofdstuk 2 is er een uit twee fasen bestaand dosisplanning- en optimalisatie systeem ontwikkeld om automatisch 77Gy 5-velden intensiteitsgemoduleerde radiotherapie (intensity modulated radiotherapy, IMRT) plannen te maken waarbij verschillende gebieden met verschillende doseringen (simultaneous integrated boost, SIB) bestraald worden voor de behandeling van prostaatkanker. Een retrospectieve planningsstudie was uitgevoerd, waarin voor een set van 100 patiënten het automatisch gegenereerde dosisplan vergeleken was met het werkelijk afgestraalde klinische plan. Vervolgens was er een klinische pilotstudie uitgevoerd waarin de plannen prospectief werden vergeleken om te bruikbaarheid van het systeem te onderzoeken. De tijd nodig voor handmatige handelingen in het planningsproces was gereduceerd tot <5 minuten. De retrospectieve planningsstudie liet zien dat voor 98 plannen alle klinische dosiscriteria behaald waren. Voor de blaas en het rectum waren er significante reducties van het volume dat 72Gy ontving. De variantie tussen de plannen was gereduceerd. Tijdens de klinische prospectieve pilot voldeden 20 van de 21 plannen aan alle dosiscriteria en

waren er 17 geselecteerd voor behandeling. Het automatische dosisplanning- en optimalisatie systeem is in staat om op efficiënte wijze patiëntspecifieke, geoptimaliseerde en verbeterde plannen te genereren van klinische kwaliteit. Het was geïntroduceerd als de standaard optie dosisplanning voor prostaatkanker in de kliniek.

De belofte van de MRI-gestuurde lineaire versneller (MR-linac) is dat het alle anatomische veranderingen tijdens de radiotherapiebehandeling kan visualiseren en het dosisplan daarop aan kan passen om de patiënt een verder geoptimaliseerde bestraling te kunnen geven. Er is echter altijd een evenwichtige wisselwerking tussen hoeveel tijd je aan het adapteren van het plan besteedt en de plankwaliteit, welke kan afnemen over tijd door veranderingen in de anatomie tijdens de planadaptatie. In hoofdstuk 3 worden de verschillende methoden voor dagelijkse planadaptatie gepresenteerd en toegepast op vijf verschillende casussen met variërende anatomische doelgebieden en tumorgroottes: prostaat, rectum, slokdarm en lymfeklier oligometastasen (enkele en meerdere). De plannen werden geëvalueerd aan de hand van de klinische dosiscriteria en de tijd nodig voor planoptimalisatie was gemeten. De tijd welke nodig was voor planadaptatie zat tussen de 17 en 485 seconden. De meer geavanceerde planadaptatiemethoden resulteerden over het algemeen in meer dosisplannen welke voldeden aan de klinische dosiscriteria. Dagelijks volledig online herplannen is de meest robuuste planadaptatiemethode voor de Elekta Unity, wat mogelijk is voor verschillende doelgebieden in klinisch acceptabele tijden. Snellere methoden zijn beschikbaar, maar voor deze toe te passen is het verstandig deze eerst dosimetrisch verder te verkennen.

Hoofdstuk 4 beschrijft de dosimetrische impact van het online herplannen voor de stereotactische behandeling van lymfeklier oligometastasen als een methode om te corrigeren voor anatomische veranderingen tussen de bestralingen door. Dosisplannen zijn gemaakt voor 17 lymfeklieren in het bekken en para-aortische gebied met zowel een 3mm als een 8mm planning target volume (PTV) marge. Deze marge wordt toegepast rondom het klinische doelgebied om eventuele bewegingen van de tumor en patiënt en overige onnauwkeurigheden op te vangen. Dit reflecteert het huidige klinische beleid waarin 3mm wordt toegepast op klieren welke goed zichtbaar zijn op cone-beam computed tomography (CBCT) scans en 8mm voor klieren welke slecht zichtbaar zijn. De dosis-volume histogram parameters van de dosisplannen zijn geëvalueerd op de dagelijkse anatomie zoals zichtbaar in de herhaalde MRI-scans en vergeleken met online herplannen. Online herplannen gebaseerd op de MRI beelden zorgde voor significante dosimetrische verbeteringen voor rectum, blaas, darmen en sigmoid zonder verslechtering van de dosis in het doelgebied. De hoeveelheid onbedoelde overschrijdingen van dosiscriteria in het doelgebied en de risico organen was gereduceerd met 75% voor doelgebieden

met een 8mm PTV marge en 66% voor doelgebieden met een 3mm PTV marge op een CBCT gestuurde lineaire versneller (CBCT-linac) wanneer online herplannen werd toegepast. Het gebruik van online herplannen gebaseerd op de actuele anatomie zoals zichtbaar op de herhaalde MRI scans geeft goede dosimetrische uitkomsten en reduceert het aantal onbedoelde overschrijdingen van dosiscriteria in vergelijking met het reguliere positie correctie protocol.

In hoofdstuk 5 wordt de meest optimale aanpak voor planadaptatie voor MRI-gestuurde stereotactische behandeling van lymfeklier oligometastasen op de 1.5T MR-linac vastgesteld. Er is gebruik gemaakt van CT beelden van voor de behandeling en herhaalde MRI beelden van vijf patiënten met in totaal 17 pathologische lymfeklieren. Op deze opnieuw ingetekende MRI beelden zijn zes verschillende methoden van planadaptatie toegepast. Om de meest optimale methode te bepalen zijn de plannen vergeleken op klinische dosiscriteria en de vereiste tijd om het planadaptatie uit te voeren. De gemiddelde tijd bedroeg tussen de 11 en 119 seconden. De meer geavanceerde adaptatiemethoden resulteren in meer plannen welke voldoen aan de klinische dosiscriteria. De resultaten laten grote verschillen zien in de dosisdekking van het doelgebied tussen de verschillende methoden. De resultaten laten daarnaast zien dat verschillende methoden voor planadaptatie, gebaseerd op adaptatie op de dagelijkse anatomie van de patiënt, toepasbaar zijn voor MRI-gestuurde stereotactische behandeling van lymfeklier oligometastasen. De meest geavanceerde methode, in welke een volledige herplanning wordt uitgevoerd middels het optimaliseren van de segmentvormen en -gewichten na een volledige heroptimalisatie van de fluentie, zorgt voor de meest gunstige dosimetrische waarden en kan uitgevoerd worden binnen een tijdsspan (<5 minuten) welke acceptabel is voor MRI-gestuurde behandelingen.

Hoofdstuk 6 evalueert de klinisch toegepaste planadaptatiestrategie en de PTV marges welke noodzakelijk zijn voor adequate dosisdekking van het doelgebied voor de behandeling van lymfeklier oligometastasen op de 1.5T MR-linac. Daarnaast zijn de resultaten vergeleken met planadaptatie gebaseerd op enkel de nieuwe positie van de patiënt om aan te tonen dat rekening houden met de actuele anatomie van de patiënt noodzakelijk is. Tien patiënten zijn behandeld voor enkel of meervoudige lymfeklier oligometastasen in het bekken of para-aortische gebied op de 1.5T MR-linac met een voorgeschreven dosis van 5 x 7Gy en een 3mm isotrope PTV marge. Voor elke fractie was er een plan gegenereerd middels de adapt-to-shape (ATS) procedure, waarbij het plan aangepast wordt op de nieuwe anatomie en intekeningen zoals zichtbaar op de direct daarvoor gemaakte MRI beelden van de patiënt. Deze zijn vergeleken met plannen welke aangepast zijn via de adapt-to-position (ATP) procedure, waarin planadaptatie plaatsvindt op basis van de nieuwe positie van de patiënt. Hierbij wordt er geen rekening gehouden

met de huidige anatomie van de patiënt. Aan het einde van elke bestralingsfractie waren er nieuwe MRI beelden gemaakt waarop het zichtbare deel (gross tumor volume, GTV) van de tumor werd ingetekend om de dosisdekking van het GTV en te evalueren of de toegepaste PTV marge voldoet. De mediaan van het volume van de PTV welke minimaal 35Gy kreeg (V_{35Gy}) was 99.9% [90.7–100%] voor de klinisch afgestraalde ATS plannen vergeleken met 93.6% [76.3–99.7%] voor de ATP plannen. De mediaan van de GTV V_{35Gy} tijdens behandeling was respectievelijk 100% [98–100%] op de MRI voor bestraling en MRI na bestraling voor ATS en 100% [93.9–100%] voor ATP. De toegepaste 3mm isotrope PTV marge was adequaat. Voor gemetastaseerde lymfeklieren in het bekken en para-aortale gebied zorgt MRI-gestuurde radiotherapie met planadaptatie op de huidige anatomie van de patiënt voor adequate dosisdekking van het GTV en het PTV. Over het algemeen bleef de dosisdekking van het GTV adequaat gedurende de behandeling voor zowel ATS als ATP-gebaseerde planadaptatie, maar waren er door gebruik van de ATS procedure meer fracties waar aan alle dosiscriteria voldaan werd.

In hoofdstuk 7 worden de dosisdekking en dosiscriteria van de eerste 1.5T MR-linac stereotactische behandelingen voor enkele en meerdere lymfeklier oligometastasen geëvalueerd en vergeleken met de situatie wanneer deze patiënten op een conventionele CBCT-linac behandeld zouden zijn. Hiervoor is gebruikgemaakt van patiëntdata van 14 patiënten met enkele lymfeklier oligometastasen en 6 patiënten met meerdere (2-3) metastasen. Alle patiënten zijn behandeld op de 1.5T MR-linac met een voorgeschreven dosis van 5 x 7Gy op 95% van het PTV. Daarnaast was er voor elke patiënt een CBCT-linac dosisplan gemaakt. De dosimetrische verschillen tussen deze plannen werden vergeleken voor elke fractie na berekening van het CBCT-plan op de dagelijkse patiëntanatomie. De dosisdekking van het GTV was geëvalueerd op basis van de MRI beelden gemaakt direct voorafgaand aan de bestraling en de MRI beelden direct na bestraling. Voor zowel de enkele als meerdere lymfeklier oligometastasen had de GTV V_{35Gy} een mediaan van 100% voor zowel de MR-linac als de CBCT-linac dosisplannen voorafgaand en na bestraling. Hierin zijn geen significante verschillen gevonden. Het percentage plannen dat voldeed aan alle dosiscriteria was respectievelijk verbeterd van 19% naar 84% en van 20% naar 67% voor enkele en meerdere lymfeklieren oligometastasen. Evaluatie van de dosisdekking en de dosiscriteria voor de eerste klinische 1.5T MR-linac stereotactische behandelingen van lymfeklier oligometastasen vergeleken met conventionele CBCT-linac behandelingen laten een kleinere hoeveelheid overschrijdingen van de dosiscriteria zien. De dosisdekking van het GTV was vergelijkbaar. Voordeel is voornamelijk behaald voor patiënten welke behandeld worden voor meerdere lymfeklier metastasen: er wordt rekening gehouden met geometrische deformaties, dosis kan afgestraald worden in één plan en marges

zijn gereduceerd.

Automatische dosisplanning en verschillende MRI-gestuurde planadaptatiemethoden zijn besproken. Het werk beschreven in dit proefschrift bevat daarnaast de introductie van stereotactische behandeling van lymfeklier oligometastasen op de 1.5T MR-linac door het simuleren van de potentiele dosimetrische winst, het bepalen van de meest geschikte planadaptatiestrategie en door het evalueren van de behandelingen ten opzichte van de conventionele CBCT-linac behandeling en alternatieve strategieën. Essentieel gezien beschrijft dit proefschrift een mogelijke blauwdruk voor de introductie van nieuwe MRI-gestuurde adaptieve behandelingen op de 1.5T MR-linac.

References

References

[1] Delaney, G., Jacob, S., Featherstone, C., and Barton, M. (2005). The role of radiotherapy in cancer treatment: estimating optimal utilization from a review of evidence-based clinical guidelines. *Cancer*, volume 104(6):1129–37. ISSN 0008-543X (Print) 0008-543x.

[2] Baskar, R., Lee, K.A., Yeo, R., and Yeoh, K.W. (2012). Cancer and radiation therapy: current advances and future directions. *International journal of medical sciences*, volume 9(3):193–199. ISSN 1449-1907.

[3] Khan, F.M. and Gibbons, J.P. (2014). *Khan's the physics of radiation therapy*. Lippincott Williams Wilkins. ISBN 1451182457.

[4] Hoskin, P. (2019). *External Beam Therapy*. Oxford University Press. ISBN 0191090336.

[5] Holthusen, H. (1936). Erfahrungen über die verträglichkeitsgrenze für röntgenstrahlen und deren nutzanwendung zur verhütung von schäden. *Strahlentherapie*, volume 57:254–269.

[6] Dörr, W. (2015). Radiobiology of tissue reactions. *Annals of the ICRP*, volume 44(s1):58–68.

[7] Withers, H.R. (1985). Biologic basis for altered fractionation schemes. *Cancer*, volume 55(9 Suppl):2086–95. ISSN 0008-543X (Print) 0008-543x.

[8] van Herk, M., Remeijer, P., Rasch, C., and Lebesque, J.V. (2000). The probability of correct target dosage: dose-population histograms for deriving treatment margins in radiotherapy. *Int J Radiat Oncol Biol Phys*, volume 47(4):1121–35. ISSN 0360-3016 (Print) 0360-3016.

[9] van Herk, M. (2004). Errors and margins in radiotherapy. *Semin Radiat Oncol*, volume 14(1):52–64. ISSN 1053-4296 (Print) 1053-4296.

[10] Heerkens, H.D., Reerink, O., Intven, M.P.W., et al. (2017). Pancreatic tumor motion reduction by use of a custom abdominal corset. *Phys Imag Radiat Oncol*, volume 2:7–10. ISSN 2405-6316.

[11] Pilipuf, M.N., Goble, J.C., and Kassell, N.F. (1995). A noninvasive thermoplastic head immobilization system. *Journal of neurosurgery*, volume 82(6):1082–1085. ISSN 0022-3085.

[12] Ahnesjö, A. and Aspradakis, M.M. (1999). Dose calculations for external photon beams in radiotherapy. *Physics in Medicine and Biology*, volume 44(11):R99–R155. ISSN 0031-9155 1361-6560.

[13] Xiao, Y., Galvin, J., Hossain, M., and Valicenti, R. (2000). An optimized forward-planning technique for intensity modulated radiation therapy. *Medical Physics*, volume 27(9):2093–2099. ISSN 0094-2405.

[14] Taylor, A. and Powell, M.E.B. (2004). Intensity-modulated radiotherapy–what is it? *Cancer imaging : the official publication of the International Cancer Imaging Society*, volume 4(2):68–73. ISSN 1470-7330 1740-5025.

[15] Webb, S. (2003). The physical basis of imrt and inverse planning. *Br J Radiol*, volume 76(910):678–89. ISSN 0007-1285 (Print) 0007-1285.

[16] Voet, P.W., Dirkx, M.L., Breedveld, S., et al. (2013). Toward fully automated multicriterial plan generation: a prospective clinical study. *International Journal of Radiation Oncology* Biology* Physics*, volume 85(3):866–872. ISSN 0360-3016.

[17] Voet, P.W., Dirkx, M.L., Breedveld, S., et al. (2014). Fully automated volumetric modulated arc therapy plan generation for prostate cancer patients. *International Journal of Radiation Oncology* Biology* Physics*, volume 88(5):1175–1179. ISSN 0360-3016.

[18] Wu, B., McNutt, T., Zahurak, M., et al. (2012). Fully automated simultaneous integrated boosted–intensity modulated radiation therapy treatment planning is feasible for head-and-neck cancer: a prospective clinical study. *International Journal of Radiation Oncology* Biology* Physics*, volume 84(5):e647–e653. ISSN 0360-3016.

[19] Wu, B., Pang, D., Simari, P., et al. (2013). Using overlap volume histogram and imrt plan data to guide and automate vmat planning: a head-and-neck case study. *Medical physics*, volume 40(2):021714. ISSN 0094-2405.

[20] Purdie, T.G., Dinniwell, R.E., Letourneau, D., Hill, C., and Sharpe, M.B. (2011). Automated planning of tangential breast intensity-modulated radiotherapy using heuristic optimization. *International Journal of Radiation Oncology* Biology* Physics*, volume 81(2):575–583. ISSN 0360-3016.

[21] Purdie, T.G., Dinniwell, R.E., Fyles, A., and Sharpe, M.B. (2014). Automation and intensity modulated radiation therapy for individualized high-quality tangent breast treatment plans. *International Journal of Radiation Oncology* Biology* Physics*, volume 90(3):688–695. ISSN 0360-3016.

[22] Hussein, M., Heijmen, B.J.M., Verellen, D., and Nisbet, A. (2018). Automation in intensity modulated radiotherapy treatment planning—a review of recent innovations. *The British Journal of Radiology*, volume 91(1092):20180270. ISSN 0007-1285.

[23] Heijkoop, S.T., Langerak, T.R., Quint, S., et al. (2014). Clinical implementation of an online adaptive plan-of-the-day protocol for nonrigid motion management in locally advanced cervical cancer imrt. *International Journal of Radiation Oncology*Biology*Physics*, volume 90(3):673–679. ISSN 0360-3016.

[24] van de Schoot, A.J.A.J., Visser, J., van Kesteren, Z., et al. (2016). Beam configuration selection for robust intensity-modulated proton therapy in cervical cancer using pareto front comparison. *Physics in Medicine and Biology*, volume 61(4):1780–1794. ISSN 0031-9155 1361-6560.

[25] Meijer, G.J., van der Toorn, P.P., Bal, M., et al. (2012). High precision bladder cancer irradiation by integrating a library planning procedure of 6 prospectively generated sib imrt plans with image guidance using lipiodol markers. *Radiotherapy and Oncology*, volume 105(2):174–179. ISSN 0167-8140.

[26] Nwankwo, O., Sihono, D.S.K., Schneider, F., and Wenz, F. (2014). A global quality assurance system for personalized radiation therapy treatment planning for the prostate (or other sites). *Physics in Medicine and Biology*, volume 59(18):5575–5591. ISSN 0031-9155 1361-6560.

[27] Lin, K.M., Simpson, J., Sasso, G., Raith, A., and Ehrgott, M. (2013). Quality assessment for vmat prostate radiotherapy planning based on data envelopment analysis. *Physics in Medicine and Biology*, volume 58(16):5753–5769. ISSN 0031-9155 1361-6560.

[28] Wang, Y., Heijmen, B.J.M., and Petit, S.F. (2017). Prospective clinical validation of independent dvh prediction for plan qa in automatic treatment planning for prostate cancer patients. *Radiotherapy and Oncology*, volume 125(3):500–506. ISSN 0167-8140.

[29] Verellen, D., De Ridder, M., Linthout, N., et al. (2007). Innovations in image-guided radiotherapy. *Nat Rev Cancer*, volume 7(12):949–60. ISSN 1474-1768 (Electronic) 1474-175X (Linking).

[30] Oldham, M., Létourneau, D., Watt, L., et al. (2005). Cone-beam-ct guided radiation therapy: A model for on-line application. *Radiotherapy and oncology*, volume 75(3):271. E1–271. E8. ISSN 0167-8140.

[31] Litzenberg, D., Dawson, L.A., Sandler, H., et al. (2002). Daily prostate targeting using implanted radiopaque markers. *Int J Radiat Oncol Biol Phys*, volume 52(3):699–703.

[32] Dehnad, H., Nederveen, A.J., Heide, U.A.v.d., et al. (2003). Clinical feasibility study for the use of implanted gold seeds in the prostate as reliable positioning markers during megavoltage irradiation. *Radiother Oncol*, volume 67(3):295–302. ISSN 0167-8140.

[33] Purdie, T.G., Bissonnette, J.P., Franks, K., et al. (2007). Cone-beam computed tomography for on-line image guidance of lung stereotactic radiotherapy: localization, verification, and intrafraction tumor position. *Int J Radiat Oncol Biol Phys*, volume 68(1):243–52. ISSN 0360-3016 (Print) 0360-3016 (Linking).

[34] Acharya, S., Fischer-Valuck, B.W., Kashani, R., et al. (2016). Online magnetic resonance image guided adaptive radiation therapy: first clinical applications. *International Journal of Radiation Oncology* Biology* Physics*, volume 94(2):394–403. ISSN 0360-3016.

[35] Mutic, S. and Dempsey, J.F. (2014). The viewray system: magnetic resonance-guided and controlled radiotherapy. *Semin Radiat Oncol*, volume 24(3):196–9. ISSN 1532-9461 (Electronic) 1053-4296 (Linking).

[36] Raaymakers, B.W., Jurgenliemk-Schulz, I.M., Bol, G.H., et al. (2017). First patients treated with a 1.5 t mri-linac: clinical proof of concept of a high-precision, high-field mri guided radiotherapy treatment. *Phys Med Biol*, volume 62(23):L41–L50. ISSN 1361-6560 (Electronic) 0031-9155 (Linking).

[37] Noel, C.E., Parikh, P.J., Spencer, C.R., et al. (2015). Comparison of onboard low-field magnetic resonance imaging versus onboard computed tomography for anatomy visualization in radiotherapy. *Acta Oncol*, volume 54(9):1474–82. ISSN 1651-226X (Electronic) 0284-186X (Linking).

[38] Barillot, I. and Reynaud-Bougnoux, A. (2006). The use of mri in planning radiotherapy for gynaecological tumours. *Cancer Imaging*, volume 6(1):100–106. ISSN 1740-5025 1470-7330.

[39] Winkel, D., Bol, G.H., Kiekebosch, I.H., et al. (2018). Evaluation of online plan adaptation strategies for the 1.5t mr-linac based on "first-in-man" treatments. *Cureus*, volume 10(4):e2431. ISSN 2168-8184 (Print) 2168-8184 (Linking).

[40] Timmerman, R.D., Kavanagh, B.D., Cho, L.C., Papiez, L., and Xing, L. (2007). Stereotactic body radiation therapy in multiple organ sites. *J Clin Oncol*, volume 25(8):947–52. ISSN 1527-7755 (Electronic) 0732-183X (Linking).

[41] Timmerman, R., Paulus, R., Galvin, J., et al. (2010). Stereotactic body radiation therapy for inoperable early stage lung cancer. *JAMA*, volume 303(11):1070–1076. ISSN 1538-3598 0098-7484.

[42] Benedict, S.H., Yenice, K.M., Followill, D., et al. (2010). Stereotactic body radiation therapy: the report of aapm task group 101. *Med Phys*, volume 37(8):4078–101. ISSN 0094-2405 (Print) 0094-2405 (Linking).

[43] Park, H.J., Chang, A.R., Seo, Y., et al. (2015). Stereotactic body radiotherapy for recurrent or oligometastatic uterine cervix cancer: A cooperative study of the korean radiation oncology group (krog 14-11). *Anticancer Res*, volume 35(9):5103–10. ISSN 1791-7530 (Electronic) 0250-7005 (Linking).

[44] Choi, C.W., Cho, C.K., Yoo, S.Y., et al. (2009). Image-guided stereotactic body radiation therapy in patients with isolated para-aortic lymph node metastases from uterine cervical and corpus cancer. *Int J Radiat Oncol Biol Phys*, volume 74(1):147–53. ISSN 1879-355X (Electronic) 0360-3016 (Linking).

[45] Jereczek-Fossa, B.A., Fanetti, G., Fodor, C., et al. (2017). Salvage stereotactic body radiotherapy for isolated lymph node recurrent prostate cancer: Single institution series of 94 consecutive patients and 124 lymph nodes. *Clin Genitourin Cancer*, volume 15(4):e623–e632. ISSN 1938-0682 (Electronic) 1558-7673 (Linking).

[46] Yeung, R., Hamm, J., Liu, M., and Schellenberg, D. (2017). Institutional analysis of stereotactic body radiotherapy (sbrt) for oligometastatic lymph node metastases. *Radiat Oncol*, volume 12(1):105. ISSN 1748-717X (Electronic) 1748-717X (Linking).

[47] Casamassima, F., Livi, L., Masciullo, S., et al. (2012). Stereotactic radiotherapy for adrenal gland metastases: University of florence experience. *International Journal of Radiation Oncology • Biology • Physics*, volume 82(2):919–923. ISSN 0360-3016.

[48] Plichta, K., Camden, N., Furqan, M., et al. (2017). Sbrt to adrenal metastases provides high local control with minimal toxicity. *Advances in radiation oncology*, volume 2(4):581–587. ISSN 2452-1094.

[49] Owen, D., Laack, N.N., Mayo, C.S., et al. (2014). Outcomes and toxicities of stereotactic body radiation therapy for non-spine bone oligometastases. *Practical Radiation Oncology*, volume 4(2):e143–e149. ISSN 1879-8500.

[50] Fowler, J., Chappell, R., and Ritter, M. (2001). Is / for prostate tumors really low? *International Journal of Radiation Oncology*Biology*Physics*, volume 50(4):1021–1031. ISSN 0360-3016.

[51] Tree, A.C., Khoo, V.S., Eeles, R.A., et al. (2013). Stereotactic body radiotherapy for oligometastases. *The Lancet Oncology*, volume 14(1):e28–e37. ISSN 14702045.

[52] Bouman-Wammes, E.W., van Dodewaard-De Jong, J.M., Dahele, M., et al. (2017). Benefits of using stereotactic body radiotherapy in patients with metachronous oligometastases of hormone-sensitive prostate cancer detected by [18f]fluoromethylcholine pet/ct. *Clinical Genitourinary Cancer*, volume 15(5):e773–e782. ISSN 1558-7673.

[53] Ost, P., Reynders, D., Decaestecker, K., et al. (2017). Surveillance or metastasis-directed therapy for oligometastatic prostate cancer recurrence: A prospective, randomized, multicenter phase ii trial. *Journal of Clinical Oncology*, volume 36(5):446–453. ISSN 0732-183X.

[54] Taylor, L.G., Canfield, S.E., and Du, X.L. (2009). Review of major adverse effects of androgen-deprivation therapy in men with prostate cancer. *Cancer*, volume 115(11):2388–2399. ISSN 0008-543X.

[55] Ponti, E., Lancia, A., Ost, P., et al. (2017). Exploring all avenues for radiotherapy in oligorecurrent prostate cancer disease limited to lymph nodes: A systematic review of the role of stereotactic body radiotherapy. *Eur Urol Focus*, volume 3(6):538–544. ISSN 2405-4569 (Electronic) 2405-4569 (Linking).

[56] Detti, B., Bonomo, P., Masi, L., et al. (2015). Stereotactic radiotherapy for isolated nodal recurrence of prostate cancer. *World J Urol*, volume 33(8):1197–203. ISSN 1433-8726 (Electronic) 0724-4983 (Linking).

[57] Muldermans, J.L., Romak, L.B., Kwon, E.D., Park, S.S., and Olivier, K.R. (2016). Stereotactic body radiation therapy for oligometastatic prostate cancer. *Int J Radiat Oncol Biol Phys*, volume 95(2):696–702. ISSN 1879-355X (Electronic) 0360-3016 (Linking).

[58] Podgorsak, E. and Kainz, K. (2006). Radiation oncology physics: A handbook for teachers and students. *International Atomic Energy Agency*.

[59] Nelms, B.E., Robinson, G., Markham, J., et al. (2012). Variation in external beam treatment plan quality: an inter-institutional study of planners and planning systems. *Practical radiation oncology*, volume 2(4):296–305. ISSN 1879-8500.

[60] Das, I.J., Cheng, C.W., Chopra, K.L., et al. (2008). Intensity-modulated radiation therapy dose prescription, recording, and delivery: patterns of variability among institutions and treatment planning systems. *Journal of the National Cancer Institute*, volume 100(5):300–307. ISSN 1460-2105.

[61] Lagendijk, J., Raaymakers, B.W., Van Der Heide, U., et al. (2002). Mri guided radiotherapy: Mri as position verification system for imrt. *Radiotherapy and Oncology*, volume 64(5):S75–S76.

[62] Lagendijk, J.J.W., Raaymakers, B.W., and van Vulpen, M. (2014). The magnetic resonance imaging–linac system. *Seminars in Radiation Oncology*, volume 24(3):207–209. ISSN 1053-4296.

[63] Raaymakers, B., Lagendijk, J., Overweg, J., et al. (2009). Integrating a 1.5 t mri scanner with a 6 mv accelerator: proof of concept. *Physics in Medicine & Biology*, volume 54(12):N229. ISSN 0031-9155.

[64] Breedveld, S., Storchi, P.R., Voet, P.W., and Heijmen, B.J. (2012). icycle: Integrated, multicriterial beam angle, and profile optimization for generation of coplanar and noncoplanar imrt plans. *Med Phys*, volume 39(2):951–63. ISSN 0094-2405 (Print) 0094-2405. Breedveld, Sebastiaan Storchi, Pascal R M Voet, Peter W J Heijmen, Ben J M Journal Article United States Med Phys. 2012 Feb;39(2):951-63. doi: 10.1118/1.3676689.

[65] Quan, E.M., Li, X., Li, Y., et al. (2012). A comprehensive comparison of imrt and vmat plan quality for prostate cancer treatment. *International Journal of Radiation Oncology* Biology* Physics*, volume 83(4):1169–1178. ISSN 0360-3016.

[66] Song, Y., Wang, Q., Jiang, X., et al. (2016). Fully automatic volumetric modulated arc therapy plan generation for rectal cancer. *Radiotherapy and Oncology*, volume 119(3):531–536. ISSN 0167-8140.

[67] Quan, E.M., Chang, J.Y., Liao, Z., et al. (2012). Automated volumetric modulated arc therapy treatment planning for stage iii lung cancer: how does it compare with intensity-modulated radio therapy? *International Journal of Radiation Oncology* Biology* Physics*, volume 84(1):e69–e76. ISSN 0360-3016.

[68] Nijkamp, J., Pos, F.J., Nuver, T.T., et al. (2008). Adaptive radiotherapy for prostate cancer using kilovoltage cone-beam computed tomography: first clinical results. *International Journal of Radiation Oncology* Biology* Physics*, volume 70(1):75–82. ISSN 0360-3016.

[69] Werensteijn-Honingh, A.M., Kroon, P.S., Winkel, D., et al. (2019). Feasibility of stereotactic radiotherapy using a 1.5t mr-linac: Multi-fraction treatment of pelvic lymph node oligometastases. *Radiotherapy and Oncology*, volume 134:50–54. ISSN 0167-8140.

[70] Kleijnen, J.P.J.E., van Asselen, B., Burbach, J.P.M., et al. (2015). Evolution of motion uncertainty in rectal cancer: implications for adaptive radiotherapy. *Physics in Medicine and Biology*, volume 61(1):1–11.

[71] Stemkens, B., Glitzner, M., Kontaxis, C., et al. (2017). Effect of intra-fraction motion on the accumulated dose for free-breathing mr-guided stereotactic body radiation therapy of renal-cell carcinoma. *Physics in Medicine & Biology*, volume 62(18):7407.

[72] Kontaxis, C., Bol, G.H., Stemkens, B., et al. (2017). Towards fast online intrafraction replanning for free-breathing stereotactic body radiation therapy with the mr-linac. *Phys Med Biol*, volume 62(18):7233–7248. ISSN 1361-6560 (Electronic) 0031-9155 (Linking).

[73] Van der Heide, U.A., Houweling, A.C., Groenendaal, G., Beets-Tan, R.G., and Lambin, P. (2012). Functional mri for radiotherapy dose painting. *Magnetic resonance imaging*, volume 30(9):1216–1223.

[74] van Rossum, P.S., van Lier, A.L., van Vulpen, M., et al. (2015). Diffusion-weighted magnetic resonance imaging for the prediction of pathologic response to neoadjuvant chemoradiotherapy in esophageal cancer. *Radiotherapy and Oncology*, volume 115(2):163–170.

[75] Ahunbay, E.E., Peng, C., Chen, G.P., et al. (2008). An on-line replanning scheme for interfractional variations. *Med Phys*, volume 35(8):3607–15. ISSN 0094-2405 (Print) 0094-2405 (Linking).

[76] Jonsson, J.H., Karlsson, M.G., Karlsson, M., and Nyholm, T. (2010). Treatment planning using mri data: an analysis of the dose calculation accuracy for different treatment regions. *Radiation oncology*, volume 5(1):62.

[77] Hoogcarspel, S.J., Van der Velden, J.M., Lagendijk, J.J., Van Vulpen, M., and Raaymakers, B.W. (2014). The feasibility of utilizing pseudo ct-data for online mri based treatment plan adaptation for a stereotactic radiotherapy treatment of spinal bone metastases. *Physics in Medicine & Biology*, volume 59(23):7383.

[78] Raaijmakers, A., Raaymakers, B.W., and Lagendijk, J.J. (2005). Integrating a mri scanner with a 6 mv radiotherapy accelerator: dose increase at tissue–air interfaces in a lateral magnetic field due to returning electrons. *Physics in Medicine & Biology*, volume 50(7):1363.

[79] Winkel, D., Werensteijn-Honingh, A.M., Kroon, P.S., et al. (2019). Individual lymph nodes: "see it and zap it". *Clinical and Translational Radiation Oncology*. ISSN 2405-6308.

[80] Winkel, D., Bol, G.H., Werensteijn-Honingh, A.M., et al. (2019). Evaluation of plan adaptation strategies for stereotactic radiotherapy of lymph node oligometastases using online magnetic resonance image guidance. *Physics and Imaging in Radiation Oncology*, volume 9:58–64.

[81] Kontaxis, C., Bol, G.H., Lagendijk, J.J., and Raaymakers, B.W. (2015). A new methodology for inter- and intrafraction plan adaptation for the mr-linac. *Phys Med Biol*, volume 60(19):7485–97. ISSN 0031-9155.

[82] Kontaxis, C., Bol, G.H., Kerkmeijer, L.G., Lagendijk, J.J., and Raaymakers, B.W. (2017). Fast online replanning for interfraction rotation correction in prostate radiotherapy. *Medical physics*, volume 44(10):5034–5042.

[83] Zachiu, C., de Senneville, B.D., Moonen, C.T.W., Raaymakers, B.W., and Ries, M. (2018). Anatomically plausible models and quality assurance criteria for online mono- and multimodal medical image registration. *Phys Med Biol*, volume 63(15):155016. ISSN 0031-9155.

[84] Jaffray, D.A., Siewerdsen, J.H., Wong, J.W., and Martinez, A.A. (2002). Flat-panel cone-beam computed tomography for image-guided radiation therapy. *Int J Radiat Oncol Biol Phys*, volume 53(5):1337–1349. ISSN 0360-3016.

[85] Bohoudi, O., Bruynzeel, A.M.E., Senan, S., et al. (2017). Fast and robust online adaptive planning in stereotactic mr-guided adaptive radiation therapy (smart) for pancreatic cancer. *Radiother Oncol*, volume 125(3):439–444. ISSN 0167-8140.

[86] Timmerman, R.D. and Kavanagh, B.D. (2005). Stereotactic body radiation therapy. *Curr Probl Cancer*, volume 29(3):120–57. ISSN 0147-0272 (Print) 0147-0272 (Linking).

[87] Scorsetti, M., Clerici, E., and Comito, T. (2014). Stereotactic body radiation therapy for liver metastases. *J Gastrointest Oncol*, volume 5(3):190–7. ISSN 2078-6891 (Print) 2078-6891 (Linking).

[88] Kerkhof, E.M., Balter, J.M., Vineberg, K., and Raaymakers, B.W. (2010). Treatment plan adaptation for mri-guided radiotherapy using solely mri data: a ct-based simulation study. *Phys Med Biol*, volume 55(16):N433–40. ISSN 0031-9155.

[89] Henke, L., Kashani, R., Yang, D., et al. (2016). Simulated online adaptive magnetic resonance-guided stereotactic body radiation therapy for the treatment of oligometastatic disease of the abdomen and central thorax: Characterization of potential advantages. *Int J Radiat Oncol Biol Phys*, volume 96(5):1078–1086. ISSN 1879-355X (Electronic) 0360-3016 (Linking).

[90] Nomden, C.N., de Leeuw, A.A., Roesink, J.M., et al. (2014). Intra-fraction uncertainties of mri guided brachytherapy in patients with cervical cancer. *Radiotherapy and Oncology*, volume 112(2):217–220.

[91] Verkooijen, H.M., Kerkmeijer, L.G.W., Fuller, C.D., et al. (2017). R-ideal: A framework for systematic clinical evaluation of technical innovations in radiation oncology. *Front Oncol*, volume 7:59. ISSN 2234-943X.

[92] Grimm, J., LaCouture, T., Croce, R., et al. (2011). Dose tolerance limits and dose volume histogram evaluation for stereotactic body radiotherapy. *Journal of applied clinical medical physics*, volume 12(2):267–292.

[93] Wiersema, L., Borst, G., Nakhaee, S., et al. (2017). First igrt results for sbrt bone and lymph node oligometastases within the pelvic region. *Radiother Oncol*, volume 123:S1006.

[94] Gerlich, A., Van der Velden, J., Fanetti, G., et al. (2017). Ep-1620: The immobilizing effect of the vacuum cushion in spinal sbrt and the impact of pain. *Radiotherapy and Oncology*, volume 123:S876–S877.

[95] Seravalli, E., van Haaren, P.M.A., van der Toorn, P.P., and Hurkmans, C.W. (2015). A comprehensive evaluation of treatment accuracy, including end-to-end tests and clinical data, applied to intracranial stereotactic radiotherapy. *Radiother Oncol*, volume 116(1):131–138. ISSN 0167-8140.

[96] Velema, L., Bondar, M., Mens, J., and Hoogeman, M. (2012). Oc-0463 nodal ctv deformation cannot be neglected in highly conformal radiotherapy of cervical cancer patients. *Radiotherapy and Oncology*, volume 103:S185–S186.

[97] Schippers, M.G., Bol, G.H., de Leeuw, A.A., et al. (2014). Position shifts and volume changes of pelvic and para-aortic nodes during imrt for patients with cervical cancer. *Radiother Oncol*, volume 111(3):442–5. ISSN 1879-0887 (Electronic) 0167-8140 (Linking).

[98] van de Bunt, L., Jürgenliemk-Schulz, I.M., de Kort, G.A.P., et al. (2008). Motion and deformation of the target volumes during imrt for cervical cancer: What margins do we need? *Radiother Oncol*, volume 88(2):233–240. ISSN 0167-8140.

[99] Liu, F., Erickson, B., Peng, C., and Li, X.A. (2012). Characterization and management of interfractional anatomic changes for pancreatic cancer radiotherapy. *International Journal of Radiation Oncology* Biology* Physics*, volume 83(3):e423–e429.

[100] Peng, C., Ahunbay, E., Chen, G., et al. (2011). Characterizing interfraction variations and their dosimetric effects in prostate cancer radiotherapy. *International Journal of Radiation Oncology* Biology* Physics*, volume 79(3):909–914.

[101] Thor, M., Bentzen, L., Hysing, L.B., et al. (2013). Prediction of rectum and bladder morbidity following radiotherapy of prostate cancer based on motion-inclusive dose distributions. *Radiotherapy and Oncology*, volume 107(2):147–152.

[102] Thornqvist, S., Hysing, L.B., Tuomikoski, L., et al. (2016). Adaptive radiotherapy strategies for pelvic tumors - a systematic review of clinical implementations. *Acta Oncol*, volume 55(8):943–58. ISSN 1651-226X (Electronic) 0284-186X (Linking).

[103] Wahl, M., Descovich, M., Shugard, E., et al. (2017). Interfraction anatomical variability can lead to significantly increased rectal dose for patients undergoing stereotactic body radiotherapy for prostate cancer. *Technol Cancer Res Treat*, volume 16(2):178–187. ISSN 1533-0338 (Electronic) 1533-0338 (Linking).

[104] Greco, C., Zelefsky, M.J., Lovelock, M., et al. (2011). Predictors of local control after single-dose stereotactic image-guided intensity-modulated radiotherapy for extracranial metastases. *Int J Radiat Oncol Biol Phys*, volume 79(4):1151–7. ISSN 1879-355X (Electronic) 0360-3016 (Linking).

[105] Salama, J.K., Hasselle, M.D., Chmura, S.J., et al. (2012). Stereotactic body radiotherapy for multisite extracranial oligometastases: final report of a dose escalation trial in patients with 1 to 5 sites of metastatic disease. *Cancer*, volume 118(11):2962–70. ISSN 0008-543x.

[106] Jereczek-Fossa, B.A., Beltramo, G., Fariselli, L., et al. (2012). Robotic image-guided stereotactic radiotherapy, for isolated recurrent primary, lymph node or metastatic prostate cancer. *Int J Radiat Oncol Biol Phys*, volume 82(2):889–97. ISSN 1879-355X (Electronic) 0360-3016 (Linking).

[107] van de Schoot, A.J.A.J., de Boer, P., Visser, J., et al. (2017). Dosimetric advantages of a clinical daily adaptive plan selection strategy compared with a non-adaptive strategy in cervical cancer radiation therapy. *Acta Oncologica*, volume 56(5):667–674. ISSN 0284-186X.

[108] Li, Y., Hoisak, J.D., Li, N., et al. (2015). Dosimetric benefit of adaptive re-planning in pancreatic cancer stereotactic body radiotherapy. *Med Dosim*, volume 40(4):318–24. ISSN 1873-4022.

[109] Clark, G.M., Popple, R.A., Prendergast, B.M., et al. (2012). Plan quality and treatment planning technique for single isocenter cranial radiosurgery with volumetric modulated arc therapy. *Pract Radiat Oncol*, volume 2(4):306–313. ISSN 1879-8500.

[110] Chen, G., Wang, K., and Li, X. (2009). Independent interfraction motion of regional lymph nodes and breast targets in image-guided radiotherapy of breast cancer. *International Journal of Radiation Oncology*Biology*Physics*, volume 75(3, Supplement):S208. ISSN 0360-3016.

[111] Bol, G.H., Lagendijk, J.J., and Raaymakers, B.W. (2013). Virtual couch shift (vcs): accounting for patient translation and rotation by online imrt re-optimization. *Phys Med Biol*, volume 58(9):2989–3000. ISSN 0031-9155.

[112] Antonuk, L.E. (2002). Electronic portal imaging devices: A review and historical perspective of contemporary technologies and research. *Physics in Medicine and Biology*, volume 47(6):R31–R65.

[113] Lagendijk, J.J.W., Raaymakers, B.W., Raaijmakers, A.J.E., et al. (2008). Mri/linac integration. *Radiother Oncol*, volume 86(1):25–29. ISSN 0167-8140.

[114] Lamb, J., Cao, M., Kishan, A., et al. (2017). Online adaptive radiation therapy: Implementation of a new process of care. *Cureus*, volume 9(8):e1618. ISSN 2168-8184.

[115] Baumann, R., Koncz, M., Luetzen, U., Krause, F., and Dunst, J. (2018). Oligometastases in prostate cancer : Metabolic response in follow-up psma-pet-cts after hypofractionated igrt. *Strahlenther Onkol*, volume 194(4):318–324. ISSN 1439-099X (Electronic) 0179-7158 (Linking).

[116] Loi, M., Frelinghuysen, M., Klass, N.D., et al. (2018). Locoregional control and survival after lymph node sbrt in oligometastatic disease. *Clin Exp Metastasis*. ISSN 1573-7276 (Electronic) 0262-0898 (Linking).

[117] Winkel, D., Kroon, P.S., Werensteijn-Honingh, A.M., et al. (2018). Simulated dosimetric impact of online replanning for stereotactic body radiation therapy of lymph node oligometastases on the 1.5t mr-linac. *Acta Oncol*, pp. 1–8. ISSN 0284-186X.

[118] Henke, L., Kashani, R., Robinson, C., et al. (2018). Phase i trial of stereotactic mr-guided online adaptive radiation therapy (smart) for the treatment of oligometastatic or unresectable primary malignancies of the abdomen. *Radiother Oncol*, volume 126(3):519–526. ISSN 0167-8140.

[119] Goodburn, R.J., Tijssen, R.H.N., and Philippens, M.E.P. (2018). Ep-2147: Comparison of spatial-distortion maps for mrsim versus mr-linac in the brain and pelvis at 1.5t. *Radiother Oncol*, volume 127:S1184–S1185. ISSN 0167-8140.

[120] Winkel, D., Kroon, P., Hes, J., et al. (2017). Ep-1663: Automated full-online replanning of sbrt lymph node oligometastases for the mr-linac. *Radiother Oncol*, volume 123:S904. ISSN 0167-8140.

[121] Hissoiny, S., Raaijmakers, A.J., Ozell, B., Despres, P., and Raaymakers, B.W. (2011). Fast dose calculation in magnetic fields with gpumcd. *Phys Med Biol*, volume 56(16):5119–29. ISSN 1361-6560 (Electronic) 0031-9155 (Linking).

[122] Wells, W. M., r., Viola, P., Atsumi, H., Nakajima, S., and Kikinis, R. (1996). Multi-modal volume registration by maximization of mutual information. *Med Image Anal*, volume 1(1):35–51. ISSN 1361-8415 (Print) 1361-8415 (Linking).

[123] Wu, J., Haycocks, T., Alasti, H., et al. (2001). Positioning errors and prostate motion during conformal prostate radiotherapy using on-line isocentre set-up verification and implanted prostate markers. *Radiother Oncol*, volume 61(2):127–133. ISSN 0167-8140.

[124] Pang, E.P.P., Knight, K., Fan, Q., et al. (2018). Analysis of intra-fraction prostate motion and derivation of duration-dependent margins for radiotherapy using real-time 4d ultrasound. *Phys Imag Radiat Oncol*, volume 5:102–107. ISSN 2405-6316.

[125] Brunner, T.B., Nestle, U., Grosu, A.L., and Partridge, M. (2015). Sbrt in pancreatic cancer: What is the therapeutic window? *Radiother Oncol*, volume 114(1):109–116. ISSN 0167-8140.

[126] Palacios, M.A., Bohoudi, O., Bruynzeel, A.M.E., et al. (2018). Role of daily plan adaptation in mr-guided stereotactic ablative radiation therapy for adrenal metastases. *Int J Radiat Oncol Biol Phys*, volume 102(2):426–433. ISSN 0360-3016.

[127] Tyran, M., Cao, M., Raldow, A.C., et al. (2018). Stereotactic magnetic resonance-guided online adaptive radiotherapy for oligometastatic breast cancer: A case report. *Cureus*, volume 10(3):e2368. ISSN 2168-8184 (Print) 2168-8184 (Linking).

[128] Kotte, A.N., Hofman, P., Lagendijk, J.J., van Vulpen, M., and van der Heide, U.A. (2007). Intrafraction motion of the prostate during external-beam radiation therapy: analysis of 427 patients with implanted fiducial markers. *Int J Radiat Oncol Biol Phys*, volume 69(2):419–25. ISSN 0360-3016 (Print) 0360-3016 (Linking).

[129] Cramer, A.K., Haile, A.G., Ognjenovic, S., et al. (2013). Real-time prostate motion assessment: image-guidance and the temporal dependence of intra-fraction motion. *BMC Med Phys*, volume 13(1):4. ISSN 1756-6649 (Print) 1756-6649 (Linking).

[130] Pathmanathan, A.U., van As, N.J., Kerkmeijer, L.G.W., et al. (2018). Magnetic resonance imaging-guided adaptive radiation therapy: A "game changer" for prostate treatment? *Int J Radiat Oncol Biol Phys*, volume 100(2):361–373. ISSN 1879-355X (Electronic) 0360-3016 (Linking).

[131] De Bleser, E., Tran, P.T., and Ost, P. (2017). Radiotherapy as metastasis-directed therapy for oligometastatic prostate cancer. *Curr Opin Urol*, volume 27(6):587–595. ISSN 0963-0643.

[132] Otake, S. and Goto, T. (2019). Stereotactic radiotherapy for oligometastasis. *Cancers*, volume 11(2):133. ISSN 2072-6694.

[133] Hellman, S. and Weichselbaum, R.R. (2005). Importance of local control in an era of systematic therapy. *Nature Clinical Practice Oncology*, volume 2(2):60–61.

[134] Steuber, T., Jilg, C., Tennstedt, P., et al. (2018). Standard of care versus metastases-directed therapy for pet-detected nodal oligorecurrent prostate cancer following multi-modality treatment: A multi-institutional case-control study. *Eur Urol Focus*. ISSN 2405-4569.

[135] Timmerman, R.D., Bizekis, C.S., Pass, H.I., et al. (2009). Local surgical, ablative, and radiation treatment of metastases. *CA Cancer J Clin*, volume 59(3):145–70. ISSN 0007-9235 (Print) 0007-9235.

[136] Aitken, K.L. and Hawkins, M.A. (2015). Stereotactic body radiotherapy for liver metastases. *Clin Oncol (R Coll Radiol)*, volume 27(5):307–15. ISSN 0936-6555.

[137] Shultz, D.B., Filippi, A.R., Thariat, J., et al. (2014). Stereotactic ablative radiotherapy for pulmonary oligometastases and oligometastatic lung cancer. *J Thorac Oncol*, volume 9(10):1426–33. ISSN 1556-0864.

[138] Comito, T., Cozzi, L., Clerici, E., et al. (2014). Stereotactic ablative radiotherapy (sabr) in inoperable oligometastatic disease from colorectal cancer: a safe and effective approach. *BMC Cancer*, volume 14:619. ISSN 1471-2407.

[139] Andratschke, N., Alheid, H., Allgäuer, M., et al. (2018). The sbrt database initiative of the german society for radiation oncology (degro): patterns of care and outcome analysis of stereotactic body radiotherapy (sbrt) for liver oligometastases in 474 patients with 623 metastases. *BMC cancer*, volume 18(1):283–283. ISSN 1471-2407.

[140] Scorsetti, M., Comito, T., Clerici, E., et al. (2018). Phase ii trial on sbrt for unresectable liver metastases: long-term outcome and prognostic factors of survival after 5 years of follow-up. *Radiat Oncol*, volume 13(1):234. ISSN 1748-717x.

[141] Ost, P., Reynders, D., Decaestecker, K., et al. (2018). Surveillance or metastasis-directed therapy for oligometastatic prostate cancer recurrence: A prospective, randomized, multicenter phase ii trial. *Journal of Clinical Oncology*, volume 36(5):446–453. ISSN 0732-183X.

[142] Lancia, A., Zilli, T., Achard, V., et al. (2019). Oligometastatic prostate cancer: The game is afoot. *Cancer Treatment Reviews*, volume 73:84–90. ISSN 0305-7372.

[143] Palacios-Eito, A., Béjar-Luque, A., Rodríguez-Liñán, M., and García-Cabezas, S. (2019). Oligometastases in prostate cancer: Ablative treatment. *World journal of clinical oncology*, volume 10(2):38–51. ISSN 2218-4333.

[144] Chance, W.W., Nguyen, Q.N., Mehran, R., et al. (2017). Stereotactic ablative radiotherapy for adrenal gland metastases: Factors influencing outcomes, patterns of failure, and dosimetric thresholds for toxicity. *Pract Radiat Oncol*, volume 7(3):e195–e203. ISSN 1879-8500.

[145] Ippolito, E., D'Angelillo, R.M., Fiore, M., et al. (2015). Sbrt: A viable option for treating adrenal gland metastases. *Reports of practical oncology and radiotherapy : journal of Greatpoland Cancer Center in Poznan and Polish Society of Radiation Oncology*, volume 20(6):484–490. ISSN 1507-1367 2083-4640.

[146] Moghul, M., Somani, B., Lane, T., et al. (2019). Detection rates of recurrent prostate cancer: (68)gallium (ga)-labelled prostate-specific membrane antigen versus choline pet/ct scans. a systematic review. *Therapeutic advances in urology*, volume 11:1756287218815793–1756287218815793. ISSN 1756-2872 1756-2880.

[147] Pasqualetti, F., Panichi, M., Sainato, A., et al. (2016). [(18)f]choline pet/ct and stereotactic body radiotherapy on treatment decision making of oligometastatic prostate cancer patients: preliminary results. *Radiat Oncol*, volume 11:9. ISSN 1748-717X (Electronic) 1748-717X (Linking).

[148] Laliscia, C., Fabrini, M.G., Delishaj, D., et al. (2017). Clinical outcomes of stereotactic body radiotherapy in oligometastatic gynecological cancer. *Int J Gynecol Cancer*, volume 27(2):396–402. ISSN 1525-1438 (Electronic) 1048-891X (Linking).

[149] Siva, S., Bressel, M., Murphy, D.G., et al. (2018). Stereotactic abative body radiotherapy (sabr) for oligometastatic prostate cancer: A prospective clinical trial. *Eur Urol*, volume 74(4):455–462. ISSN 0302-2838.

[150] Winkel, D., Bol, G., Werensteijn-Honingh, A., et al. (2018). Po-0848: Dose escalation and hypofractionation for sbrt of lymph node oligometastases on the 1.5t mri-linac. *Radiotherapy and Oncology*, volume 127:S443–S444. ISSN 0167-8140.

[151] Winkel, D., Bol, G., Werensteijn-Honingh, A.M., et al. (2019). Ep-2006 dosimetric benefit of the first clinical sbrt of lymph node oligometastases on the 1.5t mr-linac. *Radiotherapy and Oncology*, volume 133:S1098–S1099.

[152] Gordon, J.J. and Siebers, J.V. (2007). Convolution method and ctv-to-ptv margins for finite fractions and small systematic errors. *Phys Med Biol*, volume 52(7):1967–90. ISSN 0031-9155 (Print) 0031-9155.

[153] de Boer, H.C. and Heijmen, B.J. (2001). A protocol for the reduction of systematic patient setup errors with minimal portal imaging workload. *Int J Radiat Oncol Biol Phys*, volume 50(5):1350–65. ISSN 0360-3016 (Print) 0360-3016.

[154] Tijssen, R.H.N., Philippens, M.E.P., Paulson, E.S., et al. (2019). Mri commissioning of 1.5t mr-linac systems – a multi-institutional study. *Radiotherapy and Oncology*, volume 132:114–120. ISSN 0167-8140.

[155] Stroom, J.C. and Heijmen, B.J. (2002). Geometrical uncertainties, radiotherapy planning margins, and the icru-62 report. *Radiother Oncol*, volume 64(1):75–83. ISSN 0167-8140 (Print) 0167-8140.

[156] Tanderup, K., Viswanathan, A.N., Kirisits, C., and Frank, S.J. (2014). Magnetic resonance image guided brachytherapy. *Seminars in Radiation Oncology*, volume 24(3):181–191. ISSN 1053-4296.

[157] Sturdza, A., Pötter, R., Fokdal, L.U., et al. (2016). Image guided brachytherapy in locally advanced cervical cancer: Improved pelvic control and survival in retroembrace, a multicenter cohort study. *Radiotherapy and Oncology*, volume 120(3):428–433. ISSN 0167-8140.

[158] Pötter, R., Tanderup, K., Kirisits, C., et al. (2018). The embrace ii study: The outcome and prospect of two decades of evolution within the gec-estro gyn working group and the embrace studies. *Clinical and Translational Radiation Oncology*, volume 9:48–60. ISSN 2405-6308.

[159] Rijkmans, E.C., Nout, R.A., Rutten, I.H., et al. (2014). Improved survival of patients with cervical cancer treated with image-guided brachytherapy compared with conventional brachytherapy. *Gynecol Oncol*, volume 135(2):231–8. ISSN 0090-8258.

[160] Tanderup, K., Fokdal, L.U., Sturdza, A., et al. (2016). Effect of tumor dose, volume and overall treatment time on local control after radiochemotherapy including mri guided brachytherapy of locally advanced cervical cancer. *Radiother Oncol*, volume 120(3):441–446. ISSN 0167-8140.

[161] Nguyen, P.L., Chen, M.H., Zhang, Y., et al. (2012). Updated results of magnetic resonance imaging guided partial prostate brachytherapy for favorable risk prostate cancer: implications for focal therapy. *J Urol*, volume 188(4):1151–6. ISSN 0022-5347.

[162] Fischer-Valuck, B.W., Henke, L., Green, O., et al. (2017). Two-and-a-half-year clinical experience with the world's first magnetic resonance image guided radiation therapy system. *Adv Radiat Oncol*, volume 2(3):485–493. ISSN 2452-1094 (Print) 2452-1094.

[163] Witte, M.G., van der Geer, J., Schneider, C., Lebesque, J.V., and van Herk, M. (2004). The effects of target size and tissue density on the minimum margin required for random errors. *Med Phys*, volume 31(11):3068–79. ISSN 0094-2405 (Print) 0094-2405.

[164] Pantarotto, J.R., Piet, A.H., Vincent, A., van Sornsen de Koste, J.R., and Senan, S. (2009). Motion analysis of 100 mediastinal lymph nodes: potential pitfalls in treatment planning and adaptive strategies. *Int J Radiat Oncol Biol Phys*, volume 74(4):1092–9. ISSN 1879-355X (Electronic) 0360-3016 (Linking).

[165] Yorke, E., Xiong, Y., Han, Q., et al. (2016). Kilovoltage imaging of implanted fiducials to monitor intrafraction motion with abdominal compression during stereotactic body radiation therapy for gastrointestinal tumors. *Int J Radiat Oncol Biol Phys*, volume 95(3):1042–1049. ISSN 0360-3016.

[166] McPartlin, A.J., Li, X.A., Kershaw, L.E., et al. (2016). Mri-guided prostate adaptive radiotherapy – a systematic review. *Radiotherapy and Oncology*, volume 119(3):371–380. ISSN 0167-8140.

[167] Kerkhof, E.M., van der Put, R.W., Raaymakers, B.W., et al. (2009). Intrafraction motion in patients with cervical cancer: The benefit of soft tissue registration using mri. *Radiotherapy and Oncology*, volume 93(1):115–121. ISSN 0167-8140.

[168] Nijkamp, J., Swellengrebel, M., Hollmann, B., et al. (2012). Repeat ct assessed ctv variation and ptv margins for short- and long-course pre-operative rt of rectal cancer. *Radiotherapy and Oncology*, volume 102(3):399–405. ISSN 0167-8140.

[169] Winkel, D., Bol, G.H., Kroon, P.S., et al. (2019). Adaptive radiotherapy: The elekta unity mr-linac concept. *Clinical and Translational Radiation Oncology*. ISSN 2405-6308.

[170] Roper, J., Chanyavanich, V., Betzel, G., Switchenko, J., and Dhabaan, A. (2015). Single-isocenter multiple-target stereotactic radiosurgery: Risk of compromised coverage. *Int J Radiat Oncol Biol Phys*, volume 93(3):540–6. ISSN 1879-355X (Electronic) 0360-3016 (Linking).

[171] Quan, K., Xu, K.M., Lalonde, R., et al. (2015). Treatment plan technique and quality for single-isocenter stereotactic ablative radiotherapy of multiple lung lesions with volumetric-modulated arc therapy or intensity-modulated radiosurgery. *Front Oncol*, volume 5:213. ISSN 2234-943X (Print) 2234-943x.

[172] Chang, J. (2017). A statistical model for analyzing the rotational error of single isocenter for multiple targets technique. *Med Phys*, volume 44(6):2115–2123. ISSN 2473-4209 (Electronic) 0094-2405 (Linking).

[173] Müller, B.S., Shih, H.A., Efstathiou, J.A., Bortfeld, T., and Craft, D. (2017). Multicriteria plan optimization in the hands of physicians: a pilot study in prostate cancer and brain tumors. *Radiation Oncology*, volume 12(1):168. ISSN 1748-717X.

[174] Hansen, C.R., Bertelsen, A., Hazell, I., et al. (2016). Automatic treatment planning improves the clinical quality of head and neck cancer treatment plans. *Clinical and Translational Radiation Oncology*, volume 1:2–8. ISSN 2405-6308.

[175] Zhang, Y., Li, T., Xiao, H., et al. (2018). A knowledge-based approach to automated planning for hepatocellular carcinoma. *J Appl Clin Med Phys*, volume 19(1):50–59. ISSN 1526-9914.

[176] Ueda, Y., Fukunaga, J.i., Kamima, T., et al. (2018). Evaluation of multiple institutions' models for knowledge-based planning of volumetric modulated arc therapy (vmat) for prostate cancer. *Radiation Oncology*, volume 13(1):46. ISSN 1748-717X.

[177] Fan, J., Wang, J., Chen, Z., et al. (2019). Automatic treatment planning based on three-dimensional dose distribution predicted from deep learning technique. *Med Phys*, volume 46(1):370–381. ISSN 0094-2405.

[178] Delaney, A.R., Dahele, M., Tol, J.P., et al. (2017). Using a knowledge-based planning solution to select patients for proton therapy. *Radiotherapy and Oncology*, volume 124(2):263–270. ISSN 0167-8140.

[179] Lechner, W., Kragl, G., and Georg, D. (2013). Evaluation of treatment plan quality of imrt and vmat with and without flattening filter using pareto optimal fronts. *Radiotherapy and Oncology*, volume 109(3):437–441. ISSN 0167-8140.

[180] Ottosson, R.O., Engström, P.E., Sjöström, D., et al. (2009). The feasibility of using pareto fronts for comparison of treatment planning systems and delivery techniques. *Acta Oncologica*, volume 48(2):233–237. ISSN 0284-186X.

[181] van Sornsen de Koste, J.R., Palacios, M.A., Bruynzeel, A.M.E., et al. (2018). Mr-guided gated stereotactic radiation therapy delivery for lung, adrenal, and pancreatic tumors: A geometric analysis. *Int J Radiat Oncol Biol Phys*, volume 102(4):858–866. ISSN 0360-3016.

[182] Ginn, J.S., O'Connell, D., Thomas, D.H., Low, D.A., and Lamb, J.M. (2018). Model-interpolated gating for magnetic resonance image–guided radiation therapy. *International Journal of Radiation Oncology*Biology*Physics*, volume 102(4):885–894. ISSN 0360-3016.

[183] Kim, J.I., Lee, H., Wu, H.G., et al. (2017). Development of patient-controlled respiratory gating system based on visual guidance for magnetic-resonance image-guided radiation therapy. *Med Phys*, volume 44(9):4838–4846. ISSN 0094-2405.

[184] Crijns, S.P., Bakker, C.J., Seevinck, P.R., et al. (2012). Towards inherently distortion-free mr images for image-guided radiotherapy on an mri accelerator. *Phys Med Biol*, volume 57(5):1349–58. ISSN 1361-6560 (Electronic) 0031-9155 (Linking).

[185] Glitzner, M., Crijns, S.P., de Senneville, B.D., Lagendijk, J.J., and Raaymakers, B.W. (2015). On the suitability of elekta's agility 160 mlc for tracked radiation delivery: closed-loop machine performance. *Phys Med Biol*, volume 60(5):2005–17. ISSN 0031-9155.

[186] Kupelian, P. and Sonke, J.J. (2014). Magnetic resonance-guided adaptive radiotherapy: a solution to the future. *Semin Radiat Oncol*, volume 24(3):227–32. ISSN 1053-4296.

[187] Barbaro, B., Vitale, R., Valentini, V., et al. (2012). Diffusion-weighted magnetic resonance imaging in monitoring rectal cancer response to neoadjuvant chemoradiotherapy. *International Journal of Radiation Oncology*Biology*Physics*, volume 83(2):594–599. ISSN 0360-3016.

[188] Heethuis, S.E., Goense, L., van Rossum, P.S.N., et al. (2018). Dw-mri and dce-mri are of complementary value in predicting pathologic response to neoadjuvant chemoradiotherapy for esophageal cancer. *Acta Oncol*, volume 57(9):1201–1208. ISSN 0284-186x.

[189] Pollard, J.M., Wen, Z., Sadagopan, R., Wang, J., and Ibbott, G.S. (2017). The future of image-guided radiotherapy will be mr guided. *The British journal of radiology*, volume 90(1073):20160667–20160667. ISSN 1748-880X 0007-1285.

[190] Johnstone, E., Wyatt, J.J., Henry, A.M., et al. (2018). Systematic review of synthetic computed tomography generation methodologies for use in magnetic resonance imaging-only radiation therapy. *Int J Radiat Oncol Biol Phys*, volume 100(1):199–217. ISSN 0360-3016.

[191] Maspero, M., H F Savenije, M., Dinkla, A., et al. (2018). *Fast synthetic CT generation with deep learning for general pelvis MR-only Radiotherapy*.

[192] Nath, S.K., Lawson, J.D., Simpson, D.R., et al. (2010). Single-isocenter frameless intensity-modulated stereotactic radiosurgery for simultaneous treatment of multiple brain metastases: Clinical experience. *International Journal of Radiation Oncology*Biology*Physics*, volume 78(1):91–97. ISSN 0360-3016.

Publications

Journal articles

Winkel D., Bol G.H., Kroon P.S., van Asselen B., Hackett S.S., Werensteijn-Honingh A.M., Intven M.P.W., Eppinga W.S.C., Tijssen R.H.N., Kerkmeijer L.G.W., de Boer H.C.J., Mook S., Meijer G.J., Hes J., Willemsen-Bosman M., de Groot-van Breugel E.N., Jürgenliemk-Schulz I.M., Raaymakers B.W. (2019) Adaptive radiotherapy: the Elekta Unity MR-linac concept. *Clinical and Translational Radiation Oncology* 18, 54-59

Winkel D., Werensteijn-Honingh A.M., Kroon P.S., Eppinga W.S.C., Bol G.H., Intven M.P.W., de Boer H.C.J., Snoeren, L.M.W., Hes J., Raaymakers B.W., Jürgenliemk-Schulz I.M. (2019) Individual Lymph Nodes:"See it and Zap it". *Clinical and Translational Radiation Oncology* 18, 46-53

Werensteijn-Honingh A.M., Kroon P.S., **Winkel D.,** Aalbers E.M., van Asselen B., Bol G.H., Brown K.J., Eppinga W.S.C., van Es C.A., Glitzner M., de Groot-van Breugel E.N., Hackett S.S., Intven M.P.W., Kok J.G.M., Kontaxis C., Kotte A.N., Lagendijk J.J.W., Philippens M.E.P., Tijssen R.H.N., Wolthaus J.W.H., Woodings S.J., Raaymakers B.W., Jürgenliemk-Schulz I.M. (2019) Feasibility of stereotactic radiotherapy using a 1.5 T MR-linac: Multi-fraction treatment of pelvic lymph node oligometastases. *Radiotherapy and Oncology* 134, 50-54

Winkel D., Bol G.H., Werensteijn-Honingh A.M., Kiekebosch I.H., van Asselen B., Intven M.P.W., Eppinga W.S.C., Raaymakers B.W., Jürgenliemk-Schulz I.M., Kroon P.S. (2019) Evaluation of plan adaptation strategies for stereotactic radiotherapy of lymph node oligometastases using online magnetic resonance image guidance. *Physics and Imaging in Radiation Oncology* 9, 58-64

Winkel D., Kroon P.S., Werensteijn-Honingh A.M., Bol G.H., Raaymakers B.W., Jürgenliemk-Schulz I.M. (2018) Simulated dosimetric impact of online replanning for stereotactic body radiation therapy of lymph node oligometastases on the 1.5 T MR-linac. *Acta Oncologica* 57(12), 1705-1712

Winkel D., Bol G.H., Kiekebosch I.H., van Asselen B., Kroon P.S., Jürgenliemk-Schulz I.M., Raaymakers B.W. (2018) Evaluation of Online Plan Adaptation Strategies for the 1.5T MR-linac Based on "First-In-Man" Treatments. *Cureus* 10(4), e2431

Winkel D., Bol G.H., van Asselen B., Hes J., Scholten V., Kerkmeijer L.G.W., Raaymakers B.W. (2016) Development and clinical introduction of automated radiotherapy treatment planning for prostate cancer. *Physics in Medicine & Biology* 61(24) 8587-8595

Submitted article

Winkel D., Bol G.H., Werensteijn-Honingh A.M., Intven M.P.W., Eppinga W.S.C., Hes J., Snoeren, L.M.W., Sikkes G.G., Gadellaa-van Hooijdonk C.G.M., Raaymakers B.W., Jürgenliemk-Schulz I.M., Kroon P.S. (2019) Target coverage and dose criteria based evaluation of the first clinical 1.5T MR-linac SBRT treatments of lymph node oligometastases compared with conventional CBCT-linac treatment.

Abstracts and conference proceedings

Winkel D., Bol G.H., Werensteijn-Honingh A.M., Intven M.P.W., Eppinga W.S.C., Hes J., Snoeren L.M.W., Raaymakers B.W., Jürgenliemk-Schulz I.M., Kroon P.S. (2019). Clinical Dosimetric Benefit of the first 1.5T MR-Linac SBRT treatments of lymph node oligometastases compared to conventional CBCT-Linac treatment. *MRinRT 2019*

Winkel D., Bol G.H., Kroon P.S., van Asselen B., Hackett S.S., Werensteijn-Honingh A.M., Intven M.P.W., Eppinga W.S.C., Tijssen R.H.N., Kerkmeijer L.G.W., de Boer H.C.J., Mook S., Meijer G.J., Hes J., Willemsen-Bosman M., Sikkes G.G., de Groot-van Breugel E.N., Jürgenliemk-Schulz I.M., Raaymakers B.W. (2019) Exploration of methods for online plan adaptation on the 1.5T MR-linac. *ICCR 2019*

Winkel D., Bol G.H., Werensteijn-Honingh A.M., Intven M.P.W., Eppinga W.S.C., van Asselen B., Hes J., Raaymakers B.W., Jürgenliemk-Schulz I.M., Kroon P.S. (2019) Dosimetric benefit of the first clinical SBRT of lymph node oligometastases on the 1.5 T MR-linac. *ESTRO 2019*

Werensteijn-Honingh A.M., Kroon P.S., **Winkel D.,** Aalbers E.M., van Asselen B., Bol G.H., Brown K.J., Eppinga W.S.C., Glitzner M., de Groot-van Breugel

E.N., Hackett S.S., Intven M.P.W., Kok J.G.M., Kotte A.N., Lagendijk J.J.W., Philippens M.E.P., Tijssen R.H.N., Wolthaus J.W.H., Woodings S.J., Raaymakers B.W., Jürgenliemk-Schulz I.M. (2019) First clinical experiences with SBRT on the 1.5 T MR-linac for pelvic lymph node oligometastases. *ESTRO 2019*

Winkel D., Kroon P.S., Werensteijn-Honingh A.M., Kiekebosch I.H., Hes J., Intven M.P.W., Eppinga W.S.C., Bol G.H., Raaymakers B.W., Jürgenliemk-Schulz I.M. (2018) R-IDEAL phase 0 simulation study: Investigation of the potential dosimetric benefits of treating lymph node oligometastases on the 1.5T MR-linac. *MRinRT 2018*

Winkel D., Bol G.H., Werensteijn-Honingh A.M., Kiekebosch I.H., Hes J., Intven M.P.W., Eppinga W.S.C., Raaymakers B.W., Jürgenliemk-Schulz I.M., Kroon P.S. (2018) Dose escalation and hypofractionation for SBRT of lymph node oligometastases on the 1.5 T MRI-Linac. *ESTRO 2018*

Kiekebosch I.H., **Winkel D.,** Werensteijn-Honingh A.M., Hes J., Intven M.P.W., Eppinga W.S.C., Bol G.H., Raaymakers B.W., Jürgenliemk-Schulz I.M., Kroon P.S. (2018) 1.5 T MRI-Linac treatment planning for multiple lymph node oligometastases in the pelvic area. *ESTRO 2018*

Winkel D., Kroon P.S., Werensteijn-Honingh A.M., Hes J., Bol G.H., Jürgenliemk-Schulz I.M., Raaymakers B.W. (2017) Dosimetric impact of MR-linac treatment on SBRT of lymph node oligometastases poorly visible on CBCT. *AAPM 2017*

Winkel D., Kroon P.S., Hes J., Bol G.H., Raaymakers B.W., Jürgenliemk-Schulz I.M. (2017) Automated full-online replanning of SBRT lymph node oligometastases for the MR-linac. *ESTRO 2017*

Winkel D., Bol G.H., van Asselen B., Hes J., Scholten V., Raaymakers B.W. (2016) Development and clinical introduction of automated radiotherapy treatment planning for prostate cancer. *ICCR 2016*

Dankwoord

Dit proefschrift zou niet tot stand zijn gekomen dankzij de directe of indirecte input, steun en hulp van velen. Daarom wil ik hier graag iedereen hartelijk bedanken die hieraan, op welke manier dan ook, heeft bijgedragen. De afgelopen jaren heb ik met veel plezier met vele collega's samengewerkt en enkele hiervan wil ik dan ook in het bijzonder bedanken.

Beste Bas, bedankt dat jij als mijn promotor mij de mogelijkheden en de kans hebt gegeven om dit onderzoek binnen de afdeling uit te kunnen voeren. Al tijdens de afstudeerfase van mijn masteropleiding was je betrokken als begeleider. Enigszins afwijkend van het originele plan zijn we begonnen met het implementeren van automatische dosisplanning en na mijn afstuderen heb je mij het vertrouwen, de mogelijkheid en de vrijheid gegeven om hier verder mee te gaan. Al snel ging het onderzoek richting de MR-linac en planadaptatie en heeft dat geleid tot dit proefschrift. Bedankt voor alle goede gesprekken en discussies die we de afgelopen jaren hebben gevoerd en voor alle inspiratie, motivatie, nieuwe inzichten en input. Ik heb veel van je geleerd en zet dit graag voort.

Gijs en Petra, bedankt voor de goede en fijne begeleiding als copromotoren gedurende mijn promotietraject. Gijs, ook jij was al vanaf de afstudeerfase van mijn masteropleiding betrokken als dagelijks begeleider. Jouw ideeën en input waren altijd erg waardevol en hielpen mij altijd weer op weg als ik even "vast zat" met mijn onderzoek. Petra, kort na het begin van mijn promotietraject sloot jij aan als copromotor en zijn we met zijn allen aan de gang gegaan voor de introductie van de lymfeklier oligometastasen op de MR-linac. Je onuitputtelijke enthousiasme, suggesties en ideeën hebben veel innovaties naar de kliniek gebracht. Ook ben ik er zeker van dat je op termijn deze innovaties ook op persoonlijk vlak zal doorvoeren en eindelijk een automaat gaat rijden. Bedankt dat ik altijd jullie kamer binnen kon stormen voor discussies en feedback. Ik had mij geen beter team kunnen wensen tijdens dit traject.

Ina, uiteindelijk ben jij ook erg betrokken geraakt bij dit project met de introductie van de lymfeklier oligometastasen op de 1.5T MR-linac. Bedankt voor alle waardevolle input vanuit een klinisch perspectief. Dit heeft een groot deel van

het onderzoek gedurende mijn promotietraject mogelijk gemaakt en heeft enorm bijgedragen aan dit proefschrift. Jij gaat altijd tot het uiterste voor de patiënt en jouw eindeloze inzet voor zowel de kliniek als het onderzoek is inspirerend.

Beste leden van de beoordelingscommissie, prof. dr. J.H.E. Kuball, prof. dr. M. Verheij, prof. dr. H.M. Verkooijen, prof. dr. U.A. van der Heide en prof. dr. S. Horenblas, hartelijk dank voor het lezen en beoordelen van dit proefschrift en voor het plaatsnemen in de oppositie.

Ik wil graag de gehele tumorwerkgroep urologie bedanken voor hun bijdrage en input voor de ontwikkeling en de klinische implementatie van de automatische dosisplanning voor prostaat en blaas. Daarnaast wil ik de hele oligo-groep bedanken voor hun bijdrage met betrekking tot de implementatie van de lymfeklieren oligometastasen op de MR-linac. Martijn en Wietse, bedankt voor jullie inbreng vanuit klinisch perspectief. Anita, in het bijzonder wil ik jou daarbij bedanken voor jouw waardevolle inhoudelijke en taalkundige suggesties op veel van de stukken in dit proefschrift. Ook wil ik de gyn-, oes- en rectumgroep bedanken voor het beschikbaar stellen van data voor het onderzoek beschreven in dit proefschrift.

Dank aan de klinisch fysici betrokken bij dit proefschrift. Bram, door jou colleges is mijn interesse voor de radiotherapie aangewakkerd en ben ik dan ook op dit pad terecht gekomen. Bedankt hiervoor en voor al jouw expertise en suggesties ten opzichte van dosisplanning. Hans, bedankt voor je input op het gebied van prostaatkanker en marge-analyses. Sara en Jochem, bedankt voor het uitvoeren van diverse QA metingen en analyses.

Bijzondere dank aan alle laboranten van de radiotherapie welke in de afgelopen jaren direct of indirect hebben bijgedragen aan dit proefschrift. Jochem, al vanaf het begin was jij betrokken als specialistisch laborant en was jij altijd de "go-to" voor praktische vragen en feedback op de dosisplannen. Het *i*MRL team: Christel, Eline, Gonda, Ilse en Lieke, bedankt voor de fijne samenwerking en jullie praktische hulp als ik ergens niet uitkwam. Ook wil ik nog in het bijzonder de volgende laboranten bedanken: Mirjam, Loek, Roel, Tuan, Ellart, Nicole en stagiaire Sanne.

Ik wil in het bijzonder mijn kamergenoten van de gezelligste kamer van de afdeling: Q.0S.4.37 bedanken. Joris, Hans, Sophie en Robin, al vanaf mijn afstudeerproject ben ik bij jullie op de kamer terecht gekomen. Niet enkel bedankt voor de gezelligheid, de leuke gesprekken en vele koffie-momentjes, maar ook voor al jullie praktische hulp, tips en suggesties welke mij goed op weg hebben geholpen. Ook waren de theebel (Hans), het beschikbaar stellen van het Nespresso apparaat (Joris) en

het regelmatig doorgeven van de sneeuwhoogtes (Sophie) van essentieel belang. Gaandeweg gingen er mensen weg en kwamen er weer nieuwe kamergenoten bij. Soraya, je spreekt inmiddels beter Nederlands dan Robin, ga zo door. Jorine, dankzij jouw planning liep het altijd goed en het was elke dag weer een verrassing hoe je haar er bij stond. Daan, binnenkort dan toch eindelijk die Lexus. Steven, bedankt voor je baksels, maar toch miste er altijd wel iets. Pouleleider Mick, altijd weer paraat om de telefoon door te verbinden, maar misschien moet je iets minder 'boer zoekt vrouw', 'wie is de mol' en 'heel Holland bakt' kijken. Daarnaast ook alle overige en tijdelijke kamergenoten: Thomas, Stefan, Filipa, Sanam, Victor, Cathalijne en Marcia, bedankt voor de gezelligheid, leuke gesprekken en vele koffie-momentjes.

De sfeer en betrokkenheid van de hele afdeling waren buitengewoon goed. Dit heeft allemaal bijgedragen aan een ontzettend fijn promotietraject. Bedankt hiervoor aan alle verdere collega's; Markus, Charis, Tristan, Bjorn, Jean-Paul, Stan, Alexis, Anette, Astrid, Matteo, Tom, Maarten, Maxence, Ellis, Pim, Gert, Simon, Jan, Rob, Nico en iedereen die ik nog vergeet te noemen. Veel dank voor jullie directe en indirecte input, maar ook voornamelijk de gezelligheid tijdens uitjes, congressen, lunches en gewoon bij het koffieapparaat.

Mijn vrijwilligerswerk bij het Rode Kruis is inmiddels een belangrijk deel van mijn leven geworden. Daarvoor wil ik iedereen bedanken met wie ik de afgelopen jaren de nodige ontspannende momenten en avonturen heb beleefd. In het bijzonder wil ik daarvoor mijn vrienden en collega's van afdeling Culemborg, noodhulpteam Gelderland-Zuid en natuurlijk de Jeugd Rode Kruis Culemborg groep. Daarnaast wil ik ook een aantal Rode Kruis vrienden en collega's van elders bedanken: Adrie, Henk, Mariejanne, Joke, Karin, Hanna en iedereen die ik mogelijk vergeet. Bedankt voor jullie steun, hulpbereidheid en het mede mogelijk maken van de vele inzetten, projecten en dingen die ik graag onderneem.

Ich danke auch meinen Kollegen und Freunden des Deutschen Roten Kreuzes und des Jugendrotkreuzes aus Hürben und Berghausen für die gute internationale Zusammenarbeit und die lustige und angenehme Zeit. Eine relativ zufällige Begegnung führte in kurzer Zeit zu einem tollen internationalen Projekt und vielen neuen Freundschaften. Insbesondere möchte ich mich bei den Familien Mai, Graf, Morlock und Windschnurer für ihre Gastfreundschaft bedanken. Ich fühle mich immer willkommen bei euch. An meine Dönergruppe: nächstes Mal gebe ich aus! Raphael, mein kleiner Freund seit dem ersten Moment und wahrscheinlich noch für eine lange Zeit. Lena, vielen Dank für die großartige Zusammenarbeit und Freundschaft, die hoffentlich noch viele Jahre andauern wird.

Hans en Francis, bedankt dat jullie mijn paranimfen willen zijn tijdens deze bijzondere gebeurtenis. Met jullie erbij gaat het zeker goedkomen en wordt het een topfeest.

Mijn ouders, bedankt voor jullie vertrouwen, steun en kansen welke ik in mijn leven van jullie heb gekregen. Davey, bedankt voor de praktische ondersteuning. Hiervoor ben ik jullie ontzettend dankbaar en dit heeft mede geleid tot dit proefschrift.

Curriculum Vitae

Dennis Winkel was born in Culemborg, The Netherlands, on 18 February 1989. After attending primary school in Culemborg, he obtained his VWO diploma at *O.R.S. Lek en Linge* in Culemborg in 2007. Then he studied Computer Science at the *University of Utrecht* starting in 2007. After finishing the Bachelor program in 2011, he followed the Master program Biomedical Image Sciences at the *University of Utrecht* and graduated in 2015. His master thesis was carried out at the *Department of Radiotherapy* of the *University Medical Center Utrecht*, under the supervision of prof. dr. B.W. Raaymakers and dr. G.H. Bol. on the topic of automated radiotherapy treatment planning for prostate cancer. After his Master graduation, he started as a PhD student at the *Department of Radiotherapy* of the *University Medical Center Utrecht* under supervision of prof dr. B.W. Raaymakers, dr. G.H. Bol and dr. ir. P.S. Kroon. His research topics were automated treatment planning and online treatment adaptation strategies for the 1.5T MR-linac of which the results are presented in this thesis. Dennis will continue working as a computer scientist at the *Department of Radiotherapy* of the *University Medical Center Utrecht* focusing on automated and adaptive treatment planning.